

Distribution Agreement

In presenting this thesis or dissertation as a partial fulfillment of the requirements for an advanced degree from Emory University, I hereby grant to Emory University and its agents the non-exclusive license to archive, make accessible, and display my thesis or dissertation in whole or in part in all forms of media, now or hereafter known, including display on the world wide web. I understand that I may select some access restrictions as part of the online submission of this thesis or dissertation. I retain all ownership rights to the copyright of the thesis or dissertation. I also retain the right to use in future works (such as articles or books) all or part of this thesis or dissertation.

Signature:

Carolina Montañez Harm

THE IMPACT OF GENETIC VARIATION ON RGS AND G PROTEIN SIGNALING IN PHYSIOLOGY AND DISEASE

By

Carolina Montañez Harm
Doctor of Philosophy (Ph.D.)

Graduate Division of Biological and Biomedical Sciences
Molecular and Systems Pharmacology

John R. Hepler, Ph.D. (Advisor)

Victor Faundez, M.D., Ph. D. (Committee Member)

Randy Hall, Ph. D. (Committee Member)

Stephen Traynelis, Ph. D. (Committee Member)

Accepted:

Kimberly Jacob Arriola, Ph.D., MPH
Dean of the James T. Laney Graduate School of Graduate Studies

Date

**THE IMPACT OF GENETIC VARIATION ON RGS AND G PROTEIN
SIGNALING IN PHYSIOLOGY AND DISEASE**

By

**Carolina Montañez Harm
Bachelor of Science, University of Puerto Rico Cayey, 2016**

Advisor: John R. Hepler, Ph. D.

An abstract of
A dissertation submitted to the Faculty of the James T. Laney School of Graduate
Studies of Emory University in partial fulfillment of the requirements for the degree of
Doctor of Philosophy
Graduate Division of Biological and Biomedical Sciences
Molecular Systems and Pharmacology
2022

Abstract

THE IMPACT OF GENETIC VARIATION ON RGS AND G PROTEIN SIGNALING IN PHYSIOLOGY AND DISEASE

By
Carolina Montañez Harm

Regulators of G protein signaling (RGS) proteins modulate G protein-coupled receptor (GPCR) signaling by acting as negative regulators of G proteins. RGS proteins critically regulate cell physiology and pathophysiology. Each RGS protein has a distinct G protein selectivity profile that correlates to a finely tuned GPCR-G protein response. Human genetic variant information has expanded rapidly in recent years, including cancer-linked mutations in RGS proteins. Genetic variants in RGS proteins contribute to complex polygenic human traits and pathologies by causing differences in protein function that is critical for signaling regulation and physiology. Recent genome-wide association studies (GWAS) have identified point mutations in RGS proteins that are associated with pathologies such as cancers and other diseases (e.g. RGS14 in chronic kidney disease). In this body of work, I explored a new analytical method, 3DMTR and permutation analysis, to define regions of genetic intolerance in 15 RGS proteins and prioritize which cancer-linked mutants in selected RGS proteins to test for altered function. Using complimentary cellular and biochemical approaches, RGS4, RGS10 and RGS14 were tested for effects on GPCR-G α activation, G α binding properties, and downstream cAMP levels. My findings show that 3DMTR identified intolerant residues that overlap with cancer-linked mutations cause phenotypic changes that negatively impact GPCR-G protein signaling and suggests that 3DMTR is a potentially useful bioinformatics tool for predicting functionally important protein residues. In addition to these findings, my studies expand our knowledge of the multifunctional signaling protein RGS14 by defining its role in regulating PTH1R-G protein signaling linked to phosphate transport in chronic kidney disease. My studies reveal that PTHR1 stimulates intracellular cAMP by coupling to G α_s , as expected. However, quite unexpectedly, I also found that RGS14 stimulates intracellular calcium independent of G α_q coupling. Human RGS14 binds to the PDZ protein NHERF1. I found that RGS14 and NHERF1 each block PTH-stimulated calcium, but not cAMP accumulation, indicating that RGS14 and NHERF1 regulate PTHR1-calcium signaling by a previously unknown mechanism. These studies expand on the fine-tuning roles of RGS14 and other RGS proteins in mediating G protein signaling and crosstalk between GPCRs and other signaling pathways linked to physiology and disease.

**THE IMPACT OF GENETIC VARIATION ON RGS AND G PROTEIN
SIGNALING IN PHYSIOLOGY AND DISEASE**

By

**Carolina Montañez Harm
Bachelor of Science, University of Puerto Rico Cayey, 2016**

Advisor: John R. Hepler, Ph. D.

A dissertation submitted to the Faculty of the James T. Laney School of Graduate
Studies of Emory University in partial fulfillment of the requirements for the degree of
Doctor of Philosophy
Graduate Division of Biological and Biomedical Sciences
Molecular Systems and Pharmacology
2022

ACKNOWLEDGMENTS

To my mentors

Words cannot express my gratitude and respect to my thesis and research advisor Dr. John R. Hepler. I am extremely thankful for his invaluable advice, continuous support, and patience during my PhD study. His immense knowledge, experience and passion for science have encouraged me to be a better scientist. He is a brilliant scientist, and a great role model.

My gratitude extends to my committee members: Dr. Randy Hall, Dr. Stephen Traynelis and Dr. Victor Faundez. They generously gave their time and shared their knowledge, expertise, constructive criticism, and technical support through the years. Thank you for showing me what brilliant and hard-working scientist can accomplish.

To my colleagues and friends

I would like to thank all the members, past and present, of the Hepler Lab: Katherine Squires, Kyle Gerber, Suneela Ramineni, Nicholas Harbin and Sara Bramlett. Thank you for a cherished time spend together. This brilliant friends and colleagues inspired me over the years. It is their kind help, support, lengthy science discussions, and mentorship that have made my time at Emory so pleasant and exciting.

I cannot forget friends who cheered me on and celebrated each accomplishment. Thank you for being there for me when the challenges of graduate school seemed too great to overcome. Many thanks: Trisha, Juleva, Jaqueline, Roxana, Lauren, Bijan, Darius, Valerie, Mary G., Destiny, Ada, Lola, Pedro, Juan Carlos, and Wilfredo.

To my family

Finally, I would like to express the deepest gratitude to *mi bella familia y esposo*. Without their tremendous encouragement, it would have been impossible for me to complete my doctoral degree.

Tío Javier, Titi Lisy, Prima Liz, thank you for your infinite love, support, and advice. It's been a long journey and I could have not made it without your continuous encouragement and optimism.

It was my grandparents who from an early age inspired me to be ambitious in my pursuits. Gracias, abuelo y abuela, for teaching me that my job in life is to keep learning, to be happy, and humble.

I could have not undertaken this journey without the support of my husband, Peyton. You have been continually supportive of my graduate education. Thank you for being understanding of the PhD life and for always caring about the status of my HEK293 cells. You have provided me endless encouragement in this academic journey, you have celebrated with me even when the little things go right. I am truly thankful for having you and Chimi in my life.

Thank you to my wonderful parents, Tere y Manolo, for always believing in me. I am forever indebted to my parents for giving me the opportunities and experiences that have made me who I am. I'm lucky to have extremely smart, witty, and enthusiastic parents, that never doubted I would make it to the finish line, even when I didn't believe in myself.

DEDICATION

This thesis work is dedicated to my husband, Peyton, who has been a constant source of support and encouragement during this exciting and challenging journey. This work is also dedicated to my supportive and enthusiastic parents, Tere y Manolo, who have always loved me unconditionally and have shown me to work hard and aspire to achieve.

TABLE OF CONTENTS

	PAGE
1. CHAPTER 1: INTRODUCTION	1
1.1. Foundations in the GPCR-G protein field	2
1.2. Conventional GPCR and G protein signaling	5
1.3. Regulators of G protein signaling (RGS) in physiology and disease	6
1.3.1. The R4 Family	10
1.3.2. The R7 Family	11
1.3.3. The RZ Family	12
1.3.4. The R12 Family	13
1.4. Regulator of G protein signaling 14 in physiology and disease	15
1.4.1. RGS14 is a multifunctional signaling protein	15
1.4.2. The role of RGS14 in the brain	19
1.4.3. The role of RGS14 outside of the brain	23
2. CHAPTER 2: FUNCTIONAL ASSESSMENT OF CANCER-LINKED MUTATIONS IN SENSITIVE REGIONS OF RGS PROTEINS PREDICTED BY 3DMTR ANALYSIS	26
2.1. Abstract	27
2.2. Introduction	29
2.3. Materials and Methods	32
2.4. Results	39
2.5. Discussion	70
2.6. Supplemental Information	76
3. CHAPTER 3: HUMAN RGS14 AND NHERF1 REGULATE PTH1R-G PROTEIN SIGNALING EVENTS LINKED TO PHOSPHATE UPTAKE IN KIDNEY	88
3.1. Abstract	89
3.2. Introduction	90
3.3. Materials and Methods	93
3.4. Results	97
3.5. Discussion	104
4. CHAPTER 4: DISCUSSION AND CONCLUDING REMARKS	108
4.1. Introduction	109
4.2. Discussion and Future Directions	111
4.3. Concluding Remarks	126
5. BIBLIOGRAPHY	127

LIST OF FIGURES AND TABLES

PAGE NUMBER

FIGURE 1.1: REGULATOR OF G PROTEIN SIGNALING (RGS) PROTEIN FAMILY AND G ALPHA PROTEIN SELECTIVITY	9
FIGURE 1.2: HUMAN RGS14 STRUCTURE: DOMAINS, MOTIFS, AND BINDING PARTNERS.	18
FIGURE 2.1: COMPARISON OF RGS14 1DMTR AND 3DMTR PERMUTATION ANALYSIS.	42
FIGURE 2.2: THE 3DMTR PERMUTATION ANALYSIS IDENTIFIES SIGNIFICANTLY INTOLERANT RESIDUES WITHIN THE RGS DOMAIN THAT WERE NOT IDENTIFIED BY 1DMTR.	46
TABLE 2.1: TOLERANT AND INTOLERANT RESIDUES FROM RGS DOMAINS OF INTEREST THAT ALSO OVERLAP WITH HIGHLY DELETERIOUS SOMATIC MUTATIONS WERE SELECTED FOR ASSESSMENT OF THEIR IMPACT ON RGS FUNCTION	48
FIGURE 2.3: ASSESSMENT OF FUNCTIONAL IMPACT OF RGS14 SOMATIC MUTATIONS ON GPCR-G PROTEIN ACTIVATION AND G PROTEIN BINDING	54
FIGURE 2.4: ASSESSMENT OF FUNCTIONAL IMPACT OF RGS10 SOMATIC MUTATIONS ON GPCR-G PROTEIN ACTIVATION AND G PROTEIN BINDING.	58
FIGURE 2.5: ASSESSMENT OF FUNCTIONAL IMPACT OF RGS4 SOMATIC MUTATIONS ON GPCR-G PROTEIN ACTIVATION AND G PROTEIN BINDING.	61
FIGURE 2.6: ASSESSMENT OF FUNCTIONAL IMPACT OF WILD TYPE VS MUTANT FORMS OF RGS14, RGS10 AND RGS4 ON A2A-AR-G PROTEIN DIRECTED INHIBITION OF CAMP LEVELS.	65
FIGURE 2.7:	

ASSESSMENT OF THE FUNCTIONAL IMPACT OF WILD TYPE VS MUTANT FORMS OF RGS14, RGS10 AND RGS4 ON FSK-STIMULATED CAMP PRODUCTION BY ADENYLYL CYCLASE (AC).	68
TABLE 2.2:	
THE 3DMTR ANALYSIS IS A BETTER PREDICTOR OF KEY PROTEIN RESIDUES FOR FUNCTIONAL IMPACT OF SOMATIC MUTATIONS THAN 1DMTR.	71
SUPPLEMENTAL FIGURE 2.1:	
RASTER PLOT OF ALL RGS PROTEINS WITH AVAILABLE CRYSTAL STRUCTURE.	76
SUPPLEMENTAL FIGURE 2.2:	
RASTER PLOT OF RGS PROTEINS IN COMPLEX WITH ACTIVE FORMS OF THEIR GA PARTNERS.	78
SUPPLEMENTAL TABLE 2.1:	
3D STRUCTURE INFORMATION FOR ANALYZED RGS PROTEINS.	79
SUPPLEMENTAL FIGURE 2.3:	
3DMTR-PERMUTATION ANALYSIS COMPARING RGS4 AND RGS10.	81
SUPPLEMENTAL FIGURE 2.4:	
RGS WT AND MUTANT PROTEIN EXPRESSION IN HEK 293 CELLS USED FOR KINETIC BRET.	82
SUPPLEMENTAL TABLE 2.2:	
COMPARISON OF VARIOUS BIOINFORMATIC TOOLS FOR THEIR PREDICTIVE VALUES FOR CHANGE-OF-FUNCTION IN AMINO ACIDS OF RGS14, RGS10 AND RGS4	83
FIGURE 3.1:	
PTH1R SIGNALS STRONGLY THROUGH GaS.	100
FIGURE 3.2:	
RGS14 AND NHERF1 DO NOT AFFECT PTHR-GaS COUPLING OR CAMP FORMATION.	101
FIGURE 3.3:	
RGS14 AND NHERF1 DO NOT AFFECT PTHR-GaQ COUPLING BUT DO AFFECT CALCIUM LEVELS.	102
FIGURE 3.4:	
RGS14 ROLE IN PTH-PTHR SIGNALING.	107

FIGURE 4.1:	
THE 3DMTR PERMUTATION ANALYSIS IDENTIFIES INTOLERANT AND TOLERANT RESIDUES WITHIN THE RGS DOMAIN OF RGS PROTEINS	114
FIGURE 4.2:	
A2AR SIGNALS VIA GS IN HEK CELLS AND WT RGS14/RGS10 DECREASE CAMP ACCUMULATION.	119
FIGURE 4.3:	
MODEL FIGURE: POSSIBLE MECHANISMS BY WHICH RGS14 INHIBITS PHOSPHATE UPTAKE AND REGULATES CALCIUM FLUX IN KIDNEY CELLS	124

CHAPTER 1: INTRODUCTION

This chapter has been assembled in part from the published^{1,2} and submitted³ manuscripts:

¹Squires KE, **Montañez-Miranda C**, Pandya RR, Torres MP, and Hepler JR (2017). **Genetic Analysis of Rare Human Variants of Regulators of G Protein Signaling (RGS) Proteins and Their Role in Human Physiology and Disease**. *Pharmacol Rev.*

²Harbin NH, Bramlett SN, **Montañez-Miranda C**, Terzioglu G, and Hepler JR (2021.) **RGS14 Regulation of Post-Synaptic Signaling and Spine Plasticity in Brain**. *Int. J. Mol. Sci.*

³**Montañez-Miranda C**, Bramlett SN, Hepler JR (2022). **RGS14 expression in CA2 hippocampus, amygdala, and basal ganglia: Implications for human brain physiology and disease**. *Hippocampus*.

1.1 FOUNDATIONS OF THE GPCR-G PROTEIN FIELD

Understanding how cells communicate has been the center of attention of many scientists for decades. Because of these researchers' efforts, today we can appreciate the molecular mechanism that explains how cells communicate by releasing chemical messengers that dictate cell physiology. These messengers are a diverse array of chemical signals, or ligands, that include hormones, neurotransmitters, chemokines, sensory receptors, odorants, and photons of light. G protein-coupled receptors (GPCRs) represent the largest and most ubiquitous group of cell surface receptors. These receptors are characterized by a seven-transmembrane (7TM) configuration and activate G proteins transducing the signals into intracellular responses.

The discoveries and developments that led to our understanding of GPCR-G protein signaling started between the 1960s and 1970s. During this time, Sutherland discovered the second messenger cAMP (Robison and Sutherland, 1971), while Krebs discovered the effector of cAMP action (cAMP-dependent protein kinase) (Walsh et al., 1968). In 1971, Rodbell proposed the existence of a guanine nucleotide regulatory protein that acts as a GTP dependent transducer between hormone receptors, adenylyl cyclase (AC) and cAMP production (Rodbell et al., 1971). Gilman and colleagues later demonstrated the existence of this factor as a necessary third protein independent of receptor or AC (Ross and Gilman, 1977). In subsequent studies, the Gilman group purified the first G protein, calling it G_s, "s" for "stimulatory" protein, demonstrating that the guanine nucleotide regulatory component observed by Rodbell consisted of a G_s subunit and a regulatory G $\beta\gamma$ dimer, together existing as a functional G_s heterotrimer to link receptors to activation of AC (Gilman, 1987; Northup et al., 1980). A distinct pertussis toxin-sensitive

factor was later described to inhibit AC (Hazeki and Ui, 1981). It was then purified and identified as a second hormone-regulated G protein, termed Gai for the “inhibitory” actions (Katada et al., 1984). In 1985, this group was the first to reconstitute the three component complex to demonstrate the activation/deactivation cycle GPCR-G α -Effector complex (May et al., 1985) and propose the now accepted mechanism of hormone/neurotransmitter actions. This research group then cloned, purified, and solved the crystal structures of G α s (Graziano et al., 1987; Harris et al., 1985; Sunahara et al., 1997), a non-retinal G $\beta\gamma$ complex (Gao et al., 1987; Ueda et al., 1994; Wall et al., 1995), the Gai1 heterotrimeric complex (Coleman et al., 1994; Linder et al., 1990) and the first of the isoforms for AC (Krupinski et al., 1989; Tesmer et al., 1997b) to elucidate the mechanism of receptor and dual G protein regulation of AC activity (Gilman, 1987). Collaborative work between Melvin Simon at Cal Tech, the Gilman group and other labs went on to identify the family of heterotrimeric G proteins classified into 4 subfamilies that regulate the actions of all GPCRs (Hepler and Gilman, 1992). These include the G α s subfamily (G α s and G α olf) that activates AC, the Gai family (Gai1, Gai2, Gai3, Gao, Gat, and Gaz) that inhibits adenylyl cyclase, the G α q family (G α q, G α 11, G α 14, G α 16) that activates phospholipase C, and the G α 13/13 family that activates Rho family monomeric GTPases to regulate actin cytoskeleton.

In the 1980s, the groups of Robert Lefkowitz and Marc Caron were able to successfully purify, for the first time, the GPCR adrenoreceptor β 2 (β 2-AR) (Benovic et al., 1984; Shorr et al., 1981), α 2A-AR (Regan et al., 1986), and α 1B-AR (Lomasney et al., 1986). In 1986, Brian Kobilka, in the laboratory of Robert Lefkowitz, and in collaboration with a team of scientists at Merck Sharpe and Dohme, were able to clone the gene and cDNA encoding

the hamster β 2-AR and subsequently create a genomic library (Dixon et al., 1986). This led to the rapid discovery of many other receptors that resembled those of the 7TM receptor gene family that share a sequence homology and structure. Currently there are ~800 annotated GPCRs involved in almost every physiological function including the regulation of neurotransmitters, hormones, metabolites, odors, and ions (Schoneberg and Liebscher, 2021). GPCRs are the most targeted receptor family, with 34% of the pharmaceuticals used today (Hauser et al., 2017).

Between the 1980s and 1990s researchers noticed a discrepancy between the biochemical GTPase activity of $G\alpha$ subunits and the turnoff rate of physiological signals (Kaur et al., 2011). To understand this phenomenon, studies were done in yeast and worm models. Haploid yeast secretes pheromones that act on the GPCRs of the opposing mating yeast. In 1982, a mutant pheromone-supersensitive yeast strain *sst2* showed long lasting pheromone effects when compared to WT yeast (Chan and Otte, 1982). The studies showed the effect of the *sst2* protein (*sst2p*) to have direct action on G protein, showing *sst2p* to be the first identified RGS protein (Dietzel and Kurjan, 1987; Dohlman et al., 1995). Meanwhile, studies in *C. elegans* identified the gene *EGL-10*, a RGS protein that suppresses serotonin signaling through *Gao* protein (Koelle and Horvitz, 1996). Gilman and colleagues then defined RGS proteins GAP activity at *Gai* and *Gaq* family $G\alpha$ subunits (Berman et al., 1996). Following this discovery, researchers focused on defining the biochemical properties, tissue-specific expression, protein complex formation and regulation of RGS proteins (Kaur et al., 2011).

This series of discoveries explain the molecular basis of cell signaling and communication from the outside to the inside of the cell, by involving an input receiver

(receptor), a transducer (G protein), and an effector enzyme (such as adenylyl cyclase). These discoveries laid the foundation for all future work on GPCR-G-RGS complex and downstream signaling studies, including my dissertation work understanding how human mutations in RGS proteins affect GPCR-G protein signaling.

1.2 CONVENTIONAL G-PROTEIN COUPLED RECEPTORS (GPCR) AND G PROTEIN SIGNALING

G protein coupled receptors (GPCRs) and linked G protein signaling pathways regulate vital physiological processes by transducing extracellular stimuli and regulating intracellular effectors important for cell and organ physiology (Bourne et al., 1990; Hamm, 1998; Hepler and Gilman, 1992). Following stimulation by extracellular stimuli (hormones or neurotransmitters and others), GPCRs activate heterotrimeric G proteins ($G\alpha\beta\gamma$) by acting as guanine nucleotide exchange factors (GEFs). Activation of the GPCR-G protein complex initiates a conformational change in $G\alpha$ that promotes the exchange of inactive guanosine diphosphate (GDP) for active guanosine triphosphate (GTP) that binds to $G\alpha$ causing a dissociation from the $\beta\gamma$ subunits (Gilman, 1987; Hamm, 1998; Ross and Wilkie, 2000). Termination of downstream signaling occurs due to the relatively slow intrinsic GTPase activity of $G\alpha$ subunits hydrolyze GTP to GDP, allowing $G\alpha$ to re-associate with $G\beta\gamma$ (Hamm, 1998; Ross and Wilkie, 2000). Regulators of G proteins Signaling (RGS) proteins are critical mediators of G-proteins by tightly mediating the magnitude and duration of the intracellular signaling response stabilizing the transition state conformation and lowering the free energy required to activate the hydrolysis reaction. RGS proteins act as GTPase-accelerating proteins (GAPs) for specific $G\alpha$

subunits and accelerate the exchange of GTP to GDP, terminating the signaling cascades (Berman et al., 1996; Dohlman and Thorner, 1997; Hepler et al., 1997; Hunt et al., 1996; Kozasa et al., 1998; Watson et al., 1996).

GPCR rapid signal turnoff is also accomplished by receptor phosphorylation by GPCR kinases (GRKs). However, this process differs from RGS function. By binding active GPCRs and phosphorylating them, GRKs reduce G protein coupling of active GPCR. Arrestin then recognizes the active phosphorylated GPCR and outcompetes the G protein. Arrestin binding leads to receptor desensitization, internalization, dephosphorylation and recycling. The arrestin-receptor complex acts as a scaffold facilitating different signaling cascades, such as Raf-MEK-ERK (Gurevich and Gurevich, 2019). The N-terminus of all GRKs is homologous to the RGS protein RGS domain, termed RGS homology domain (RH) (Day et al., 2004). However, the GRK RGS homology domain is different from others by having a distinct binding interface for G α subunits. It is thought that the GRK RH functions to provide specificity for the GRK to interact with a particular G α subunit or GPCR/G α complex (Day et al., 2004). In contrast to the canonical RGS proteins, the RH domain of GRKs possess a weak ability to activate intrinsic GTPase of G proteins, instead it reduces the G α q/11 regulated signaling by sequestering active G α q/11 or by blocking the receptor (Carman et al., 1999; Dhimi et al., 2002; Gurevich and Gurevich, 2019; Ribeiro et al., 2009).

1.3 REGULATORS OF G PROTEIN SIGNALING (RGS) IN PHYSIOLOGY AND DISEASE

RGS proteins are a large family (20 members) of diverse multifunctional signaling proteins that are classified into four subfamilies based on sequence homology and the presence of additional non-RGS domains (Hollinger and Hepler, 2002; Ross and Wilkie, 2000; Willars, 2006). Functional proteins share a conserved RGS domain that interacts with specific active G α subunits and catalyzes the transition state of GTP hydrolysis by G α (Tesmer et al., 1997a). While many RGS proteins are small simple proteins that serve as dedicated GAPs, some are larger more complex proteins with other domains and signaling partners with roles outside of their canonical GAP function (Gerber et al., 2016; Hollinger and Hepler, 2002). Figure 1.1 shows a map of all RGS members, and the G protein selectivity associated to each family.

GPCRs transmit extracellular signals into target cells via G protein activation, and RGS proteins determine the magnitude and duration of the cellular responses initiated. A minor disturbance in the GPCR-G-RGS complex can initiate pathology by disrupting the signaling cascade. Several publications have implicated RGS proteins to play a role in pathology including: cancer (Hurst and Hooks, 2009), inflammation (Xie et al., 2016), cardiovascular processes (Stewart et al., 2012), and neurodegenerative diseases (Ahlers-Dannen et al., 2020). Some RGS proteins (RGS2, 4, 7, 9-2, and 14) have been involved in diseases by altering pre and postsynaptic neurotransmission (Gerber et al., 2016). In cancer, GPCR-RGS mediated pathways have been linked to mediate oncogenic processes (Wu et al., 2019) such as uncontrolled growth, invasion, and metastasis. For example, in ovarian cancer studies, decrease expression of RGS10 leads to cell proliferation and increased chemoresistance (Alqinyah et al., 2018; Hooks et al., 2010). Evidence shows that RGS proteins can also modulate diverse GPCR families such

as opioid, cannabinoid, and serotonin receptors in the GI tract (Salaga et al., 2016). RGS proteins are likely involved in more complex pathways that contribute to disease progression due to the role they play serving as central control point in the GPCR signaling cascade.

RGS PROTEINS










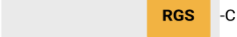








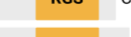

Family	Members	Gα protein selectivity
R7	RGS6 N-  -C	Go family
	RGS7 N-  -C	
	RGS9 N-  -C	
	RGS11 N-  -C	
R12	RGS14 N-  -C	Go family
	RGS12 N-  -C	
	RGS10 N-  -C	
RZ	RGS19 N-  -C	Gq/Go families
	RGS17 N-  -C	
	RGS20 N-  -C	
R4	RGS13 N-  -C	Gq/Go families
	RGS1 N-  -C	
	RGS21 N-  -C	
	RGS2 N-  -C	
	RGS18 N-  -C	
	RGS4 N-  -C	
	RGS5 N-  -C	
	RGS3 N-  -C	
	RGS8 N-  -C	
	RGS16 N-  -C	

Figure 1.1. Regulator of G protein Signaling (RGS) protein family and G alpha protein selectivity. RGS proteins are organized by family. Domains are identified by color: RGS domain in gold, DEP (disheveled EGL10-Pleckstrin homology domain) in purple, R1 in green, R2 in teal (Ras/Rap binding domains), GPR (G protein regulator motif) in magenta, GGL (G protein g subunit-like domains) in lilac, PTB (phosphotyrosine binding domain) in mint, PDZ (post synaptic density protein (PSD95), drosophila disc large tumor suppressor (Dlg1), and zonula occludens-1 protein(zo-1)domain).

1.3.1 The R4 family

Members of the R4 subfamily compose the largest and best characterized of the RGS proteins due to their early discovery and simplicity in structure. R4 family RGS proteins include: RGS1, RGS2, RGS3, RGS4, RGS5, RGS8, RGS13, RGS16, RGS18, and RGS21. All R4 family members exhibit capacity to bind and act as GAPs for both $G\alpha i/o$ and $G\alpha q$ (Hollinger and Hepler, 2002) proteins with varying specificity (Heximer, 2004; Heximer et al., 1999; Heximer et al., 1997; Huang et al., 1997) based, in some cases, on subtle structural differences (Nance et al., 2013). For example, RGS2 demonstrates much greater selectivity for $G\alpha q$ (Heximer et al., 1997), whereas RGS4 demonstrates greater selectivity for $G\alpha i$ (Hepler et al., 1997; Heximer et al., 1999). In addition to the canonical RGS domain, these small RGS proteins also share an N-terminal amphipathic α helix which, in coordination with N-terminal palmitoylation (Tu et al., 2001), facilitates plasma membrane localization (Bernstein et al., 2000; Gu et al., 2007; Heximer et al., 2001) and consequent actions on $G\alpha$ proteins. Outside of this, the N-termini of certain R4 RGS proteins show considerable diversity which determine their specificity for receptor coupling (Bernstein et al., 2004; Neitzel and Hepler, 2006) and regulation by cellular protein degradation pathways (Bodenstein et al., 2007; Davydov and Varshavsky, 2000).

RGS4 is selectively expressed in the heart and the brain (Ingi and Aoki, 2002; Zhang et al., 1998), where its expression and protein stability is tightly controlled by its N-terminus (Bastin et al., 2012; Bodenstein et al., 2007). While RGS4 protein in the heart is found at very low levels under normal cardiac physiology (Stewart et al., 2012), it can be upregulated during pathophysiology and cardiac remodeling (Felkin et al., 2011; Jaba et al., 2013; Lee et al., 2012; Mittmann et al., 2002; Owen et al., 2001). Additionally, RGS4

knockout mice are susceptible to atrial fibrillation (Opel et al., 2015). A great deal is known about RGS4 in the brain. First, RGS4 mRNA is decreased in the frontal cortex of schizophrenic patients, whereas other R4 family transcripts were not (Mirnics et al., 2001). Further, several non-coding SNVs (“SNP1”, “SNP4”, “SNP7”, and “SNP18”) are found to be associated with RGS4 expression and schizophrenia diagnosis in multiple populations (Campbell et al., 2008; Chen et al., 2004; Chowdari et al., 2008; Chowdari et al., 2002; Guo et al., 2006; Prasad et al., 2005; So et al., 2008; Williams et al., 2004). Aside from schizophrenia, RGS4 mRNA levels and SNVs have been linked with Alzheimer’s Disease (Emilsson et al., 2006) and alcoholism (Ho et al., 2010). RGS4 is associated with Parkinson’s Disease development, via decreased regulation of dopamine receptors and/or muscarinic acetylcholine receptors (Ding et al., 2006; Lerner and Kreitzer, 2012; Min et al., 2012), although results are varied (Ashrafi et al., 2017). In dopamine-depleted mice, a mouse model for Parkinson’s Disease, RGS4 is upregulated and inhibits M4 muscarinic auto receptors, an effect which is mimicked by RGS4 infusion onto untreated cells (Ding et al., 2006).

1.3.2 The R7 family

The R7 family of RGS proteins is composed of RGS6, RGS7, RGS9 and RGS11. These are highly homologous proteins mostly expressed in the nervous system where they have a role in neuronal G protein signaling controlling nociception, reward behavior, motor control, and vision (Anderson et al., 2009; Gerber et al., 2016; Gold et al., 1997). The R7 RGS proteins contain distinctive domains that form stable stoichiometric heterotrimeric complexes with accessory binding partners that control protein-protein

interaction, subcellular localization, and protein stability (Anderson et al., 2009; Sjogren, 2011). Besides the canonical RGS domain, other domains include the disheveled EGL10-Pleckstrin homology (DEP) domain, an R7 homology domain, and a G protein γ subunit-like (GGL) domain (Ahlers et al., 2016; Gerber et al., 2016; Gold et al., 1997; Sjogren, 2011). The RGS domain is located at the C terminus, where it stimulates GTP hydrolysis on *G α /o* protein subunits (Anderson et al., 2009; He et al., 2000; Hooks et al., 2003; Martemyanov and Arshavsky, 2004; Masuho et al., 2013; Posner et al., 1999; Snow et al., 1998b; Stewart et al., 2015). The GGL domain, located upstream from the RGS domain, is structurally homologous to conventional γ subunits of G proteins (Anderson et al., 2009; Posner et al., 1999) and binds G β 5 (type 5 G protein β subunit) as an obligatory partner (Anderson et al., 2009), which is crucial for protein stability (Anderson et al., 2009; Gerber et al., 2016; Sjogren, 2011; Snow et al., 1998b). Consistent with the brain expression patterns of R7 family members, various neurological conditions such as anxiety, schizophrenia, drug dependence, and visual complications have been linked with the function of these proteins.

1.3.3 The RZ family

The RZ family is composed of RGS17, RGS19 and RGS20. These all are small simple RGS proteins like the R4 family members. However, unique to the RZ family members is a conserved string of cysteine residues found near their N-termini that is palmitoylated and regulates both their membrane localization and interaction with binding partners (De Vries et al., 1996; Nunn et al., 2006). RZ proteins also function as adapter proteins for G α subunit degradation and play important roles in the regulation of

signaling and cytoskeletal events in the brain (Mao et al., 2004). All members of this family can bind to certain members of the Gai and Gaq subfamily, but with some selectivity (Glick et al., 1998; Mao et al., 2004; Tu et al., 1997).

1.3.4 The R12 family

The R12 family is a diverse group of RGS proteins, consisting of three members: RGS10, RGS12, and RGS14. Each has its own unique structure and function but share a conserved RGS sequence and dynamic nuclear shuttling (Burgon et al., 2001; Chatterjee and Fisher, 2002; Cho et al., 2005; Shu et al., 2007a; Waugh et al., 2005). While RGS10 is a small, simple RGS protein that resembles the R4 family members, RGS12 and RGS14 have larger and more complex structures that share homology. Both RGS12 and RGS14 contain accessory domains, including two tandem Ras/Rap-binding domains (R1 and R2) and a G protein regulatory (GPR) motif. The R1 domains of RGS12 and RGS14 each interact with small G proteins such as Rap2 and H-Ras to regulate MAPK signaling (Shu et al., 2010; Traver et al., 2000b; Vellano et al., 2013a; Willard et al., 2009). The GPR motif binds inactive (as opposed to active GTP-bound) G α proteins and serves as an inhibitor of GDP release (Kimple et al., 2001; Kimple et al., 2002; Kimple et al., 2004; Mittal and Linder, 2004) and also a regulator of RGS protein subcellular localization and membrane attachment (Brown et al., 2015; Shu et al., 2007a). RGS12 is expressed in humans as multiple splice variants (Chatterjee and Fisher, 2000), the longest of which (called Trans-Spliced, "RGS12-TS") contains two additional domains: a PDZ domain and a PTB domain. PDZ domains are important regulators of localization and interaction with binding partners (Dunn and Ferguson, 2015). For example, RGS12-

TS binds to CXCR2 via its PDZ domain (Snow et al., 1998a) as a means of directing to its target signaling partners. The PTB domain binds phosphotyrosines, and one report demonstrated that the PTB domain of RGS12 can attenuate PDGF-induced pERK (Sambi et al., 2006). The demonstrated roles of these accessory domains are important to consider in RGS protein function/regulation beyond the canonical RGS domains highlighted in our review here.

RGS10, at 20 kDa, is one of the smallest RGS family proteins, and is highly expressed in the brain and immune system (Gold et al., 1997; Haller et al., 2002). In humans, there are three splice variants of RGS10, differing by only a few amino acids at the N-terminus. However, these small differences can have a substantial effect on RGS10 function, as the shortest splice variant (lacking only 14 amino acids) has impaired GAP activity (Ajit and Young, 2005). RGS10 is also dynamically regulated within the cell. Palmitoylation of an N terminal cysteine targets RGS10 to the plasma membrane and enhances its GAP activity (Tu et al., 1999), while phosphorylation of a C terminal serine targets RGS10 to the nucleus and impedes its GAP activity (Burgon et al., 2001). RGS10 has been documented in the nuclei of microglia and neurons (Waugh et al., 2005), where it may serve to regulate neuroinflammation. Indeed, RGS10 has been shown to promote survival of dopaminergic neurons via regulation of neuroinflammatory pathways in nigrostriatal circuits (Lee et al., 2011; Lee et al., 2008), implicating a neuroprotective role for RGS10 in dopaminergic disorders such as Parkinson's Disease (Tansey and Goldberg, 2010). Interestingly, a polymorphism (V38M or V44M in canonical sequence) in RGS10 was found in Japanese patients with Schizophrenia, but it was not found to be significantly associated with disease due to sample size (Hishimoto et al., 2004). In

peripheral immune cells, RGS10 regulates macrophage activation (Lee et al., 2013b) and platelet activation (Hensch et al., 2016) and T lymphocytes (Lee et al., 2016), with potential roles in clotting or autoimmune diseases. Additionally, loss of RGS10 in aged mice is linked with dysregulated peripheral immune cells and inflammatory cytokines (Kannarkat et al., 2015). Last, there is a curious link between RGS10 and chemoresistant ovarian cancer (Ali et al., 2013; Cacan et al., 2014; Hooks et al., 2010; Hooks and Murph, 2015), potentially via a Rheb-GTP/mTOR pathway (Altman et al., 2015). A comprehensive review of the roles of RGS10 in neurons and immune cells was recently published (Lee and Tansey, 2015).

1.4 REGULATOR OF G PROTEIN SIGNALING 14 IN PHYSIOLOGY

1.4.1 RGS14 is a multifunctional signaling protein

The RGS domain is evolutionarily conserved among vertebrate and invertebrate species (Vatner et al., 2018). RGS14 specifically is conserved in vertebrates such as chimpanzee, rhesus monkey, dog, cow, mouse, rat, chicken, zebrafish, and frog, and in invertebrates as an early homologue (Homologene). In rodents, where RGS14 has been primarily studied, it is expressed in brain, heart, lungs, kidney, and spleen (Agudelo et al., 2018; Kardestuncer et al., 1998; Snow et al., 1997).

RGS14 is a complex multi-domain scaffolding protein that integrates G protein, mitogen activated kinase/extracellular regulated kinase (MAPK/ERK), and calcium signaling pathways (Harbin et al., 2021). RGS14 is highly selective to Gai/o through its canonical RGS domain (Cho et al., 2000b; Hollinger et al., 2001a; Traver et al., 2000b) but it also binds to other signaling partners (Figure 1.2). Through the tandem Rap/Ras

(R1/R2) binding domain (RBD) RGS14 interacts with monomeric G proteins Rap1 (Traver et al., 2000b), Rap2 (Traver et al., 2000b), H-Ras (Shu et al., 2010; Vellano et al., 2013a; Willard et al., 2009), and Raf kinases. In the heart, RGS14 diminishes myocardial remodeling and attenuates the development of cardiac remodeling through MEK-ERK1/2 signaling pathway (Li et al., 2016). Within the RBD domain RGS14 binds calcium/calmodulin (Ca²⁺/CaM) and Ca²⁺/CaM-dependent kinase II (CaMKII) (Evans et al., 2018b). The GoLoco/G protein regulatory motif (GPR) binds inactive Gαi1/3-GDP and recruits cytosolic RGS14 to the plasma membrane (Hollinger et al., 2001a; Kimple et al., 2001; Mittal and Linder, 2004).

Between the RGS and R1 domain a nuclear localization sequence (NLS) is found, while the nuclear export sequence (NES) is found within the GPR motif. RGS14 is a nucleocytoplasmic shuttling protein, its subcellular movement inside the cell is guided by the NLS, and its nuclear export is guided by XPO1 binding to the NES (Gerber et al., 2018a; Harbin et al., 2021). This shuttling movement has been reported in cultured cell lines and neurons (Branch and Hepler, 2017; Cho et al., 2005; Gerber et al., 2018a; Shu et al., 2007a; Squires et al., 2021). Studies looking at endogenous RGS14 in B35 neuroblastoma cells found that it localizes to juxtannuclear membranes encircling the nucleus, at the nuclear pore complexes on both sides of the nuclear envelope, within intranuclear membrane channels, and within both chromatin-poor and chromatin rich-regions of the nucleus in a cell cycle dependent manner (Branch and Hepler, 2017). Interestingly, recent studies have looked at human RGS14 genetic variants and how these affect RGS14 shuttling function in neurons.

Human genetic variants L505R and R507Q are located within the nuclear export sequence of RGS14 (Squires et al., 2021). These mutations affect binding to Gα1-GDP and XPO1, thus affecting normal nuclear localization. RGS14 WT localizes to the soma, dendrites, and spines of neurons while L505R concentrated in the nucleus, and R507Q exhibits a mixed phenotype (Squires et al., 2021). In addition, phosphorylation independent binding partner 14-3-3, inhibits RGS14 nuclear import and nucleocytoplasmic shuttling in neurons (Gerber et al., 2018a).

Interestingly, human, primate, and ovine RGS14 contain an extra sequence of amino acids after the GPR motif that code for the carboxy-terminal class I PDZ-recognition sequence. Recent studies in kidney physiology have shown human RGS14-PDZ motif to bind scaffolding protein NHERF1 that binds to sodium phosphate cotransporter 2a (NPT2A) and mediates renal phosphate transport (Friedman et al., 2022). Presence of human RGS14 stabilizes NPT2A-NHERF1 complex, acting as a regulator of parathyroid hormone (PTH) sensitive phosphate transport (Friedman et al., 2022).

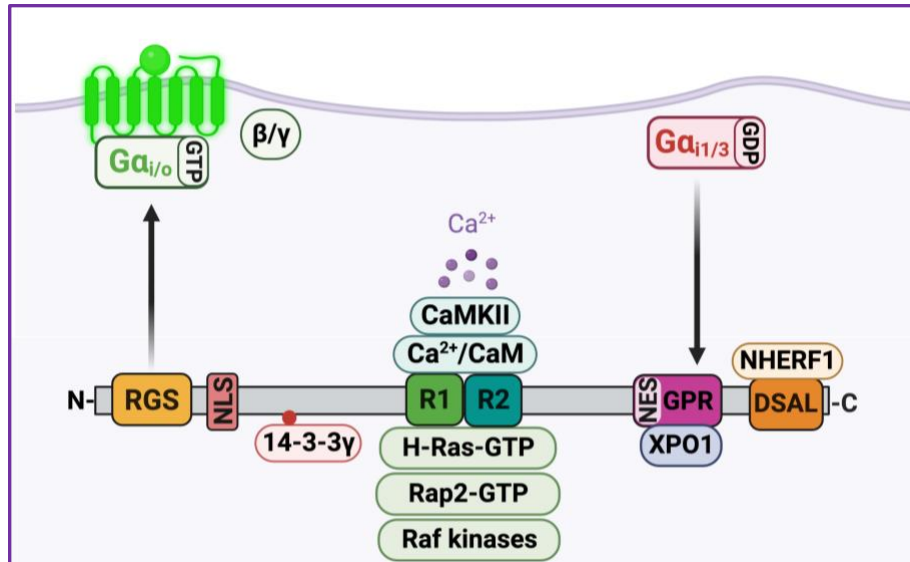


Figure 1.2 Human RGS14 structure: domains, motifs, and binding Partners.

RGS14 is a complex multifunctional signaling protein that contains multiple domains and motifs. The RGS (Regulator of G protein Signaling) domain binds active G α i/o-GTP to catalyze the GTPase activity of the G α subunit. The NLS (Nuclear Localization Sequences) motif and translocate RGS14 into the nucleus. Binding partner 14-3-3 γ binds to RGS14 in a phosphorylation dependent manner at serine 218 disrupting RGS14 interaction with active G α i at the plasma membrane. R1 and R2 are the tandem Ras/Rap binding domains where active H-Ras-GTP, Rap2A-GTP and Raf kinases bind at the R1 domain. Within the RBD domain RGS14 binds calcium/calmodulin (Ca $^{2+}$ /CaM) and Ca $^{2+}$ /CaM-dependent kinase II (CaMKII). The GoLoco/G α protein regulatory motif (GPR) binds inactive G α i1/3-GDP and recruits cytosolic RGS14 to the plasma membrane. The NES (Nuclear Export Sequence) binds XPO1 and guides RGS14 outside of the nucleus. The PDZ motif (DSAL) binds NHERF1 that binds to sodium phosphate cotransporter 2a (NPT2A) and mediates renal phosphate transport.

1.4.2 The role of RGS14 in the brain

RGS14 protein expression has been reported in rodent brain, heart, lung, kidney, and spleen (Agudelo et al., 2018; Kardestuncer et al., 1998; Snow et al., 1997). While recent studies have identified roles for RGS14 in heart (Li et al., 2016), adipocytes (Vatner et al., 2018), and kidney (Friedman et al., 2022), most studies of RGS14 have centered on understanding its role in the brain. Within brain, RGS14 is highly expressed in the hippocampus, most notably area CA2. RGS14 protein is undetectable in brain at birth but is upregulated during early postnatal development being detected at P7 and reaching highest persistent expression levels in adulthood (Evans et al., 2014). Within rodent hippocampal area CA2, RGS14 has been reported in pyramidal neurons specifically within postsynaptic dendrites and spines of pyramidal neurons (Evans et al., 2014; Lee et al., 2010a; Traver et al., 2000b).

The hippocampus plays a crucial role in many aspects of learning and memory including episodic, spatial, object recognition, social and contextual memory (Bird and Burgess, 2008; Broadbent et al., 2010; Broadbent et al., 2004; Evans et al., 2015; Harbin et al., 2021; Tzakis and Holahan, 2019). Neurons of the hippocampus have a robust capacity to express plasticity. Long term potentiation (LTP) is the stable increase in synaptic strength in responses to brief periods of synaptic stimulation that is very prominent in the hippocampus (Bliss-Moreau et al., 2011; Collingridge et al., 2004; Lynch et al., 1990). LTP is a cellular correlate and underlying mechanism of memory formation and storage (Bliss-Moreau et al., 2011; Collingridge et al., 2004; Evans et al., 2015). Area CA3-derived Schaffer collateral synapses on CA2 neurons lack the capacity to produce LTP, where RGS14 is highly expressed. However, knock-out mice lacking

RGS14 in area CA2 gain capacity for high-frequency stimulation (LTP) that was absent before, showing that RGS14 is a natural break on LTP (Evans et al., 2018d; Harbin et al., 2021; Lee et al., 2010a)

To test the effect of presence or absence of RGS14 in hippocampal based learning and memory two key mouse behavior studies were performed. First, declarative memory was measured using a novel object recognition test (Ennaceur and Delacour, 1988). When comparing signs of object recognition between WT and KO RGS14 mice, RGS14 KO spent more time exploring and contacting the novel object than WT mice (Lee et al., 2010a). Next, spatial learning was tested using the Morris water maze. This test utilizes visual cues as a guide for rodents to find a submerged platform while they navigate the swim arena (Vorhees and Williams, 2006). Both RGS14 WT and KO littermates learned the task, but RGS14-KO mice showed a significantly enhanced (and unexpected) initial learning rate that was sustained each day (Lee et al., 2010a).

Synaptic plasticity is often described in terms of changes in synaptic strength. However, plasticity also is associated with structural changes within the spine (Bernardinelli et al., 2014). Synaptic stimulation resulting in LTP induces an enlargement of dendritic spines that results from the parallel trafficking of AMPA-containing vesicles and their insertion into postsynaptic spines (Matsuzaki 2004, Nishiyama and Yasuda 2015). RGS14 is enriched in spines and dendrites and is thus well situated to play a role in structural plasticity. To explore RGS14 roles in structural plasticity, studies examined induced spine plasticity in CA1 and CA2 pyramidal neurons (Evans et al., 2018d). Hippocampal slices from RGS14 KO and WT mice expressing EGFP were subjected to two-photon glutamate uncaging and imaged using two-photon fluorescence microscopy.

RGS14 was found to negatively regulate long-term structural plasticity of dendritic spines in CA2 neurons (Evans et al., 2018d). Loss of RGS14 (KO) resulted in a large increase in structural volume change when compared to wild type (WT) mice (Evans et al., 2018d). CA2 neurons lacking RGS14 also displayed significantly enhanced spine calcium transients during plasticity induction compared to wild type control mice. Of note, viral delivery of RGS14 to CA2 neurons rescued the WT phenotype (no plasticity) whereas RGS14 delivery to CA1 neurons blocked normal plasticity there. Together, these findings indicate that RGS14 plays a vital role in synaptic plasticity by regulating synaptic strength and structural plasticity, in part, by restricting calcium in CA2 spines (Evans et al., 2018d).

Based on these findings, we speculate that the absence of RGS14 during early postnatal development (until P7) may allow for a period of enhanced learning and linked plasticity that enable pups to develop social recognition. Social recognition memory in animals is essential for social hierarchy, mate and offspring recognition, territorial defense, interspecies recognition, and for the general establishment and maintenance of groups (Ferguson et al., 2002; Tzakis and Holahan, 2019). The absence of RGS14 may lead to enhanced plasticity in CA2 that allows pups to connect with their environment and form strong bonds with their littermates and maternal bonding. After P7, the upregulation of RGS14 and its sustained expression throughout adulthood may serve to filter episodic memories, creating a period to develop new synapses that are structured based on environmental cues. Further studies will be needed to test these ideas.

RGS14 in primate brain has not been extensively explored, however recent studies have characterized the expression of RGS14 in adult rhesus macaques and humans (Squires et al., 2018a). In the rhesus macaque brain, RGS14 immunoreactivity was found

in hippocampus much like rodents, but also was highly expressed in other limbic structures and the basal ganglia. Strong immunoreactivity was observed in the caudate nucleus, putamen, substantia nigra pars reticulata, globus pallidus, and moderate staining in the amygdala (Squires et al., 2018a). RGS14 also is expressed in these brain structures in rodents (Foster et al., 2021) and speculation about RGS14 roles in these brain regions and their relationship to the hippocampus will be discussed in depth below.

Within the primate hippocampus, RGS14 was robustly expressed in CA2 and CA1 regions, but absent in CA3 and the dentate gyrus (Squires et al., 2018a). Consistent with protein expression in rodent CA2, RGS14 was found in pyramidal cell bodies and dendrites. In contrast to rodent CA1 region that shows a discrete expression of RGS14 (Lee et al., 2010a), strong RGS14 expression was found in the neuropil pre and postsynaptic profiles, pyramidal cell bodies, and proximal dendritic profiles (Squires et al., 2018a).

Neurologically healthy post-mortem human brains showed a strong RGS14 expression in pyramidal cells of CA2 and CA (Squires et al., 2018a). In contrast, RGS14 was absent in human hippocampal area CA3 (Squires et al., 2018a). Interestingly, the neuropil staining in human CA1 and CA2 was lighter than the monkey brain (Squires et al., 2018a). This phenomenon could be explained by protein degradation during post-mortem delay and immersion fixations of the tissue (Squires et al., 2018a).

Overall, RGS14 expression in human hippocampus is consistent with what is reported for rodent and monkey brain. Monkey and human brain show a strong expression of RGS14 in pyramidal neurons of area CA2 consistent with the rodent brain (Squires et al., 2018a). Strong immunoreactivity is found in cellular and neuropil of

primate CA1, specifically in glutamatergic terminals that originate from CA2 axonal projections, cell bodies, dendrites, and spine of pyramidal neurons (Squires et al., 2018a). However, the presynaptic functions of RGS14 in CA1 remain unexplored.

1.4.3 The role of RGS14 outside of the brain

RGS14 exists in peripheral tissues as well, where it plays important role in physiology. RGS14 protein expression can be found in ventricular tissue of healthy and hypertrophic mice (Li et al., 2016). In humans, RGS14 mRNA is found in the ventricular myocardium of patients with dilate and ischemic cardiomyopathy (Mittmann et al., 2002; Zhang and Mende, 2011), and RGS14 protein is detected in the left ventricle of healthy patients and those with dilated cardiomyopathy (Li et al., 2016). A recent study elucidated RGS14 role in the heart where is found to be downregulated in human failing hearts, murine hypertrophic hearts, and isolated hypertrophic cardiomyocytes (Li et al., 2016). Interestingly, its overexpression alleviated cardiac hypertrophy and dysfunction, suggesting RGS14's involvement in cardiac remodeling signaling through the MEK-ERK1/2 pathway (Li et al., 2016).

Another emerging area of RGS14 peripheral action is the kidney. Recent GWAS studies have identified single nucleotide polymorphisms (SNPs) within the RGS14 gene locus associated with kidney dysfunction (Chen et al., 2019; Mahajan et al., 2016; Urabe et al., 2012). Subjects with genetic polymorphisms within and outside the RGS14 gene locus have higher susceptibility to nephrolithiasis (Chen et al., 2019; Guan et al., 2020; Long et al., 2018a; Urabe et al., 2012; Yasui et al., 2013), reduced glomerular filtration rates (Mahajan et al., 2016), and elevated levels of serum phosphate (Kestenbaum et al.,

2010), all of which are indicative of kidney dysfunction (Brown and Razzaque, 2015). Additionally, SNPs within the RGS14 gene are associated with elevated levels of parathyroid hormone (PTH) (Robinson-Cohen et al., 2017) and fibroblast growth factor 23 (FGF23) (Robinson-Cohen et al., 2018), which are both critical for proper kidney function (Silver et al., 2012). Supporting this data, we have determined RGS14 expression in the kidney is high in human tissue, specifically in the proximal and distal tubule of the nephron (Friedman et al., 2022) further suggesting a role for RGS14 in kidney function and disease.

Much less is known about RGS14 role in the immune system. RGS14 RNA and protein is found in mouse lymphoid tissue and cells, including thymus, spleen, lymph node, peritoneal cells, white blood cells, naïve B cells and bone marrow cells (Beadling et al., 1999; Cho et al., 2000a; Reif and Cyster, 2000; Snow et al., 1997), where it is downregulated in response to B lymphocyte stimulation (Reif and Cyster, 2000). RGS14 is also expressed in THP-1 human monocytes/macrophages and in J774.A1 mouse macrophages, where it acts on α MB2 integrin during phagocytosis through the RBD domain of RGS14 (Lim et al., 2013). Recent transcriptome analysis of myeloid cells and microglia from brain revealed RGS14 mRNA expression in subsets of brain-derived myeloid cells (Bennett et al., 2016; Zhang et al., 2014), indicating a role for RGS14 in immune function in the central nervous system as well as the periphery.

Recent studies reported RGS14 expression in mouse subcutaneous/inguinal white adipose tissue (Agudelo et al., 2018; Vatner et al., 2018). Surprisingly, loss of RGS14 expression in mice leads to a reduction in white adipose tissue and increase in brown adipose tissue, resulting in improved metabolism and extending lifespan (Vatner et al.,

2018). However, the mechanism of enhanced longevity in RGS14-KO mice and body regions where RGS14 could be regulating metabolism and ageing remains unknown.

Goals of my research project

Although studies from our lab have focused mostly on understanding the role of RGS14 in synaptic signaling, I have focused on studying how RGS14 can modulate cell signaling outside of the brain in humans and the impact of genetic variation on RGS function.. Cell signaling plays a critical role in health and disease and abnormal regulation of these signaling events can lead to serious health problems. Considering the complexity of the GPCR-G-RGS signaling cascade, a slight change due to a genetic mutation can corrupt the cascade flow by disrupting protein function and cellular homeostasis. Recent GWAS (Genome-Wide Association Studies) have identified RGS14 point mutations to be associated to multiple diseases, most notably kidney dysfunction. In addition, The Catalogue of Somatic Mutations in Cancer (COSMIC) has reported RGS14 point mutations in human cancer samples. Here, I explore the role of RGS14 in cell signaling and the effect of naturally occurring mutants in renal pathophysiology and signal transduction in cancer by disrupting the cellular homeostasis.

CHAPTER 2: FUNCTIONAL ASSESSMENT OF CANCER-LINKED MUTATIONS IN SENSITIVE REGIONS OF RGS PROTEINS PREDICTED BY 3DMTR ANALYSIS

This chapter has been assembled in part from the accepted manuscript:
Montanez-Miranda C, Perszyk RE, Harbin NH, Okalova J, Ramineni S, Traynelis SF, Hepler JR (2022). **Functional assessment of cancer-linked mutations in sensitive regions of RGS proteins predicted by 3DMTR analysis.** *Mol. Pharm.*

2.1 ABSTRACT

Regulators of G protein signaling (RGS) proteins modulate G-protein coupled receptor (GPCR) signaling by acting as negative regulators of G proteins. Genetic variants in RGS proteins are associated with many diseases, including cancers, although the impact of these mutations on protein function is uncertain. Here we analyze the RGS domains of 15 RGS protein family members using a novel bioinformatic tool that measures the missense tolerance ratio (MTR) using a three-dimensional (3D) structure (3DMTR). Subsequent permutation analysis can define the protein regions that are most significantly intolerant ($P < 0.05$) in each dataset. We further focused on RGS14, RGS10, and RGS4. RGS14 exhibited seven significantly tolerant, and seven significantly intolerant residues; RGS10 had six intolerant residues; and RGS4 had eight tolerant and six intolerant residues. Intolerant and tolerant-control residues that overlap with pathogenic cancer mutations reported in the COSMIC cancer database were selected to define the functional phenotype. Using complimentary cellular and biochemical approaches, proteins were tested for effects on GPCR- $G\alpha$ activation, $G\alpha$ binding properties, and downstream cAMP levels. Identified intolerant residues with reported cancer-linked mutations RGS14-R173C/H and RGS4-K125Q/E126K, and tolerant RGS14-S127P and RGS10-S64T resulted in a loss-of-function phenotype in GPCR-G protein signaling activity. In downstream cAMP measurement, tolerant RGS14-D137Y and RGS10-S64T, and intolerant RGS10-K89M resulted in change of function phenotypes. These findings show that 3DMTR identified intolerant residues that overlap with cancer-linked mutations cause phenotypic changes that negatively impact GPCR-G

protein signaling and suggests that 3DMTR is a potentially useful bioinformatics tool for predicting functionally important protein residues.

Significance Statement Human genetic variant/mutation information has expanded rapidly in recent years, including cancer-linked mutations in RGS proteins. However, experimental testing of the impact of this vast catalogue of mutations on protein function is not feasible. We used the novel bioinformatics tool 3DMTR to define regions of genetic intolerance in RGS proteins and prioritize which cancer-linked mutants to test. We found that 3DMTR more accurately classifies loss-of-function mutations in RGS proteins than other databases thereby offering a valuable new research tool.

2.2 INTRODUCTION

Since the publication of the human genome and the development of bioinformatic sequencing tools, human genetic variant information is being identified rapidly. These advances led to the creation of many publicly available databases that reflect both healthy and diseased human populations. However, experimental testing of the vast catalogue of identified mutations is simply not feasible. Missense mutations are genetic variations where a single base pair substitution produces a different amino acid at the same position. Variations in protein structure can affect folding, stability and aggregation, thereby affecting the function of signaling proteins (Thusberg and Vihinen, 2009). Functionally relevant genetic variation has been reported in many proteins, including the regulators of G-protein signaling (RGS) (Squires et al., 2021).

RGS proteins play a vital role modulating G Protein Coupled Receptor (GPCR)-G protein signaling events. All RGS proteins share an evolutionary conserved RGS domain that binds active $G\alpha$ subunits and acts as GTPase accelerating proteins (GAPs), negatively regulating GPCR- $G\alpha$ signaling (Hollinger and Hepler, 2002; Tesmer et al., 1997a; Willars, 2006). Outside of their GAP function, RGS proteins competitively bind active $G\alpha$ and receptors to promote the rapid cycling of $G\alpha$ subunits between active and inactive states (McCoy and Hepler, 2009).

Recent deep sequencing studies have shown GPCR-G protein complexes to be frequently mutated in cancer (DiGiacomo et al., 2020; Kan et al., 2010; O'Hayre et al., 2013). GPCRs are expressed in cancerous tissues and mediate proliferation, survival, invasion, and metastasis (Gutkind, 1998; Hurst and Hooks, 2009). The pro-oncogenic effects of overexpressed constitutively activating mutations in GPCRs (DiGiacomo et al.,

2020; Moore et al., 2016; O'Hayre et al., 2013; Wright et al., 2019) and $G\alpha$ subunit, (DiGiacomo et al., 2020; Ideno et al., 2018; Nairismagi et al., 2016; Van Raamsdonk et al., 2009; Van Raamsdonk et al., 2010; Wu et al., 2011) have led to enhanced downstream signaling in reported cancer studies. Cancer-derived activated mutations in $G\alpha_o$ can induce oncogenic transformation (Garcia-Marcos et al., 2011), while inactivated mutations in $G\alpha_i/o$ -receptors can lead to enhanced cAMP activity (Chaudhary and Kim, 2021). These studies suggest that the loss of $G\alpha$ binding and GAP function in RGS proteins can promote oncogenic activity.

Multiple sequence-based analytical tools provide information and predictions about evolutionary conserved areas of a protein that are vital for structure and function (Nobrega and Pennacchio, 2004). Interestingly, sequence-based tools, like missense tolerance ratio (1DMTR) (Traynelis et al., 2017) and SIFT, access the same genetic variant databases to run their algorithms but interpret the predictive effect of a mutation in different ways. Recently, a novel tool known as 3DMTR permutation analysis (3DMTR) (Perszyk et al., 2021) has been developed but not yet widely tested. The improved 3DMTR algorithm calculates the missense tolerance ratio for the neighboring residues in three-dimensional (3D) distance from protein crystallography or cryo-EM data.

RGS proteins are divided in subfamilies based on sequence homology and other shared domains (Hepler, 1999; Sjogren and Neubig, 2010; Stewart and Fisher, 2015; Willars, 2006). Here we analyzed the RGS domains of 15 RGS proteins with reported structures, and focused on assessing three RGS proteins in particular: RGS14, RGS10 and RGS4. RGS14 and RGS10 are members of the D/R12 family. RGS14 is a complex multidomain signaling molecule selective for $G\alpha_i/o$ (Cho et al., 2000b; Vellano et al.,

2011a) and is highly expressed in brain regions essential for learning and memory (Harbin et al., 2021). RGS10 is a smaller molecule that selectively binds Gai/o members (Hunt et al., 1996; Popov et al., 1997; Watson et al., 1996). In contrast to RGS14, RGS10 is broadly expressed making it an essential regulator of physiological processes including inflammatory responses and survival signaling (Alqinyah et al., 2018). Much smaller than RGS14, RGS4 is part of the R4 subfamily and is highly expressed in brain where it has been linked to psychiatric disorders (Schwarz, 2018; Terzi et al., 2009), and in opioid reward and addiction (Sakloth et al., 2020). RGS4 is selective for Gai/o and Gaq members (Hepler et al., 1997; Tesmer et al., 1997a), preferring signaling by Gai/o over Gaq in a neuronal model (Masuho et al., 2020).

In the present study, we carry out a functional assessment of the predictive capabilities of the novel 3DMTR applied to RGS proteins. We combine this with available somatic mutational information found in cancer samples to determine the effect these genetic variants will have on RGS14/10/4 protein structure and function. We test how cancer mutations in significant regions of the protein can lead to changes in RGS function assessed by various cell based and biochemical assays.

2.3 MATERIALS AND METHODS

Three-dimensional missense tolerance with permutation analysis (3DMTR)

The 3DMTR permutation analysis is described in Perszyk, R.E. et. al. 20201 (Perszyk et al., 2021). To perform 3DMTR analysis on RGS protein structures, the encapsulated application MATLAB (Mathworks, version R2019b), available on GitHub (<https://github.com/riley-perszyk-PhD/3DMTR>, current version v2.000) was used. The protein structures of the analyzed RGS proteins were obtained from the Protein Data Bank (rcbs.org). Reference of all the crystal structures used is available in the supplementary section Table 1 (Supp. Table 1). Variant datasets of all RGS genes were downloaded from the Genome Aggregation Database (gnomAD) website (<https://gnomad.broadinstitute.org/>, version 2.1.1). The translated coding gene sequences of RGS proteins were used (RGS1, NM_002922.4; RGS2, NM_002923.4; RGS3, NM_144488.6; RGS4, NM_001102445.2; RGS5, NM_003617.4; RGS6, NM_001204416.3; RGS7, NM_001282773.2; RGS8, NM_033345.3; RGS9, NM_001081955.3; RGS10, NM_001005339.2; RGS12, NM_002926.3; RGS14, NM_006480.5; RGS16, NM_002928.4; RGS17, NM_012419.5; RGS18, NM_130782.3). The closest 21 residues were used in the 3DMTR calculations since the RGS protein domain structures are small (~120 residues) to provide more stratified scores. Permutation analysis was performed using 1000 iterations by randomizing the residue location. Permutation significance was determined where the 3DMTR score was outside the 2xSTD range (permutation standard deviation of each residue) calculated from the permutation mean score for each residue. We define the residues that are identified with permutation analysis as either significantly intolerant or significantly tolerant depending

on which tail of the permutation distribution they fall within. Additionally, having an MTR score of < 0.5 is very rare (the 5%ile score for the 1DMTR is 0.5462, <http://mtr-viewer.mdhs.unimelb.edu.au/>). Previous work suggests that the 3DMTR and the 1DMTR generally produce a similar set of MTR scores, albeit the scores are rearranged based on the different selection criteria, so we believe this cut off is also appropriate for the 3DMTR scores. Thus, we deem the residues with 3DMTR scores ≤ 0.5 as being important and will call highly intolerant.

Cell culture and reagents

Human embryonic kidney (HEK) 293 cells were cultured in 1X Dulbecco's Modified Eagle's Medium (DMEM), without phenol red indicator, supplemented with 10% fetal bovine serum (FBS), 2mmol/L L-glutamine, 100 units/mL penicillin, and 100 mg/mL streptomycin. HEK cells were kept in a humidifier incubator with 5% CO₂ at 37°C. Trypsin-EDTA 0.25% was used during cell culture procedures. Cells were seeded 8×10^5 in 2 mL of transfection medium per well in six-well plates. Transfection media was formulated with 5% FBS in DMEM phenol-red free media and polyethyleneimine (PEI) was the transfection agent used.

The Hemagglutinin (HA) epitope-tagged $\alpha 2a$ -adrenergic receptor (HA- $\alpha 2a$ -AR) construct was kindly provided by Dr. Joe Blumer (Medical University of South Carolina). The G protein used in our studies were Glu-Glu tagged G α (G α -EE) and the pertussis-resistant mutant C351G of G α (G α -CG) which was purchased from the cDNA Resource Center (cDNA.org, Bloomsberg, PA). Mas-GRK3ct-Luc and Ven-G $\beta\gamma$ were described previously (Hollins et al., 2009). Human Flag-tagged RGS14 (Flag-RGS14 WT), human

Flag-RGS14-S127P, human Flag-RGS14-D137Y, human Flag-RGS14-R173C, human Flag-RGS14-R173H, human Flag-tagged RGS10 wildtype (Flag-RGS10 WT), human Flag-RGS10-S64T, human Flag-RGS-K89M, hemagglutinin epitope-tagged rat RGS4 wildtype (HA-RGS4 WT), rat HA-RGS4-K125Q, rat HA-RGS4-E126K, rat HA-RGS4-E135K were generated as previously described (Bernstein et al., 2004; Shu et al., 2007a). Pertussis toxin #181 was purchased from List Biological Laboratories, Inc (Campbell, CA). UK 14,304 was obtained from Sigma-Aldrich (U104, St. Louis, MO). Forskolin was obtained from Sigma-Aldrich (F6886, St. Louis, MO).

Kinetic Bioluminescence Resonance Energy Transfer (BRET)

Kinetic BRET experiments were performed as previously described (Brown et al., 2016a; Lambert et al., 2010). After a 48 hr transfection, cells were resuspended in Tyrode's solution (140 mmol/L NaCl, 5 mmol/L KCl, 1 mmol/L MgCl₂, 1 mmol/L CaCl₂, 0.37 mmol/L NaH₂PO₄, 24 mmol/L NaHCO₃, 10 mmol/L HEPES, and 0.1% glucose, pH 7.4) and plated on white 96-well Optiplates (Perkin Elmer Life Sciences, Waltham, MA). Fluorescence measurements were made using the TriStar LB 941 plate reader (Berthold Technologies, Bad Wildbad, Germany) with 485-nm excitation and 530-nm emission filters to confirm acceptor expression. After a 10 min application of 5 μ mol/L coelenterazine H (Nanolight Technologies, Pinetop, AZ), *in vivo* kinetic BRET was recorded using sequential measurements through 485- and 530-nm emission filters. BRET was recorded for 30 seconds with no stimulation to establish basal BRET. After 30 seconds of basal BRET recording, α 2A-adrenergic receptor agonist UK 14,304 (100 μ M) was injected into the cells. The presence of the agonist induces G α protein activation and

the change in BRET is calculated by dividing the mas-GRK3ct-Luc signal (530 nm) by the Ven-G $\beta\gamma$ signal (485 nm) and subtracting the average BRET signal observed from the first 30 seconds of observation (basal BRET). With each experiment, a kinetic BRET control was performed using pertussis insensitive G α . Pertussis toxin was added to the transfection media to all wells. Any BRET signal recorded in the control wells transfected with pertussis sensitive G α was regarded as noise and subtracted from experimental kinetic BRET recordings. Data was collected using the MikroWin 2010 software (Mikrotek Laborsysteme GmbH, Overath, Germany) and analyzed using Microsoft Excel and GraphPad Prism 9.

Co-immunoprecipitation of RGS and G α

After a 24 hours transfection, HEK cells were washed three times with cold 1X PBS. Cells were scraped into AMF lysis buffer (50 mM Tris, 150 mM NaCl, 1 mM EDTA, 2 mM DTT, 10 mM NaF, 14 mM MgCl₂, 10 mM AlCl₃, 1X Roche protease inhibitor, 1X Halt phosphatase inhibitor) and lysed at 4°C for one hour while rotating end-over-end. Lysates were cleared by centrifuging at 13000 RPM for 10 min at 4°C. For each condition, 50 μ L of affinity gel beads were used. Anti-FLAG M2 affinity gel (Sigma A2220) was used to immunoprecipitated Flag-RGS14 and Flag-RGS10, while monoclonal anti-HA agarose beads (Sigma A2095) was used for HA-RGS4 immunoprecipitations. Affinity gel beads were washed three times with cold 1X PBS and then blocked with 4% BSA in PBS at 4°C for one hour while rotating end-over-end. Cleared cell lysate was collected for input, and the remaining lysate was added to blocked anti-FLAG M2 affinity beads or anti-HA agarose beads. Immunoprecipitation of Flag-tagged RGS from lysate was performed at

4°C for two hours while rotating end-over-end, while HA-tagged RGS was performed overnight. After immunoprecipitation, the beads-RGS complex was washed three times with cold 0.1% Tween-20 in PBS. Input and immunoprecipitated samples were denatured by boiling in Laemmli buffer for 5 min.

Analysis of immunoblots

Denatured cell lysate samples in Laemmli Buffer were resolved on 13.5% SDS-PAGE, and samples were then transferred to nitrocellulose membranes. Membranes were blocked in 5% non-fat milk for one hour at room temperature. For FLAG-tagged RGS (RGS10 WT and mutants, or RGS14 WT and mutants.), HRP-conjugated anti-FLAG antibody (Sigma A8592, 1:15,000) was diluted in TBS/T and incubated with the membranes for 45 minutes at room temperature. For HA-tagged RGS4 and mutants, Anti-HA-Peroxidase rat monoclonal antibody (Roche Cat# 12013819001, 1:5000) diluted in TBS/T was used. For Gαo, anti-EE (Covance MMS-115R, 1:1000) was diluted in 5% non-fat milk and incubated with membranes overnight at 4°C. HRP-conjugated goat anti-mouse IgG secondary antibody (Jackson ImmunoResearch 115-035-003, 1:5000) was diluted in TBS/T and incubated with membranes for 45 minutes at room temperature. Blots were developed using ECL and imaged using the ChemiDoc MP Imaging system (BioRad).

GloSensor™ cAMP assay

To measure intracellular cAMP levels, we used the GloSensor™ cAMP assay. The cAMP GloSensor™ was obtained from Promega and the assay was performed following

the manufacturer's instructions (Promega, Madison, WI, USA). HEK293 cells were harvested (15,000 cells per individual well) in tissue culture-treated 96-well flat bottom plate. Cells were kept in 37°C tissue culture incubator 5-10% CO₂ overnight. Cells were transfected with 50ng of pGloSensor-20F cAMP, 50ng α 2-AR, 50ng RGS of interest, and pcDNA in DMEM serum free media. After 24 hours, the media is removed without disrupting the cell monolayer and 100 μ L of the equilibrium medium is added (2% v/v dilution of the GloSensor cAMP Reagent stock solution). Incubation with the equilibration reagent is done for 2 hours and cells are kept in 37°C tissue culture incubator 5-10% CO₂ in the dark. After 2 hours, basal luminescence intensity was measured at 0 and at 5 minutes using a luminometer (FLUOstar) in triplicates. To measure α 2-AR-Gai/o directed inhibition of cAMP, cells are pre-incubated with 100 μ L of 100 μ M UK14,304 (agonist) or DMSO (vehicle) in HBSS for 10 minutes at room temperature following basal readings. At 10 minutes, cAMP production is stimulated by adding 10 μ M forskolin and luminescence is measured every 5 minutes for a total of 50 minutes. The data in relative light units (RLU) from triplicates wells were averaged and a response over time graph is generated. Normalization was done by dividing each time point following forskolin stimulation over basal luminescence, then each time point is divided by empty vector (50ng pcDNA alone) control. Area under the curve for each condition is calculated and the effect of the mutants is compared to the WT RGS effect in Gai/o-coupled α 2-AR stimulation of cAMP.

Data analysis and statistics

Data analysis was conducted using Microsoft Excel and GraphPad Prism 9 software. Kinetic BRET activation curves were presented as a mean of 3 or 4 experimental replicates. We then selected the maximum BRET amplitude at 100 seconds for each condition. Maximum BRET amplitude columns were compared by performing a statistical analysis using one-way analysis of variance (ANOVA) with Dunnett's test. Luminescence-based cAMP GloSensor assay relative light units (RLU) were recorded from averaged replicate wells and plotted as response over time, with a total of 4 experimental replicates. We then analyzed the area under the curve (AUC) for each condition and columns were statistically analyzed using one-way analysis of variance (ANOVA) with Dunnett's test.

2.4 RESULTS

3DMTR predicts amino acid residues in RGS proteins likely to be intolerant to mutation

RGS proteins share an evolutionary conserved ~120 amino acid RGS domain that binds activated G protein alpha subunits to act as GAPs. In this study, we examined the canonical human RGS proteins using a bioinformatic tool that evaluates the degree of variation that exists in the gnomAD database (large database of human whole exomes and genomes of healthy individuals) and determines a composite score, missense tolerance ratio (MTR) (Traynelis et al., 2017). This MTR score is determined based on the location of the linear polypeptide chain (1DMTR;(Traynelis et al., 2017)). A newly described bioinformatics tool expands on this idea to measures MTR based on the location of each residue in three-dimensional (3D) space (3DMTR;(Perszyk et al., 2021)) based on reported protein crystallography or cryo-EM data. This 3DMTR is a more accurate and improved bioinformatic tool that also utilizes a permutation analysis to calculate the relative significance of the missense tolerance ratio of a given dataset (Perszyk et al., 2021). Both 1DMTR and 3DMTR use available human variation data from neighboring residues to report population level genetic variation and measures the tolerance ratio within the entire genome.

A comparison of the 1DMTR and the 3DMTR analysis for the RGS domain of one representative RGS protein, RGS14, is shown as scatter plots in Fig. 2.1A and Fig. 2.1C. In a previous report (Squires et al., 2021), we described in detail the 1DMTR results for RGS proteins. Considering the RGS domain of RGS14 (Fig. 2.1A), the 1DMTR analysis of the RGS domain generally shows more tolerant scores (0/134 residues have 1DMTR

scores ≤ 0.5), which are shown as red shades superimposed onto the RGS domain structure (Fig. 2.1B). Structural data has been reported for the RGS domain of most RGS proteins, including RGS14 (Soundararajan et al., 2008). Using this information, we analyzed the RGS domains of 15 of 20 RGS protein family members, including RGS14, using the 3DMTR analysis (Supp. Fig. 2.1) as will be discussed further below. In contrast to 1DMTR, the 3DMTR uses the same human variation data but instead utilizing the neighboring residues in 3D space, which should be functionally more relevant to determine the tolerance ratio.

We analyzed the RGS domain of RGS14 by 3DMTR (Fig. 2.1C and 2.1D). Because the size of RGS domains (~120 aa) are much smaller than the entire RGS proteins (~200-1400 aa), the 3DMTR was calculated using the nearest 21 residues instead of the 31-residue window that has been used for larger proteins. Based on this, the 3DMTR may be a more accurate predictor of highly intolerant residues compared to the 1DMTR. We will refer to the residues that appear to have selective pressure controlling their variation as 'highly intolerant' (3DMTR score of ≤ 0.5). The 3DMTR analysis of the RGS domain of RGS14 identified several residues with highly intolerant scores (7/134 residues have 3DMTR scores ≤ 0.5 , Fig. 2.1C), shown in blue shades superimposed onto the RGS domain structure (Fig. 2.1D). Furthermore, we used permutation analysis that determines which residue scores are highly unlikely given a specific dataset (occurring in less than 5% of random permutations). It can be interpreted that the residues identified by permutation analysis that are either significantly intolerant or significantly tolerant, i.e. those that would be unexpected within each analyzed dataset (consisting of the gene sequence, protein structure, and gnomAD dataset). Primarily of note, the analysis

suggests that the significantly intolerant residues may relatively (compared to the rest of the residues in the protein) have selective pressures that limit variation in these regions. The permutation analysis of RGS14 (Fig. 2.1E) identified 14 residues that were significantly intolerant, whereas 3.4 would have been expected randomly given the dataset (based on the expected frequencies of a single tail of a normal distribution using α equal to 0.05, $0.025 * 134$ residues). Comparing the 1DMTR and 3DMTR data for RGS14, the 3DMTR analysis of the RGS domain of RGS14 predicts highly intolerant residues not found with the 1DMTR (0 with 1DMTR vs 7 with 3DMTR, total residues 134, Fisher's exact test $p = 0.0144$). The permutation analysis of RGS14 (Fig. 2.1E) identified 14 residues significantly intolerant, 7 residues highly intolerant (3DMTR score ≤ 0.5) and 7 tolerant (not highly intolerant) (3DMTR score > 0.5). The significantly intolerant residues are visualized in blue on the structure of the RGS domain of RGS14 (Fig. 1F).

Next, each RGS domain of all available structures for RGS protein family members were analyzed using 3DMTR (Fig. 2.2, Supp. Fig. 2.1). For this analysis, we utilized the reported structures of RGS protein domains that are available for 15 of the 20 RGS proteins (Supp. Fig. 2.1). Interestingly, each RGS domain presented a distinct "bar code" of significantly intolerant and significantly tolerant residues (Fig. 2.2 and Supp. Fig. 2.1). A second 3DMTR analysis was performed on four RGS protein domains in complex with active forms of their $G\alpha$ partners (Supp. Fig. 2.2: RGS1-Gai1, RGS4-Gai1, RGS10-Gai3 and RGS16-Gai1). In each of these cases, the profiles for significantly tolerant and intolerant residues differed slightly by active $G\alpha$ binding.

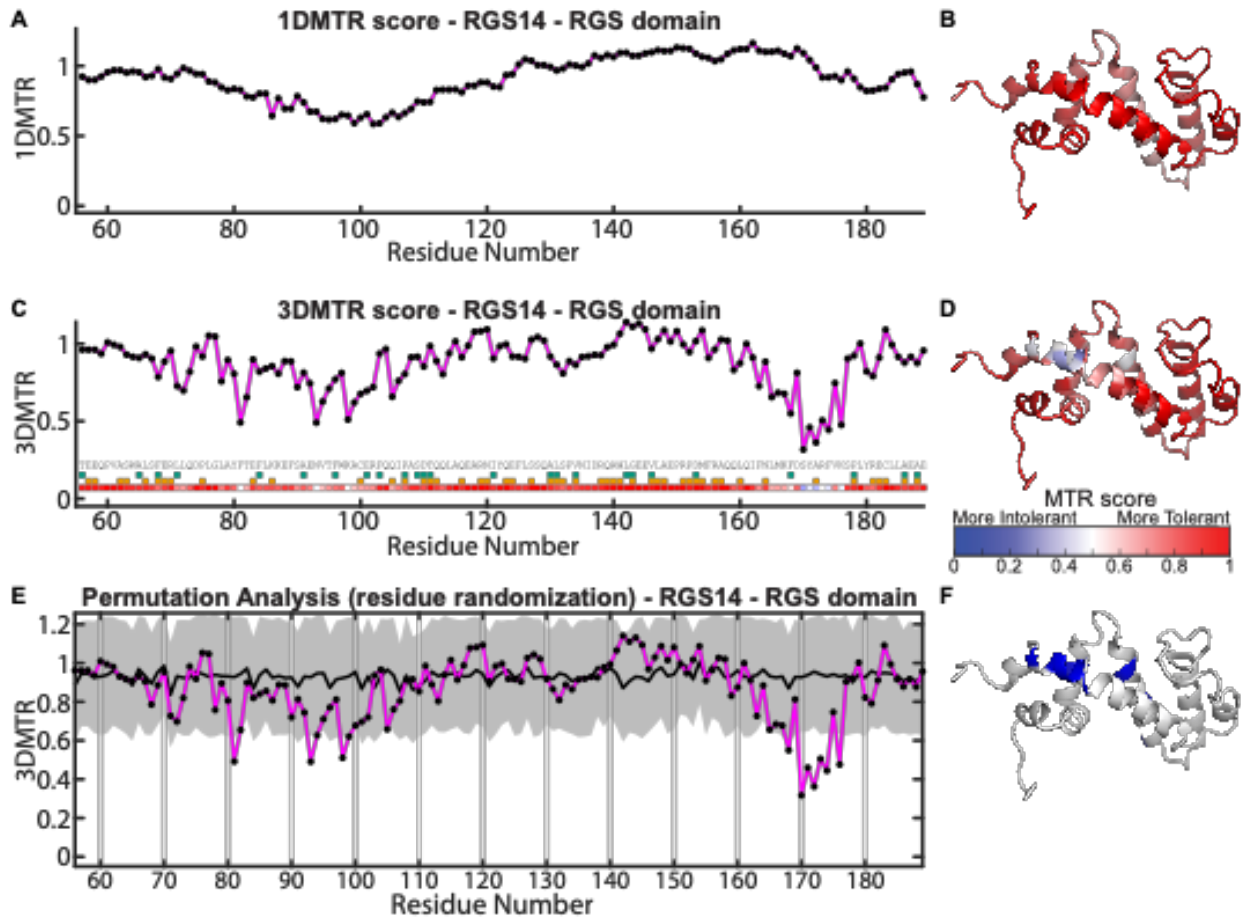


Figure 2.1. Comparison of RGS14 1DMTR and 3DMTR permutation analysis. (A) The sequential MTR score of RGS14 is calculated using gnomAD-derived human variants and is shown as a scatter plot. (B) Structural view of RGS domain of RGS14 colored to show a heatmap of the 1DMTR score (intolerant residues in blue, neutral in white, tolerant in red). (C) The MTR score of RGS14 taking into consideration three-dimensional space (3DMTR). Green squares represent a synonymous variant in that residue. Orange squares represent missense variant for the residue. Below is a linear heatmap of the MTR score for RGS14. (D) Structural view of RGS14 3DMTR raster plot scores. (E) Scatter plot of RGS14 3DMTR score (magenta line), permutation analysis score mean (black line), and 2x standard deviation around the permutation score mean

of the permutation analysis (gray areas). **(F)** Structural view of the permutation analysis raster plot significantly intolerant residues within RGS14.

We next compared the 3DMTR results for RGS14, RGS10 and RGS4. These three RGS proteins were chosen because of their involvement with various cancers and their differences in size and structure. Raster plots for RGS14 (Fig. 2.2A), RGS10 (Fig. 2.2B), and RGS4 (Fig. 2.2C) show the comparison of 1DMTR data with 3DMTR data calculated using the nearest 21 or 31 residues, as before. For each, tolerant (red) or significantly intolerant (blue) residues are shown (c21-sig). The 3DMTR analysis predicts intolerant residues not found with the 1DMTR analysis. As observed with the other RGS proteins (Supp. Fig. 2.1), the RGS domains of RGS14, RGS10, and RGS4, each presented a distinct “bar code” of significantly intolerant residues (Fig. 2.2 and Supp. Fig. 2.1-2.2).

As was the case for RGS14 (Fig. 2.1 and Fig. 2.2A), 3DMTR predicted for RGS10 more highly intolerant scores than 1DMTR (Fig. 2.2B) (1 with 1DMTR vs 7 with 3DMTR, total residues 136, Fisher’s exact test $p = 0.0663$) and for RGS4 (Fig. 2.2C) (1 with 1DMTR vs 6 with 3DMTR, total residues 128, Fisher’s exact test $p = 0.1199$). The structure of each of the RGS domains is shown with significantly tolerant and intolerant residues highlighted in red and blue, respectively (Fig. 2.2D-2.2I). Each is shown bound to the reported structure of *G α 1* (Fig. 2.2D and 2.2F), *G α 3* (Fig. 2.2E), or alone (Fig. 2.2G-2.2I). Comparison of the three RGS domain structures in the same orientation with the intolerant residues highlighted in blue (Fig. 2.2G-2.2I), shows that these residues are distributed differently within the domain structure. We next performed permutation analysis for the RGS domains of RGS10 and RGS4 (Supp. Fig. 2.3) and compared those to RGS14 (Fig. 2.1E).

The amino acid sequence for each of these RGS proteins are aligned (Fig. 2.2J). The RGS domain is highlighted in lilac, in gray are the residues that directly interact with

G α , and in orange the residues that are in the hydrophobic core (Tesmer et al., 1997a). The significant residues identified by the permutation analysis are identified with symbol under each residue letter, * for the identified residues that were also highly intolerant (MTR ≤ 0.5) and ^ for identified residues that were not highly intolerant residues (MTR > 0.5). As shown in Fig. 2.2J, the profiles of intolerant residues differ across each protein. 3DMTR identified highly intolerant residues found in the RGS hydrophobic core were residue F81 in RGS14, and I93 and F97 in RGS10. 3DMTR identified highly tolerant residues in RGS4 F91, W92 and I114 are also found in the hydrophobic core. Intolerant residues in the direct contact with G α in RGS14 are N93 and R173, and tolerant residues are RGS14-D137 and RGS4 E87 and N88. Compared with the permutation analysis for RGS14 (Fig. 2.1E), the same analysis of RGS4 identified 15 significantly intolerant residues, whereas 3.2 would have been expected randomly given the 128-residue dataset. The permutation analysis of RGS10 identified 5 residues that were significantly intolerant, whereas 3.4 would have been expected randomly given the 136-residue dataset.

We next focused on the significantly intolerant or tolerant residues in RGS14, RGS10 and RGS4 identified by the 3DMTR analysis that overlap with reported somatic pathogenic mutations found in patient cancer samples identified in the Catalogue of Somatic Mutations in Cancer (COSMIC) database (Table 2.1). Using various *in vitro* assays of RGS-G protein interaction and signaling, we test the effect of an amino acid change, due to cancer mutations, in the selected significant residues and how these affect canonical RGS function.

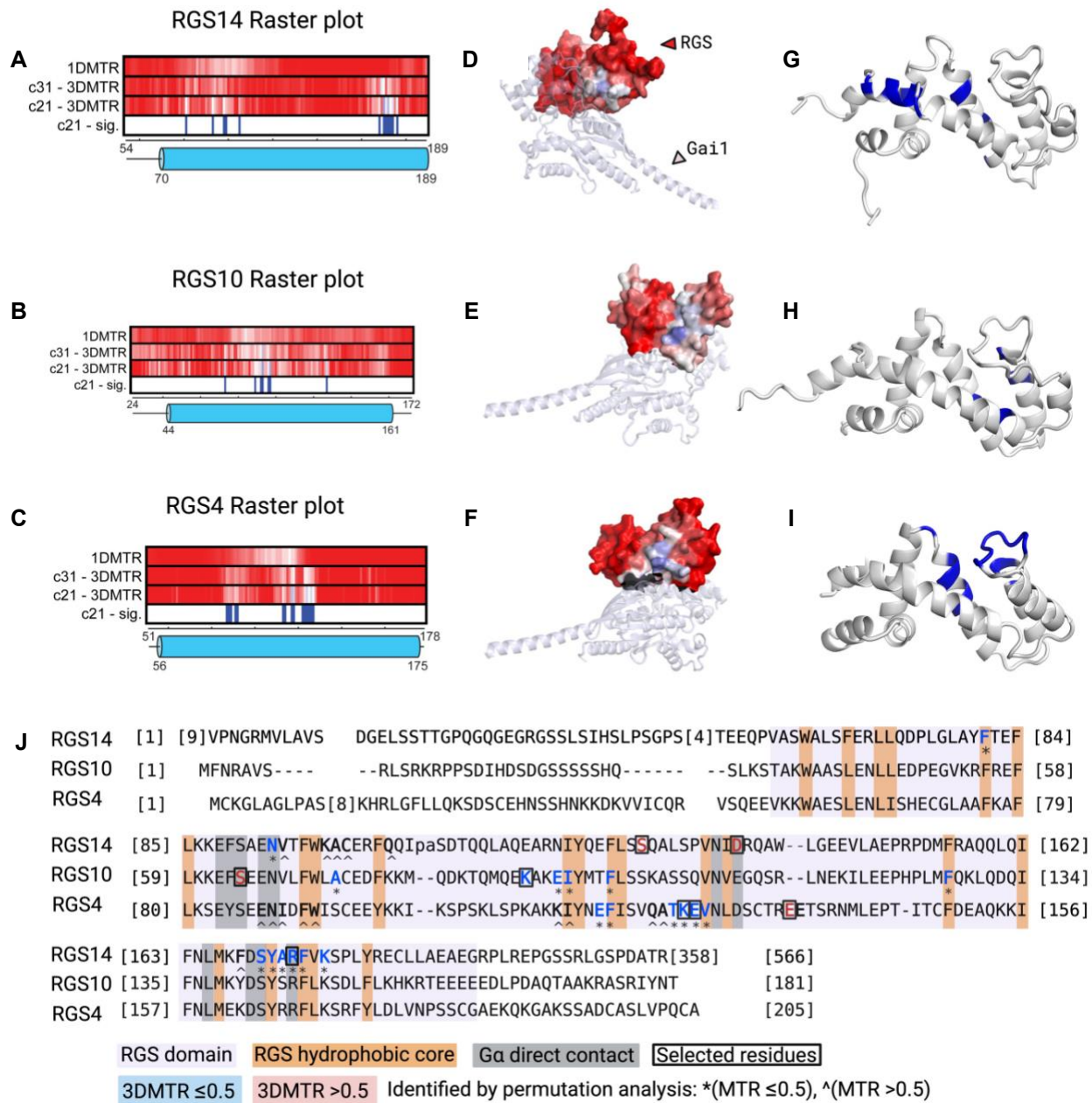


Figure 2.2. The 3DMTR permutation analysis identifies significantly intolerant residues within the RGS domain that were not identified by 1DMTR.

(A-C) Raster plot of selected RGS proteins comparing 1DMTR, 3DMTR based on the 31 neighboring residues, 3DMTR based on the 21 neighboring residues, and significantly intolerant residues based on the permutation analysis (rows labeled “c21-sig.”, labeled by a blue rectangle).

(D-F) Structural views of RGS domains colored to show a heatmap of the 21-residue 3DMTR score (intolerant residues in blue, neutral in white, tolerant in red) bound to G alpha. **(G-I)** Structural view of the 21-residue 3DMTR permutation analysis raster plot significantly tolerant/intolerant residues. **(J)** RGS protein alignment shows the RGS domain (lilac), residues in the hydrophobic core (yellow), residues in direct contact with G alpha (grey), and selected residues to test the functional consequences inside box. The residues with a 3DMTR score >0.5 are determined to be not highly intolerant (tolerant) and the color letter is red. Residues with a 3DMTR score ≤ 0.5 are determined to be highly intolerant and the color letter is blue. Residues identified via the permutation analysis are identified with symbols * ($MTR \leq 0.5$, highly intolerant) or ^ ($MTR > 0.5$, not highly tolerant).

RGS14	Pathogenic Score	Cancer Type	3DMTR (score)
S127P	0.91	Stomach Carcinoma	Tolerant (1.03)
D137Y	0.97	Prostate Carcinoma	Tolerant (0.93)
R173C	0.81	Large Intestine Carcinoma	Intolerant (0.50)
R173H	0.97	Large Intestine Carcinoma	Intolerant (0.50)
RGS10	Pathogenic Score	Cancer Type	3DMTR (score)
S64T	0.96	Lung Carcinoma	Tolerant (0.91)
K89M	0.84	Lung Carcinoma	Intolerant (0.48)
RGS4	Pathogenic Score	Cancer Type	3DMTR (score)
K125Q	0.97	Lung Carcinoma	Intolerant (0.48)
E126K	1.00	Skin Melanoma	Intolerant (0.42)
E135K	1.00	Skin Carcinoma, Melanoma, Upper Aerodigestive Tract Carcinoma	Tolerant (1.14)

Table 2.1. Tolerant and intolerant residues from RGS domains of interest that also overlap with highly deleterious somatic mutations were selected for assessment of their impact on RGS function. Amino acids reported in the COSMIC cancer database were selected based on the criteria that were predicted to be pathogenic by the FATHMM score to be highly pathogenic. Scores above 0.5 are deleterious, scores ≥ 0.7 are classified as pathogenic.

Reported pathogenic somatic mutations in RGS14, RGS10 and RGS4 that overlap with residues identified by 3DMTR to be significantly intolerant to mutation

Several bioinformatics tools (discussed below) that estimate the pathogenic potential of reported human somatic mutations are publicly available. Cells can develop somatic mutations due to imperfect replication or exposure to endogenous and exogenous mutagens (Olafsson and Anderson, 2021). Most somatic mutations will have little or no phenotypic effect, whereas a small minority of mutations can affect protein function and cell physiology leading to the progress of complex diseases (Olafsson and Anderson, 2021). These mutations occur post-zygotically and exist in a subpopulation of cells (Dou et al., 2018). Online databases like COSMIC (cancer.sanger.ac.uk/cosmic) report somatic mutations found in human cancers. COSMIC uses a FATHMM-MKL algorithm to predict the functional, molecular and phenotypic consequences of proteins missense variants using Markov models classifying the mutations as pathogenic (scores ≥ 0.7) or neutral (≤ 0.5) (Shihab et al., 2015) (Tate et al., 2018). Using these tools, we identified somatic mutations that overlap with residues in the RGS domain of RGS14, RGS10 and RGS4 identified by the 3DMTR to be either more sensitive or less sensitive to mutations (Supp. Tables 2.2-2.4).

RGS14 has been reported to be highly expressed in liver cancer and glioma (Uhlen et al., 2017). The analysis of The Cancer Genome Atlas (TCGA) and Gene Expression Omnibus (GEO) datasets have identified RGS14 as one of the five-gene signature biomarkers for Glioblastoma for Glioblastoma multiforme (GBM) (Yin et al., 2019). Somatic mutations in RGS14 that overlap with residues predicted to be highly tolerant or intolerant by the 3DMTR are shown in Supp. Table 2.2. Mutations found in RGS14 of

patient samples with large intestine carcinoma include R173C, R173H, and S170R. RGS14 somatic mutation S127P is found in gastroesophageal junction carcinoma, and D137Y is found in prostate carcinoma. Of note, coding silent mutations in RGS14 and other RGS proteins are also reported that overlap with significant residues identified by 3DMTR. For RGS14 these are residues N93, A99 and R173, and are included because the COSMIC FATHMM-MKL algorithm surprisingly and inexplicably designated some of these silent mutations to be pathogenic. Residues in RGS14 scored by the 3DMTR >0.05 and overlap with somatic mutations considered pathogenic by the COSMIC algorithm are S127P and D137Y. Residues scored by the 3DMTR ≤ 0.05 and predicted to be pathogenic are S170R, R173C, R173H, and coding silent R173.

RGS10 has been reported to be highly expressed in renal, endometrial, and cervical cancer (Uhlen et al., 2017). This ubiquitously express protein regulates physiology and signaling pathways in microglia, macrophages, T-lymphocytes, neurons, osteoclasts, cardiomyocytes, platelets, and cancer cells. It has been identified as an important regulator of cell survival and chemoresistance (Cacan et al., 2014; Hooks et al., 2010) and transcript expression is significantly suppressed in multiple ovarian cancer cell lines (Ali et al., 2013; Cacan et al., 2014). Moreover RGS10 acts as a tumor suppressor by blunting endogenous survival pathways (Cacan et al., 2014), and has been reported to regulate inflammatory signaling pathways in ovarian cancer cell survival (Alqinyah et al., 2018). Somatic mutations in RGS10 that overlap with residues deemed to be highly tolerant or intolerant by the 3DMTR are shown in Supp. Table 2.3. Mutations found in RGS10 of patient samples with lung carcinoma are S64T and coding silent A73, while K89M can be found in thyroid carcinoma samples.

Studies have shown association between RGS4 and enhanced cell viability, invasion and motility in thyroid cancer (Nikolova et al., 2008), glioma (Tatenhorst et al., 2004; Weiler et al., 2013), ovarian cancer (Puiffe et al., 2007), and triple negative breast cancer (Xie et al., 2009). Somatic mutations in RGS4 that coincide with 3DMTR identified significant residues (Supp. Table 2.4) are found in carcinoma samples of the following tissues: large intestine E87D, thyroid I89N, kidney W92C, endometrium K113N, breast Q122H and A123E, stomach A123T, and lung K125Q. Overlapping mutants were also found in melanoma including E126K, E135K, and silent coding F118 and V127 in RGS4.

Based on these findings, we chose to study selected somatic mutations in RGS14, RGS10 and RGS4 that overlap with residues identified by 3DMTR to be either tolerant or intolerant to mutation. Our goal for these studies was to test how well 3DMTR and other bioinformatic tools predict important residues for protein function and pathogenic potential. These specific residues and somatic mutations chosen for further study are listed in Table 1. Mutations in RGS14 selected for study were S127P, D137Y, R173C, and R173H (Fig. 2.3). Mutations in RGS10 selected for further study are amino acid mutation S64T and K89M (Fig. 2.4). Mutations in RGS4 chosen for further study were K125Q, E126K, and E135K (Fig. 2.5).

Assessment of somatic mutations in 3DMTR-identified tolerant and intolerant residues in GPCR/G protein activation and G protein binding

RGS14 is a member of the D/R12 subfamily and contains an RGS domain as well as accessory domains that play a role in different signaling pathways such as the tandem Ras/Rap-binding domains (R1 and R2), a G protein regulatory (GPR) motif, and a C-

terminal PDZ binding motif (Cho et al., 2000b; Friedman et al., 2022; Hollinger and Hepler, 2002; Hollinger et al., 2001a; Shu et al., 2007a; Traver et al., 2000b; Vellano et al., 2013a; Zhao et al., 2013). We first examined the effects of mutational changes in 3DMTR-defined tolerant and intolerant residues on RGS14 functions (Fig. 2.3). For these and subsequent studies (Figs. 2.4 and 2.5), we utilized a live cell biosensor (BRET) assay to measure RGS effects on GPCR/G protein activation (Brown et al., 2016a). HEK293 cells were transfected with α 2A-adrenergic receptor (α 2AR), Gao, G β 1-venus, G γ 2-venus, and the biosensor for G $\beta\gamma$ binding mas-GRK3ct-Luc, as previously reported (Brown et al., 2016a). Upon addition of α 2AR agonist UK 14,304 (100 μ M), GPCR signaling is activated leading to the dissociation of Ga and G $\beta\gamma$ -venus. The G $\beta\gamma$ -venus binds to the mas-GRK3ct-Luc biosensor resulting in an increase in BRET signal (Hollins et al., 2009). Using this model (Fig. 3A) we can test the effects of RGS mutants in α 2-adrenergic receptor-Gao protein activation.

RGS4, RGS10 and RGS14 each bind to active Gai/o protein family members including Gao1, Gao2, Gai1, Gai2, and Gai3 (Masuho et al., 2020). Of these, Gao is the most indiscriminate G alpha protein, is regulated by all canonical RGS proteins (Masuho et al., 2020), and its highly expressed in the brain where it couples α 2AR (Goldenstein et al., 2009; Nobles et al., 2005). Our previous studies compared α 2AR G-protein activation with Gao and Gai1, and Gao provided a much more robust maximum BRET amplitude signal (Brown et al., 2016a). For these reasons, we employed a live cell α 2AR-Gao model to test the effects of RGS protein mutants in G protein activation.

Using the above assay, we examined the effects of selected somatic mutations on RGS14 capacity to regulate receptor-G activation (Fig. 2.3). Four mutations were tested

including two which were scored by 3DMTR-permutation analysis as tolerant (S127P and D137Y) (Fig. 2.3C-2.3F) and two as intolerant (R173C and R173H) (Fig. 2.3G-2.3J). Wild type RGS14 and mutant proteins expressed well in HEK 293 cells (Supp. Fig. 2.4A). The relative position of these residues within the RGS domain structure are shown in Fig. 2.3B highlighted as either red (tolerant) and blue (intolerant). As shown in Figures 2.3C-2.3D and 2.3E-2.3F, somatic mutations within the tolerant residues exhibited distinct phenotypes. Whereas mutant D137Y behaved as expected (i.e., like wild type RGS14) to inhibit agonist activation of α 2AR-Gao (Fig. 2.3E-2.3F), mutant S127P exhibited a loss-of-function (LoF) phenotype (Fig. 2.3C-2.3D). In examining the two somatic mutations found in intolerant residue R173 of RGS14, both R173C (Fig. 2.3G-2.3H) and R173H (Fig. 2.3I-2.3J) behaved as expected with both mutations exhibiting a LoF phenotype. In parallel, we assessed direct binding of each RGS14 mutation with active Gao as measured by affinity capture by immunoprecipitation from HEK293 cell lysates treated with $\text{AlF}_4^-/\text{Mg}^{++}$ (AMF) to activate cellular G proteins including of Gao (Fig. 2.3K). We observed that the direct binding properties of the mutants mirrored that for RGS regulation of α 2AR-Gao activation. Specifically, mutant D137Y bound active Gao, whereas mutants S127P, R173H and R173P all failed to bind Gao (Fig. 2.3K). In summary, 3 of the 4 somatic mutations found in tolerant and intolerant residues of RGS14 as defined by 3DMTR behaved as predicted.

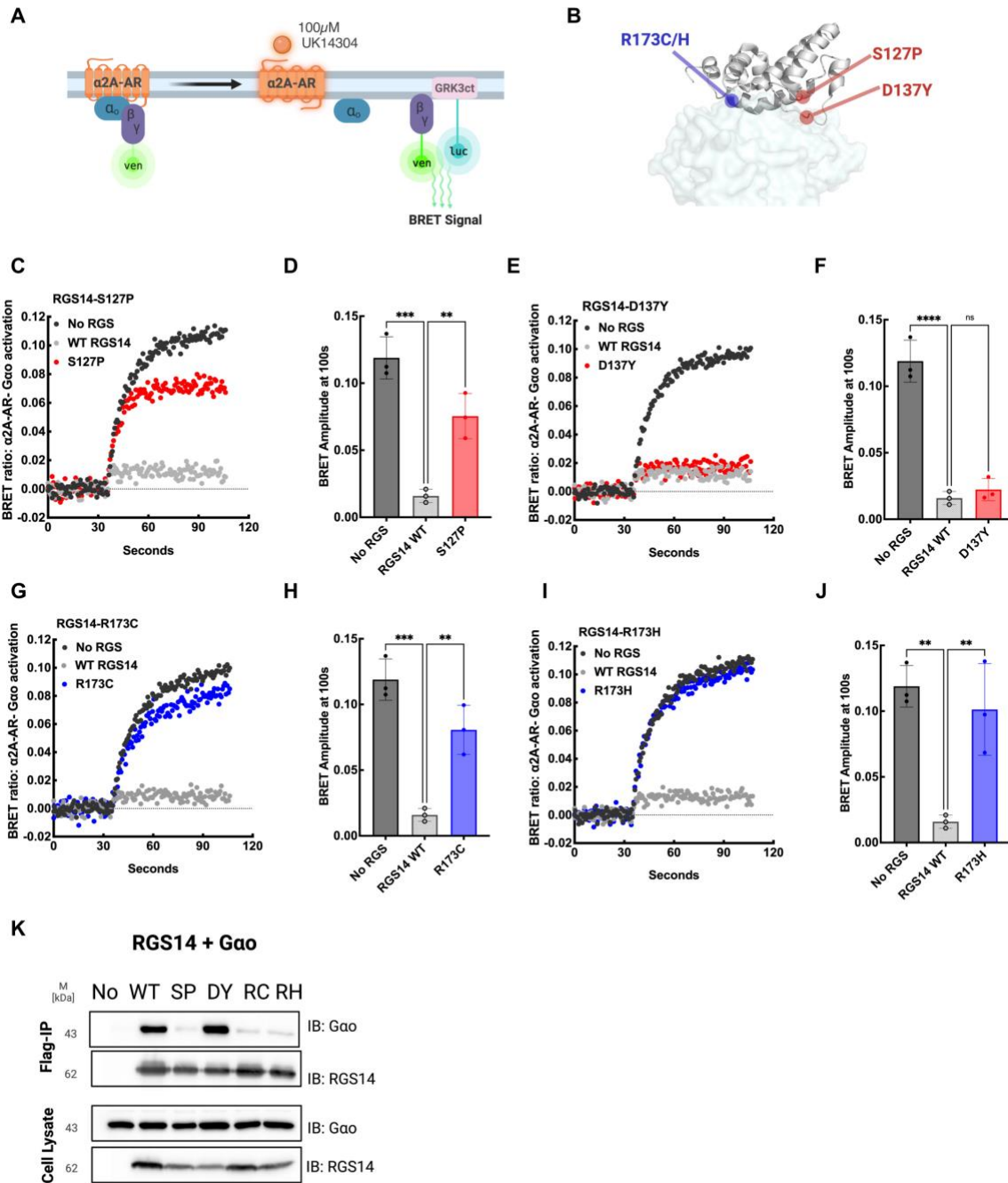


Figure 2.3. Assessment of functional impact of rgs14 somatic mutations on gpcr-g protein activation and g protein Binding.

(A) Schematic representation of kinetic BRET experiments. HEK 293 cells were transfected with 200 ng of α 2A-AR, 200 ng of Venus-G β 1 200 ng of Venus-G γ 2, 200ng of mas-GRK3ct-Luc,

1000 ng of mutant G α (PTX insensitive), and 0 or 200ng of WT Flag-RGS or 200ng of Flag tagged RGS mutant. **(B)** Structural view of selected mutated tolerant (red) and intolerant (blue) residues in RGS14. Average whole traces of BRET signal over time (n = 3) are shown comparing WT and somatic mutations. 3DMTR identified residues that led to loss of function are tolerant residues Flag-S127P **(C)**, and intolerant mutated residues Flag-R173C **(G)** and Flag-R173H **(I)**. Tolerant residue Flag-D137Y **(E)** did not lead to change of function. BRET amplitude observed at 100s was compared between 0ng RGS14, 200ng WT RGS14, and mutants Flag-S127P **(D)**, Flag-D137Y **(F)**, Flag-R173C **(H)**, and Flag-R173H **(J)**. Error bars represent mean +/- S.D. Statistical analysis was performed using one-way ANOVA with Dunnett's test (** $P < 0.005$). **(K)** Co-immunoprecipitation studies show that RGS14 mutants S127P, R173C and R173H blocked binding to G α -AIF4.

RGS10 is also part of the R12 subfamily, however, it is one of the smallest proteins in the RGS family and shares only a single conserved RGS domain in common with RGS14 and RGS12. Next, we examined the effects of selected somatic mutations on RGS10 functions using the same assay systems as described above (Fig. 2.4). In the case of RGS10, two somatic mutations were tested which were scored by 3DMTR as either tolerant (S64T) (Fig. 2.4C-2.4D) or intolerant (K89M) (Fig. 2.4E-2.4F). Wild type RGS10 and mutant proteins expressed well in HEK293 cells (Supp. Fig. 2.4B). The relative position of these residues within the RGS domain structure are shown in Fig. 2.4A highlighted as either red (tolerant) and blue (intolerant). Somatic mutations within the tolerant/intolerant residues of RGS10 exhibited phenotypes inconsistent with the 3DMTR prediction. Substituting a Thr for tolerant residue Ser64 (S64T) resulted in a partial LoF shown as a reduction in some, but not all capacity to inhibit receptor activation of G protein (Fig. 2.4C-2.4D). In contrast, substituting a Met for Lys (K89M) had no effect on RGS10 capacity to inhibit α 2AR activation of $G_{\alpha o}$ (Fig. 2.4E-2.4F). Examining these results more closely, we find that residue K89 is located on an alpha helix away from the G_{α} binding interface, while S64 is located within the binding interface (Fig. 2.4A). This could explain why mutations at these sites resulted in the observed phenotype, though opposite of what would be expected from the 3DMTR prediction. However, we cannot rule out the possibility that substitution mutations to intolerant residue K89 may lead to other change of function.

We also measured direct RGS10 binding to active $G_{\alpha o}$ (Fig. 2.4B). Results showed that the mutant phenotypes matched the functional readouts for RGS10 regulation of receptor G activation. That is, mutant K89M bound active $G_{\alpha o}$ whereas mutant S64T did not. The fact that S64T showed some capacity to inhibit receptor-G

activation but did not bind G α in the pull-down assay may reflect reduced affinity of this mutation for binding G α . In summary, neither of the two somatic mutations found in tolerant and intolerant residues of RGS10 as defined by 3DMTR behaved as predicted in this assay.

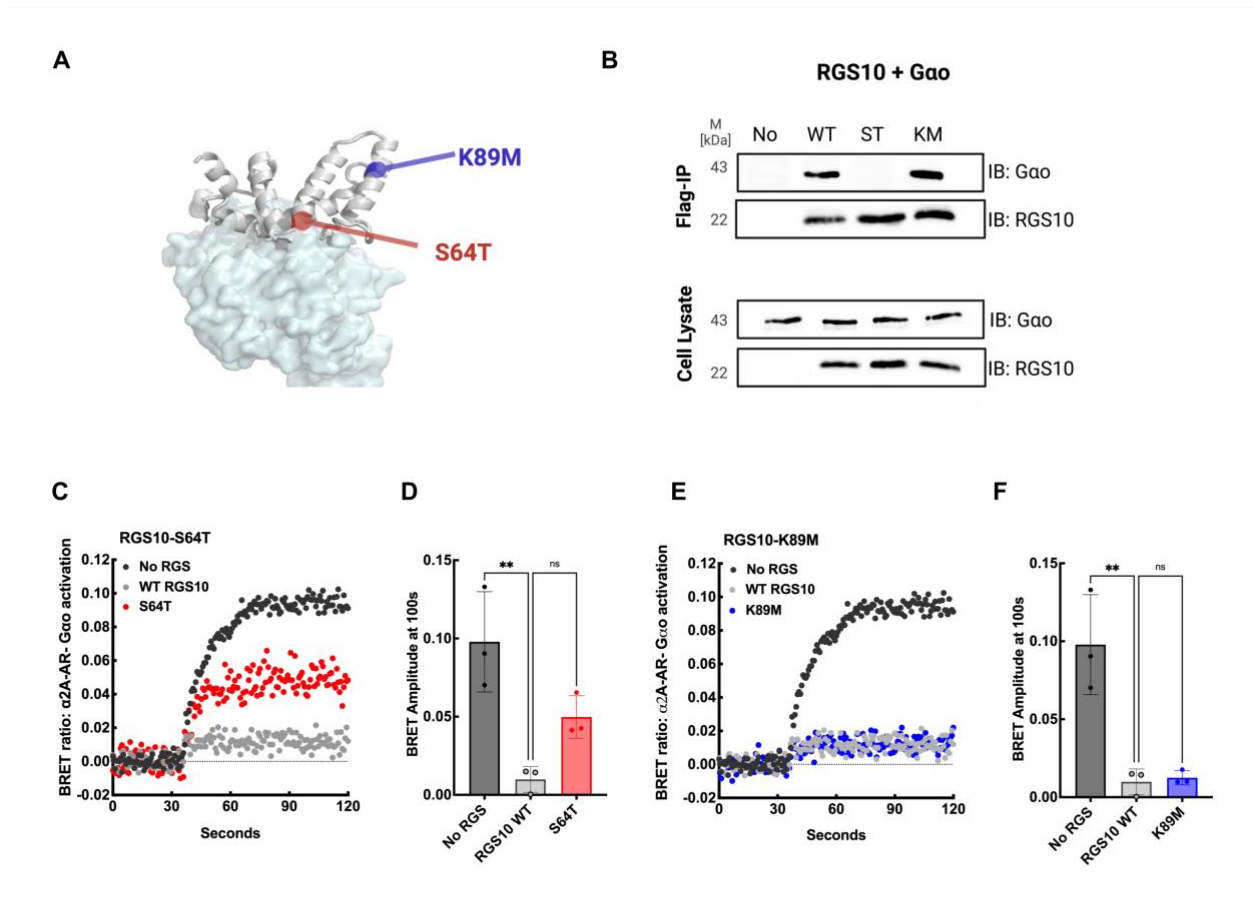


Figure 2.4. Assessment of functional impact of RGS10 somatic mutations on GPCR-G protein activation and G protein binding.

(A) Structural view of selected mutated tolerant (red) and intolerant (blue) residues in RGS10. **(B)** Co-immunoprecipitation studies show that mutants K89M bound to $G\alpha_o$ -AIF4⁺ while S64T blocked binding. Average whole traces of BRET signal over time ($n = 3$) are shown comparing WT and 3DMTR somatic mutations in identified tolerant residue Flag-S64T **(C)** and intolerant residues Flag-K89M **(E)**. BRET amplitude observed from data presented for Flag-S64T **(D)** and Flag-K89M comparison **(F)**. Tolerant residue Flag-S64T **(C-D)** led to change of function while intolerant Flag-K89M **(E-F)** did not change. Error bars represent mean \pm S.D. Statistical analysis was performed using one-way ANOVA with Dunnett's test (** $P < 0.005$).

RGS4 belongs to the B/R4 subfamily of RGS proteins, it is a small structure composed of only the RGS domain and has been linked to many cancers by regulating cell proliferation and apoptosis (He et al., 2019; Park et al., 2017; Xue et al., 2017). It has also been associated with enhanced glioma cell motility, thyroid carcinoma, and ovarian cancer (Hurst and Hooks, 2009; Hurst et al., 2009; Nikolova et al., 2008; Tatenhorst et al., 2004). RGS4 has been linked to reduced protein expression in metastatic tumors in breast cancer migration (Xie et al., 2009), suggesting that RGS4 enhancement can potentially block invasion (Sjogren, 2011). The relative position of selected somatic mutations on RGS4 are shown in Fig. 2.5A highlighted as either red (tolerant) and blue (intolerant). As with RGS14 and RGS10, we measured the effects of RGS4 on α 2AR-directed Gao activation and direct RGS binding to Gao in cell lysates. For RGS4, three somatic mutations were tested which were scored by 3DMTR as either intolerant (K125Q and E126K) (Fig. 2.5C-2.5F) or tolerant (E135K) (Fig. 2.5G-2.5H). Unlike RGS14 and RGS10, wild type RGS4 failed to completely inhibit α 2AR-directed Gao activation, as we've reported before (Brown et al., 2016a). RGS4 inhibited Gao activation by approximately 75%. Intolerant mutants K125Q and E126K of RGS4 each exhibit partial loss-of-function phenotypes (Fig. 2.5C-2.5F), largely failing to inhibit Gao activation, whereas tolerant mutation E135K (Fig. 2.5G-2.5H) behaved as wild type RGS4.

We next examined the effects of somatic mutations on RGS4 capacity to bind directly to Gao (Fig. 2.5B). Mutants K125Q and E135K each bound active Gao, whereas mutant E126K did not bind. Intolerant mutant K125Q unexpectedly bound Gao. It should be noted that the LoF effects observed for K125Q mutation (Fig. 2.5D) are only partial, and that the protein may be able to bind without fully exerting GAP effects on Gao. RGS4

mutant E126K protein levels may be low in the cells (Supp. Fig. 2.4C), but sufficiently high enough to exert GAP effects of Gao.

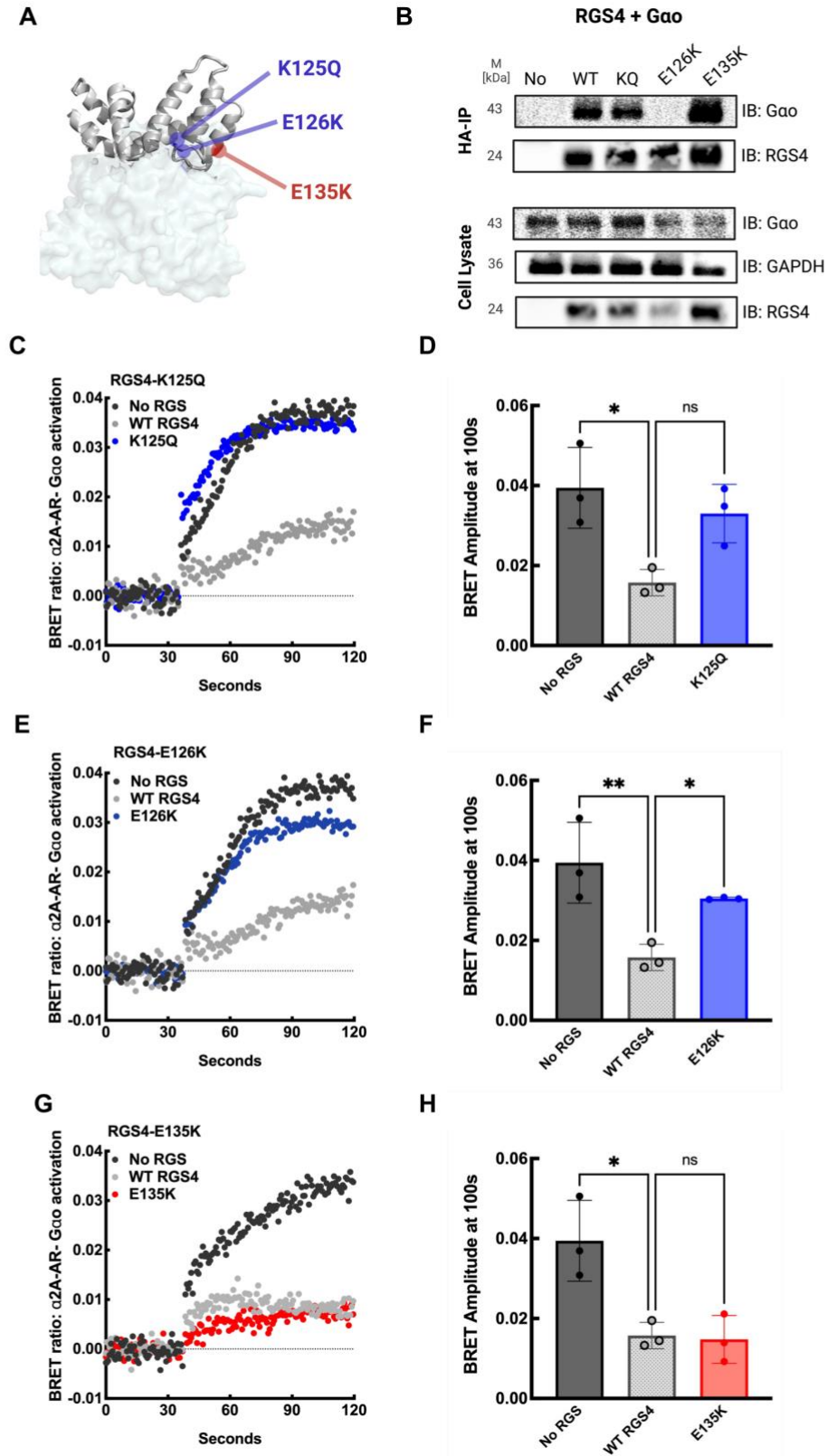


FIGURE 2.5. Assessment of functional impact of RGS4 somatic mutations on GPCR-G

protein activation and G protein binding. **(A)** Structural view of selected mutated tolerant (red) and intolerant (blue) residues in RGS4. **(B)** Co-immunoprecipitation studies show that RGS4 WT, K125Q and E135K mutants bound G α -AlF $_4^-$. Average whole traces of BRET signal over time (n = 3) are shown comparing WT and 3DMTR identified tolerant and intolerant residues HA-K125Q **(C)**, HA-E126K **(E)** and HA-E135K **(F)**. BRET amplitude at 100s observed from data presented for HA-K125Q **(D)**, HA-E126K **(F)** and HA-E135K **(G)** comparison. Intolerant mutants HA-K125Q **(C-D)**, HA-E126K **(E-F)** led to loss of function phenotypes while tolerant HA-E135K **(G-H)** did not. Error bars represent mean +/- S.D. Statistical analysis was performed using one-way ANOVA with Dunnett's test (*** $P < 0.0005$, ** $P < 0.005$, * $P < 0.05$).

The impact of somatic mutations on RGS protein regulation of intracellular cAMP levels

Findings to this point examined the impact of cancer somatic mutations on RGS protein regulation of receptor-directed G protein activation and G protein binding. The second messenger cAMP (3'-5'-cyclic adenosine monophosphate) is ubiquitously expressed and regulates cell proliferation and differentiation via PKA/Epac1 activation (Vitale et al., 2009). The cAMP-PKA signaling pathway has been linked to play roles in tumor biology. For example, in glioblastoma, increasing levels of cAMP inhibit cell growth by upregulating p21/p27 and PKA/Epac1-Rap1 signaling (Chen et al., 1998; Chen et al., 2002; Moon et al., 2012; Zhang et al., 2020). We next tested the effects of the cancer somatic mutations in key residues of RGS proteins downstream of G protein activation. For this, we examined the functions of cancer mutations of either a tolerant or an intolerant residue for each RGS protein (R173C and D137Y for RGS14, S64T and K89M for RGS10, and E126K and E135K for RGS4) in Gai/o-inhibition of adenylyl cyclase stimulated cAMP accumulation (Fig. 2.6). The accumulation of cAMP in live cells was measured using the Luciferase-based GloSensor assay (Fig. 2.6A). Studies have shown RGS4 to regulate receptor and G protein-directed inhibition of AC (Huang et al., 1997), and RGS4 and RGS10 to inhibit forskolin stimulated cAMP production in CHOK1 cells stably expressing 5-HT1A receptor (Ghavami et al., 2004). However, the effect of RGS14, RGS10 and RGS4 effect on cAMP levels in cells expressing α 2AR has not been explored. To measure RGS effects on receptor-Gai/o inhibition of cellular cAMP, cells were stimulated first with α 2AR-Gai/o coupled agonist (100uM UK 14,304) or vehicle (DMSO), followed by forskolin (10uM FSK) to stimulate adenylyl cyclase (AC) production of cAMP

(Fig. 2.6B). Of note, α 2AR has been shown to couple to both Gs and Gai/o in HEK cells (Wade et al., 1999). However, under the chosen experimental conditions, α 2AR-Gi/o coupling appears to dominate. That is, agonist activation of α 2AR-Gai/o significantly inhibited FSK-stimulated cAMP accumulation when compared to vehicle (Fig. 2.6C), indicating that FSK activation overrides any G α s contribution to cAMP formation. In each case, wild type RGS14, RGS10 and RGS4 reversed agonist-receptor-G protein inhibition of cAMP formation (Fig. 2.6D-2.6F), with RGS14 being more effective than RGS10 and RGS4. Intolerant mutant R173C in RGS14 lost capacity to reverse G protein inhibition of cAMP, whereas tolerant mutant D137Y showed a robust capacity to enhance cAMP accumulation (Fig. 2.6D). Interestingly, tolerant mutation S64T in RGS10 acted like WT RGS10, opposite to the effects in receptor-directed G protein activation and G protein binding (Fig. 2.4B-2.4D), while intolerant mutant K89M showed a robust capacity to enhance cAMP accumulation (Fig. 2.6E). Intolerant mutant E126K in RGS4 lost the capacity to reverse G-protein inhibition of cAMP, while tolerant mutant E135K acted like RGS4 WT (Fig. 2.6F). The same trends were observed here as was for receptor-directed G protein activation and G protein binding (Fig. 2.5B and 2.5E-2.5H).

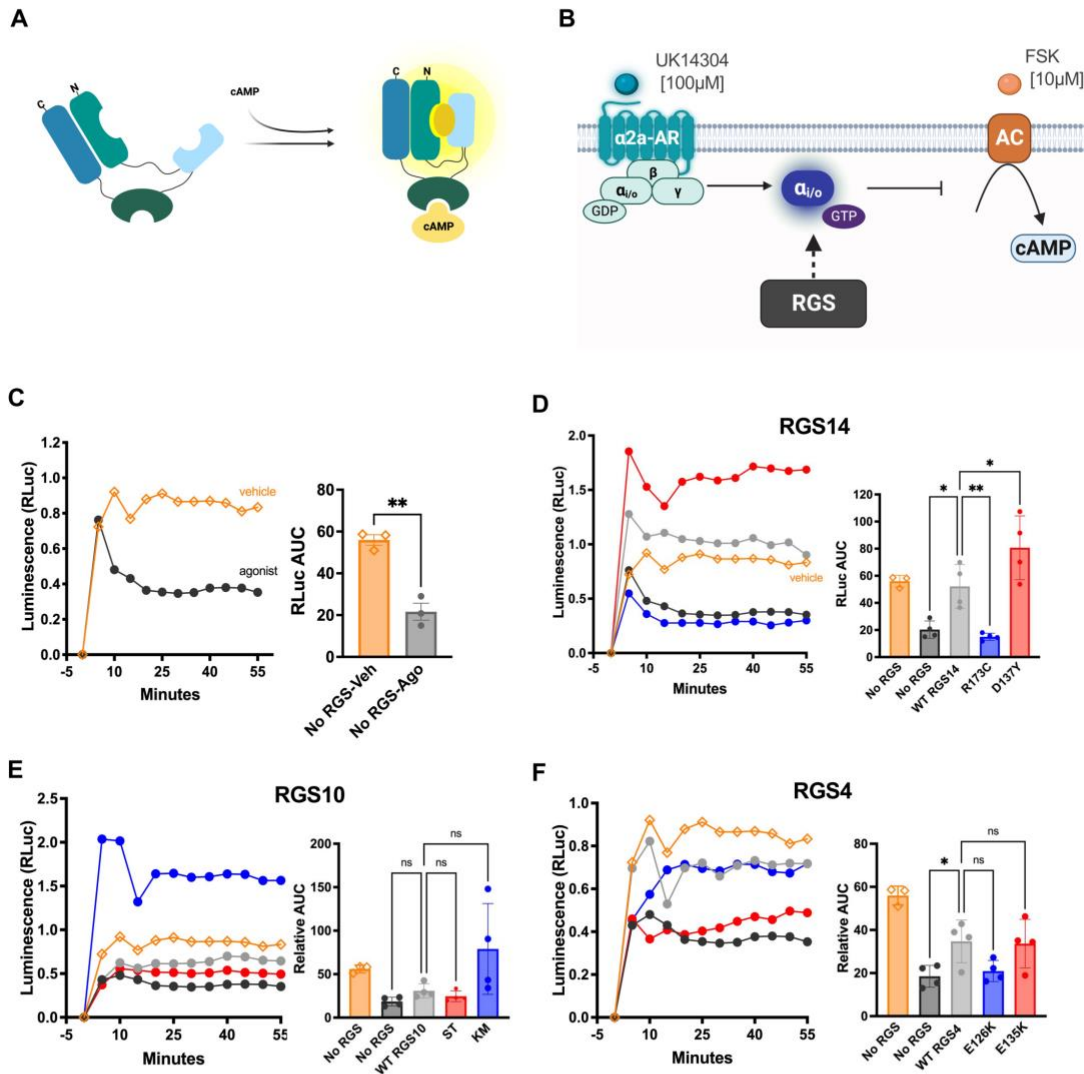


Figure 2.6. Assessment of functional impact of wild type vs mutant forms of RGS14, RGS10 and RGS4 on α 2AR -G protein directed inhibition of cAMP levels. HEK293 cells were transfected with constructs encoding gloSensor cAMP reporter, α 2AR, and RGS proteins of interest. At time 0, cells were treated with vehicle (\diamond DMSO) or agonist (\bullet 100 μ M of UK 14,304). After a 10 min incubation at RT, cells were stimulated with FSK (10 μ M). Luminescence intensity indicative of cAMP production was measured every 5 minutes for up to 50 minutes at room

temperature. Values shown in each time-course panel are means of triplicates from individual experiments, representative of 3-4 independent experiments. Data shown as +/- SD, n=3-4 independent experiments represent the relative luminescence intensity AUC (Area under the curve). **(A)** Schematic representation of the gloSensor.cAMP reporter, and **(B)** schematic representation of the assay design. **(C)** In the absence of RGS proteins, FSK alone increases cAMP levels while agonist-Gai/o stimulation leads to a significant decrease in cAMP. Bar graph shows comparative data values of AUC. **(D)** RGS14 WT compared to mutants resulted in significantly different cAMP levels over time. Bar graph shows comparative data values of AUC. **(E)** Comparison between RGS10 and mutants did not lead to any significant differences. Bar graph shows comparative data values of AUC. **(F)** Comparison between RGS4 and mutants did not lead to any significant differences. Bar graph shows comparative data values of AUC. Statistical analysis was performed measuring the AUC, using unpaired t test for C, and one-way ANOVA and Dunnett's multiple comparison test for D-F (*p<0.05, **p<0.005).

Several studies have identified RGS proteins to be regulators of adenylyl cyclase (AC) activity. RGS2 decreases accumulation of cAMP by directly interacting with type V AC (Roy et al., 2006; Salim et al., 2003), and RGS4 and RGS10 inhibited G-protein-independent cAMP production in CHOK1 cells (Ghavami et al., 2004). However, the actions of RGS14 on AC activity has not been explored. Therefore, we next examined the effect of RGS proteins on forskolin-stimulated cAMP production directly, in the absence of agonist-activated α 2AR-G protein contributions (Fig. 2.7A). Results for WT RGS14, RGS10 and RGS4 (Fig. 2.7B-2.7D) did not show an inhibition of FSK-stimulated cAMP levels in HEK293 cells transfected with α 2AR without agonist stimulation. Tolerant mutant D137Y in RGS14 showed a robust increase in cAMP levels in the absence of agonist-stimulated G_i/o -coupled receptor (Fig. 2.7B). Interestingly, tolerant mutant S64T in RGS10 showed an increase in cAMP levels when compared to WT RGS10 that had no effect (Fig. 2.7C). This trend is the opposite of the results shown in the previous assay of RGS10 mutant effects on receptor inhibition of cAMP (Fig. 2.6E). Mutations in E126K and E135K of RGS4 showed similar results to the effects shown for WT RGS4 (Fig. 2.6F).

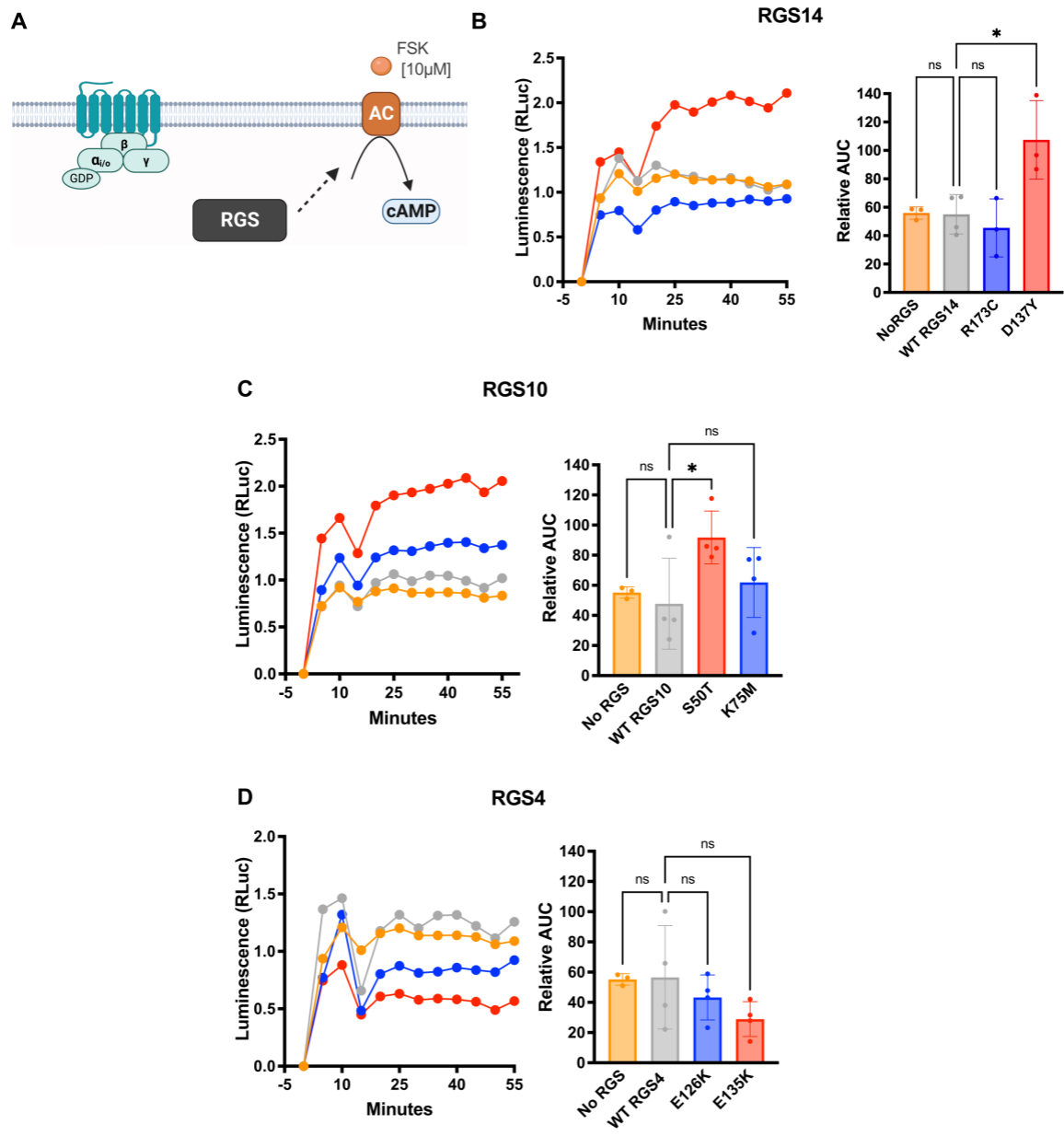


FIGURE 2.7. Assessment of the Functional Impact of Wild Type vs Mutant Forms of RGS14, RGS10 and RGS4 on FSK-Stimulated cAMP Production by Adenylyl Cyclase (AC). HEK293 cells were transfected with constructs encoding gloSensor cAMP reporter, α 2A-AR, and RGS proteins of interest. At time 0, cells were treated with vehicle (DMSO) and after a 10 min incubation at RT, cells were stimulated with FSK (10 μ M). Luminescence intensity indicative of cAMP production was measured every 5 minutes for 50 minutes at room temperature. Values shown in

each time-course panel are means of triplicates from individual experiments, representative of 3-4 independent experiments. Data shown as +/- SD, n=3-4 independent experiments represent the relative luminescence intensity AUC. (A) Schematic representation of the assay measuring the effects of RGS proteins in AC stimulated cAMP. (B) RGS14-D137Y led to a significant increase in AC stimulated cAMP levels compared to WT and other mutants. Bar graph shows comparative data values of AUC. (C) RGS10-S64T led to a significant increase in AC stimulated cAMP levels compared to WT and other mutants. Bar graph shows comparative data values of AUC. (D) There was no significant difference between RGS4 WT and mutants. Bar graph shows comparative data values of AUC. Statistical analysis was performed measuring the AUC and analyzing the difference between the conditions using one-way ANOVA and Dunnett's multiple comparison test (*p<0.05).

2.5 DISCUSSION

3DMTR analysis is a more accurate predictor than 1DMTR

In the present study, we performed a functional assessment of the predictive capabilities of the novel 3DMTR analysis applied to RGS proteins. The MTR method analyzes the regional intolerance to mutations in proteins of interest (Traynelis et al., 2017). Recent efforts have refined this tool and improved its predictive qualities (Perszyk et al., 2021). Using the 3D protein structure allows for a more refined and accurate prediction of important protein regions as it is common for non-adjacent segments of the polypeptide chain to come together in the tertiary and quaternary structure of a protein. We were able to identify important residues that show intolerance to genetic variance in most RGS domains of the RGS analogs that had a reported protein structure (Supp. Fig. 2.1-2.2). Our results show that the 3DMTR analysis is a more accurate predictor of regional intolerance when compared to its 1DMTR (Table 2.2). When we compared against the predictive qualities of other bioinformatic tools (SIFT, PROVEAN, MutPRED2; Supp. Table 2.2), 3DMTR was the most accurate at predicting intolerant residues of the protein that, if mutated, would lead to deleterious effects and change-of-function phenotypes. All nine selected residues in RGS14, RGS10 and RGS4 were predicted to be tolerant to change by the 1DMTR, while the 3DMTR predicted five of nine to be intolerant to change. The 3DMTR identified intolerant and tolerant mutated residues affected in GPCR-G protein activation and G protein binding. For RGS14, three of four, and three of three for RGS4 matched the 3DMTR-permutation analysis predictions. RGS10 mutants gave results that were opposite of expected in GPCR-G protein activation and G protein binding assessments.

RGS	Selected Mutation	1DMTR Score	CoF Prediction	3DMTR Score	CoF Prediction	CoF Effect	Matched 3DMTR
RGS14	S127P	1.04	No	1.03	No	↓	X
	D137Y	1.08	No	0.93	No	↑	●
	R173C	0.92	No	0.50	Yes	↓	●
	R173H	0.92	No	0.50	Yes	↓	●
RGS10	S64T	0.85	No	0.91	No	↓↑	X
	K89M	0.69	No	0.48	Yes	↓↑	X
RGS4	K125Q	0.94	No	0.48	Yes	↓	●
	E126K	0.99	No	0.42	Yes	↓	●
	E135K	1.22	No	1.14	No	=	●

↑ GoF, ↓ LoF, ↓↑ Mixed, = WT, ● matched prediction, x no match

TABLE 2.2. The 3DMTR analysis is a better predictor of key protein residues for functional impact of somatic mutations than 1DMTR. Here we summarize the results of the multiple functional assessments done to characterize the effects of the reported mutations. Overall, the 3DMTR analysis is a better predictor of intolerant protein regions than 1DMTR. With this information we can better predict which reported mutations will lead to a loss of function phenotype.

While greatly improved over the 1DMTR, the 3DMTR analysis was not perfect in its predictive power, with discrepancies noted after some functional assessments. The function of an RGS protein in GPCR-G protein activation and G protein binding is dependent on residue selectivity (Xie and Palmer, 2007). When the mutations examined here were tested downstream of the GPCR for RGS14 and RGS4 (e.g., cAMP accumulation), the intolerant and tolerant mutants behaved as expected in most, but not all cases. For example, the tolerant residue D137Y in RGS14 presented as tolerant in the G α coupling assay, but showed an unexpected enhanced gain-of-function effect in the cAMP assay. Another example of a mutant with a conflicting phenotype was intolerant residue K89M in RGS10. We found that K89M was tolerant and behaved as wild type protein in the G protein coupling assay but exhibited altered function in the assessment of inhibition of G α i/o-inhibition of cAMP levels causing an enhanced activity. In both cases, the cAMP assay measures adenylyl cyclase (AC) activity, and it should be noted that some RGS proteins bind directly to certain AC isoforms to stimulate their activity (Roy et al., 2006; Salim et al., 2003). In this case, tolerant D137Y RGS14 mutant and intolerant K89M RGS10 mutants could interact directly with AC, or the AC-G α complex, to stimulate AC enzyme activity. Consistent with this idea, our findings in Figure 2.7 indicate enhanced AC activity with these mutants in the absence of receptor agonist. Alternatively, the functional assessment of these assays relies on the network of residues that make direct contact with the active G α . The intolerant K89M mutation is found away from the binding site in RGS10, and this could explain why it did not lead to an altered loss-of-function phenotype in G protein coupling but did exhibit a phenotype in the cAMP assay. As a tangential side note, RGS actions on AC have not been extensively studied. Our

observations of RGS mutant effects on forskolin-stimulated AC raises the question of whether RGS proteins in general regulate AC differently with forskolin vs GPCR-Gs-activation, a topic for future study.

Despite these examples, the 3DMTR was a good overall predictor of intolerant residues that resulted in a change-of-function. The 3DMTR results need to be placed in perspective compared with other available tools, that are demonstrably less accurate predictors of change-of-function. For example, and as noted above, the COSMIC-FATHMM-MKL algorithm inexplicably designated silent mutations in residues N93, A99 and R173 of RGS14 to be pathogenic which, of course, is not possible at the protein level. In the future, the 3DMTR may also develop into a more precise tool. Specifically, as the Genome Aggregation Database (gnomAD) source data for the method collects more human synonymous and missense variant information, the analysis may be more accurate and/or require fewer residues to aggregate data that may lead to improved predictive potential.

RGS proteins in cancer and the impact of linked mutations in signaling pathways

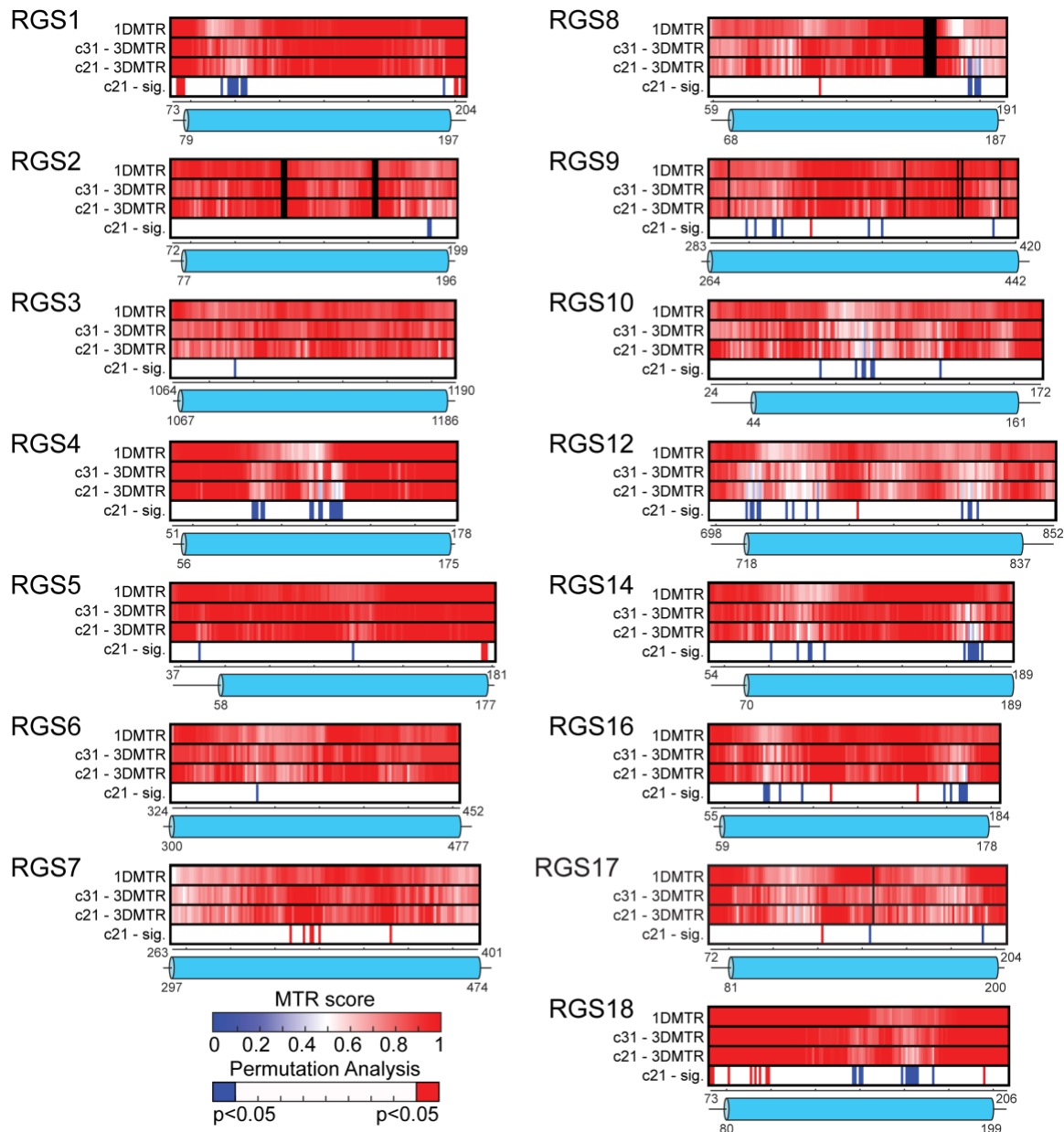
Roles for RGS proteins in GPCR-G protein signaling in human cancer have not been extensively studied, though genetic variants in RGS proteins linked to cancer have been reported (Dai et al., 2011; DiGiacomo et al., 2020; Lee et al., 2013a; Qutob et al., 2018). GPCRs have been shown to play a role in the initiation and progression of cancer, suggesting that regulators of GPCRs are also important in regulating oncogenic pathways. However, the specific roles of RGS proteins in regulating oncogenic pathways are still being studied.

In this study, we examined cancer associated mutations in RGS proteins that overlap with the significant residues identified by 3DMTR analysis. Of note, most cancer-linked mutations in RGS proteins have not been tested, except for a recent report (DiGiacomo et al., 2020). Here we tested nine cancer-linked mutations across three different RGS proteins for their functional phenotypes. These nine mutants were tested because they overlapped with residues predicted by 3DMTR to be either tolerant or intolerant to change and were predicted by the FATHMM analysis to have deleterious effect in protein function. These cancer-linked mutations were tested for their capacity to impact GPCR-G protein signaling. GPCR signaling can be altered by aberrant receptor overexpression, gain-of-function activating receptor, or mutations in downstream G protein signaling effectors, like RGS proteins, that favor oncogenicity (Gutkind, 1998). A recent study has identified 475 mutations reported in the RGS domain of RGS proteins present in 22 cancer types (DiGiacomo et al., 2020). We explored the functional effects that cancer associated mutants have in regulating RGS-G protein activation and downstream effector signaling. Eight out of the nine tested mutants led to a change-of-function phenotype. Tightly regulated GPCR-G protein-RGS signaling pathways control many important physiological events. GPCRs show selectivity to $G\alpha$ -subtypes as well as RGS proteins (Xie and Palmer, 2007), and activate/regulate specific downstream second messenger signaling pathways (e.g. cAMP) to mediate cell migration and survival (O'Hayre et al., 2014). Mutations in RGS proteins can lead to GPCR signaling dysregulation, which has been linked to roles in certain cancers (Arang and Gutkind, 2020; DiGiacomo et al., 2020). Loss-of-function mutations in RGS proteins, like RGS14-R173C/H and RGS4-E126K/K125Q, could increase G protein activity serving to promote

tumor growth mechanisms (Nishihara et al., 2004). Likewise, RGS genetic variations also could be associated with patient response to chemotherapies that specifically target GPCRs (Dai et al., 2011).

Recent advances in genome technology have allowed for a better understanding of the contribution of intolerant genetic variants in cancer pathogenesis. This, in turn, has allowed for improved diagnosis, and improved selection of cancer treatments in personalized medicine. Tools such as the novel 3DMTR analysis could enable biomedical researchers to prioritize which mutations/residues should be tested first for studying change-of-function phenotypes. Examples of this approach in other disease states such as idiopathic epilepsy have yielded remarkably promising results (Epi, 2015; Perszyk et al., 2021). Because bioinformatic tools are not perfect, the major challenge will be to make biological sense of data from large publicly available disease-linked genetic data bases and computational analysis. Our small-scale project is an example of how using the correct bioinformatic tools and testing that tool's predictive capabilities can elucidate the role of understudied genetic variants in RGS and other proteins in cancer disease progression.

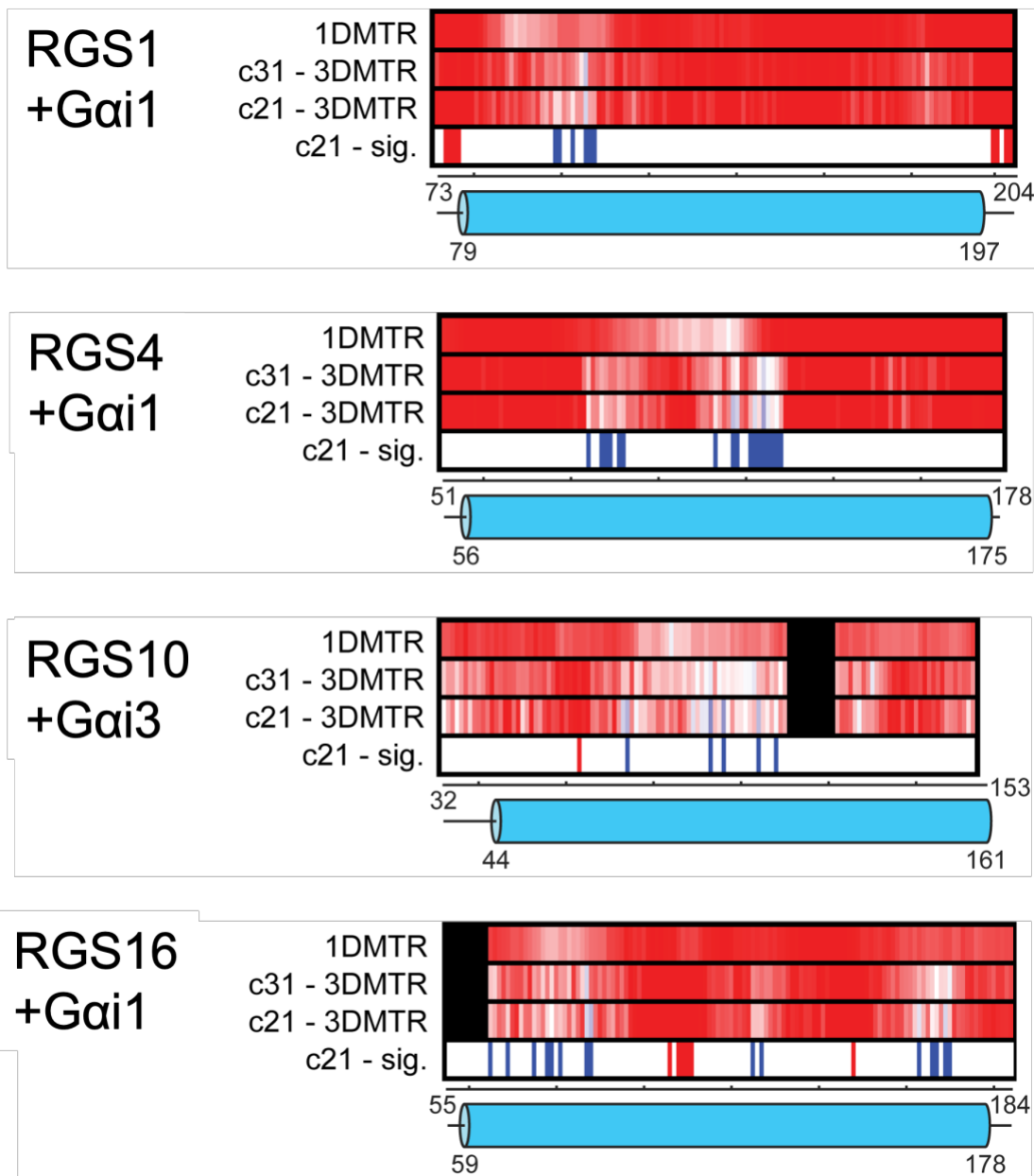
2.6 SUPPLEMENTAL INFORMATION



Supplemental Figure 2.1. Raster plot of all RGS proteins with available crystal structure.

The first row in each raster plot shows results from 1DMTR based on 31 neighboring residues in the linear sequence. Second row shows 3DMTR based on the 31 closest neighboring residues in 3D space. Third row shows 3DMTR based on the 21 closest neighboring residues. Fourth row shows significant residues based on the permutation analysis. Blue lines represent significantly

($P < 0.5$) significant residues. Bottom blue cylinder represents the RGS domain of each protein with extreme N-terminal and C-terminal residues numbered.

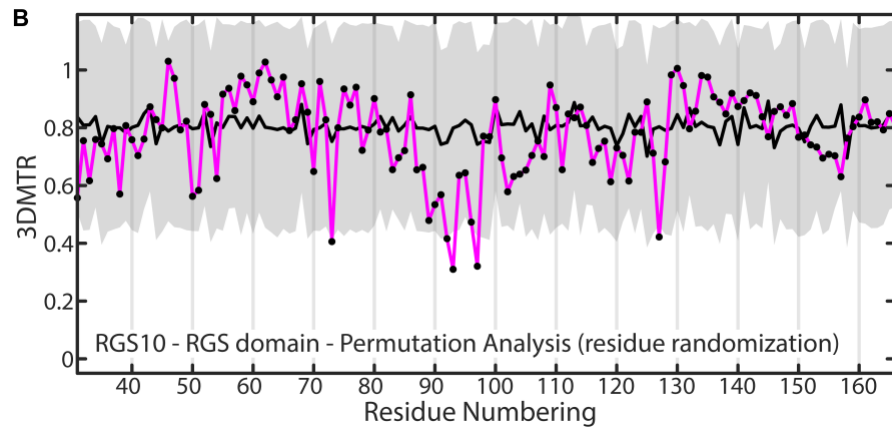
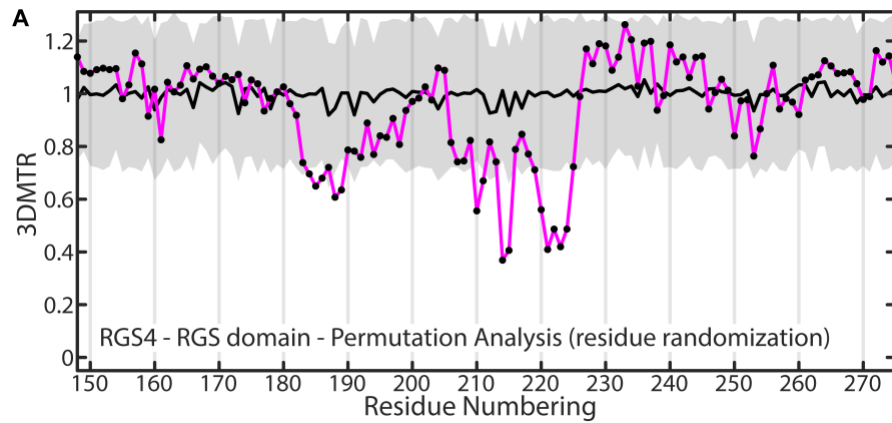


Supplemental Figure 2.2. Raster plot of RGS proteins in complex with active forms of their $G\alpha$ partners. The MTR results were calculated using the RGS 3D structure that is found in complex with G alpha subunit. See Legend of Fig S1 for details. First row in the raster plot shows results from 1DMTR followed in the second row showing 3DMTR based on the 31 neighboring residues. Third row shows 3DMTR based on the 21 neighboring residues. Fourth row shows significant residues based on the permutation analysis ($P < 0.5$). Bottom blue cylinder represents the RGS domain of each protein.

RGS protein	PDB	Deposition Authors	PMID	Link
RGS1	2BV1	Elkins, J.M., Yang, X., Soundararajan, M., et. al.	18434541	https://www.rcsb.org/structure/2BV1
RGS2	2AF0	Papagrigoriou, E., Johansson, C., Phillips, C., et. al.	18434541	https://www.rcsb.org/structure/2AF0
RGS3	2OJ4	Rezabkova, L., Boura, E., Herman, P., et. al.	20347994	https://www.rcsb.org/structure/2OJ4
RGS4	1AGR	Tesmer, J.J., Berman, D.M., Gilman, A.G., Sprang, S.R.	9108480	https://www.rcsb.org/structure/1AGR
RGS5	2CRP	Zhang, H.P., Hayashi, F., Yokoyama, S.	-	https://www.rcsb.org/structure/2CRP
RGS6	<u>2ES0</u>	Schoch, G.A., Phillips, C., Turnbull, A., et. al.	18434541	https://www.rcsb.org/structure/2ES0
RGS7	2D9J	Zhang, H.P., Nagasima, T., Hayashi, F., et. al.	-	https://www.rcsb.org/structure/2D9J
RGS8	2IHD	Turnbull, A.P., Papagrigoriou, E., Ugochukwu, E., et. al.	18434541	https://www.rcsb.org/structure/2ihd
RGS9	1FQI	Slep, K.C., Kercher, M.A., He, W., Cowan, C.W., Wensel, T.G., Sigler, P.B.	11234020	https://www.rcsb.org/structure/1FQI
RGS10	2DLR	Zhang, H.P., Nagashima, T., Hayashi, F., Yokoyama, S., RIKEN Structural Genomics/Proteomics Initiative (RSGI)	-	https://www.rcsb.org/structure/2DLR
RGS12	2EBZ	Zhang, H.P., Hayashi, F., Yokoyama, S., RIKEN Structural Genomics/Proteomics Initiative (RSGI)	-	https://www.rcsb.org/structure/2EBZ
RGS14	2JNU	Dowler, E.F., Diehl, A., Bray, J., et. al.	18434541	https://www.rcsb.org/structure/2JNU
RGS16	2BT2	Bunkoczi, G., Haroniti, A., Longman, E., et. al.	18434541	https://www.rcsb.org/structure/2BT2
RGS17	1ZV4	Schoch, G.A., Jansson, A., Elkins, J.M., et. al.	18434541	https://www.rcsb.org/structure/1ZV4
RGS18	2OWI	Higman, V.A., Leidert, M., Bray, J., et. al.	18434541	https://www.rcsb.org/structure/2OWI
RGS1 + Gai1	2GTP	Soundararajan, M., Turnbull, A.P., Ugochukwu, E., et. al.	18434541	https://www.rcsb.org/structure/2GTP
RGS4 + Gai1	1AGR	Tesmer, J.J., Berman, D.M., Gilman, A.G., Sprang, S.R.	9108480	https://www.rcsb.org/structure/1AGR
RGS10 + Gai3	2IHB	Soundararajan, M., Turnbull, A.P., Papagrigoriou, E., et. al.	18434541	https://www.rcsb.org/structure/2IHB
RGS16 + Gai1	2IK8	Soundararajan, M., Turnbull, A.P., Papagrigoriou, E., et. al.	18434541	https://www.rcsb.org/structure/2IK8

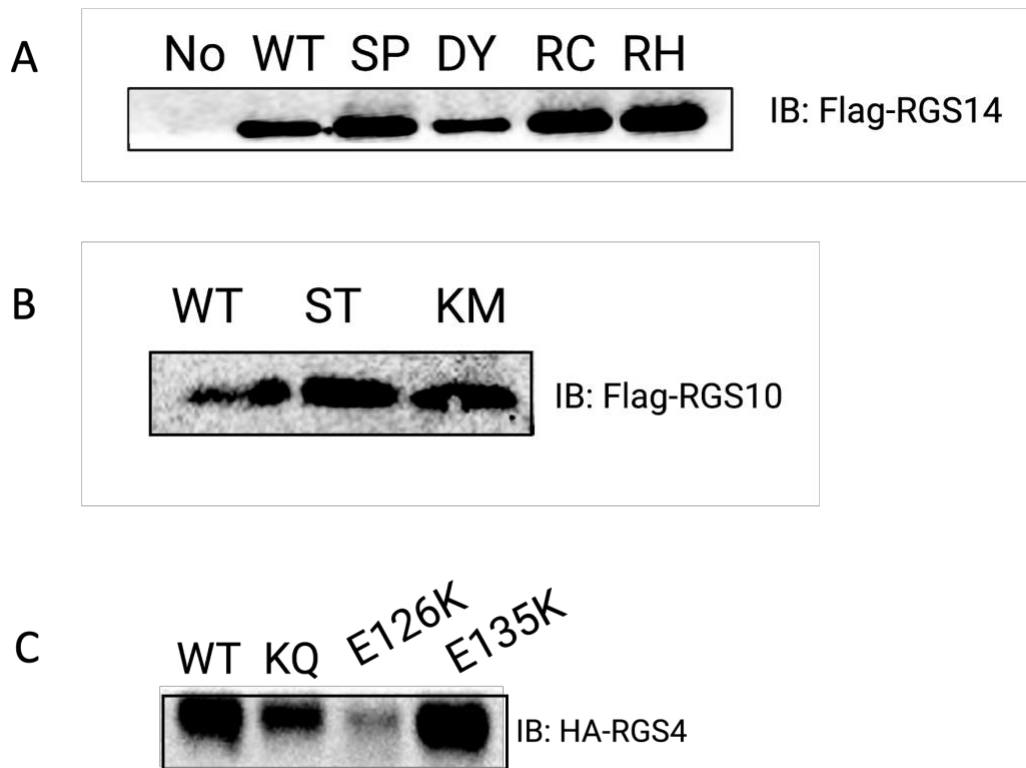
Supplemental Table 2.1. 3D structure information for analyzed RGS proteins. Protein Data Bank (PDB) information are shown for the 3D structures used in the analysis. In addition, the list

of authors who submitted the structure, the PMID where the structure was cited, and the link to the pdb database are shown.



Supplemental Figure 2.3. 3DMTR-permutation analysis comparing RGS4 and RGS10.

Scatter plot of (A) RGS4 and (B) RGS10 3DMTR score (magenta line), permutation analysis score mean (black line), and the standard deviation of the permutation analysis (gray areas).



Supplemental Figure 2.4. RGS WT and mutant protein expression in HEK 293 cells used for Kinetic BRET. To confirm RGS14, RGS10 and RGS4 WT and mutant overexpression, immunoblot analysis was performed. (A) Expression of RGS14 and mutants in cells used in Figure 3. (B) Expression of RGS10 and mutants in cells used in Figure 4. (C) Expression of RGS4 and mutants in cells used in Figure 5.

Supplemental Table 2.2. Comparison of various bioinformatic tools for their predictive values for change-of-function in amino acids of RGS14, RGS10 and RGS4. Shown are all residues within the RGS domain of RGS14 (S2), RGS10 (S3), and RGS4 (S4) that were identified by 3DMTR analysis to be significant (≤ 0.5) and have reported overlapping cancer mutation. Comparison of the various bioinformatic tools is presented with the score and prediction given to each residue based on the tool's algorithm. Publicly available variant prediction tools used in this analysis were SIFT (Sorting Intolerant From Tolerant; <http://sift.jcvi.org>; scores <0.05 are deleterious), FATHMM (Functional Analysis Through Hidden Markov Models; <http://fathmm.biocompute.org.uk>; scores >0.5 are deleterious, ≥ 0.7 pathogenic), PROVEAN (Protein Variation Effect Analyzer; <http://provean.jcvi.org>; scores < -2.5 deleterious, score > -2.5 neutral), MutPRED2 (Mutation Predictor; <http://mutpred.mutdb.org>; score >0.5 pathogenic).

RGS14		Somatic Mutation			Bioinformatic Tool Scores					
Res #	Res L	Mutation Type	AA mutation	Tissue Histology	SIFT	FATHMM	1DMTR	3DMTR	PROVEAN	MutPRED2
81	F				1.00	0.09	0.83	0.49		
93	N	N=	Coding Silent	Large Intestine Carcinoma	0.07		0.67	0.49		
94	V	M	Missense				0.62	0.63	-1.68	
98	K				0.00		0.65	0.51		
99	A	P			1.00	0.29	0.59	0.62	-4.08	
99	A	A=	Coding Silent	Skin Carcinoma	0.01					

RGS14		Somatic Mutation			Bioinformatic Tool Scores					
Res #	Res L	Mutation Type	AA mutation	Tissue Histology	SIFT	FATHMM	1DMTR	3DMTR	PROVEAN	MutPRED2
105	Q	E			0.03		0.67	0.66	-0.52	
		R			0.23				-0.46	
127	S	C			0.02	0.91	1.04	1.03		
		P	Missense	Gastroesophageal junction Carcinoma	0.00	0.97			-3.54	0.78
137	D	Y	Missense	Prostate Carcinoma	0.00	0.96	1.08	0.93	-7.70	0.92
168	F						1.07	0.55		
170	S	R	Missense	Large Intestine Carcinoma			1.09	0.32		
171	Y						1.04	0.46		
172	A				0.00	0.81	0.99	0.36		
173	R	C	Missense	Large Intestine Carcinoma	0.00	0.97	0.92	0.50	-7.31	0.72
		H	Missense	Large Intestine Carcinoma	1.00	0.74			-4.57	0.60

RGS14		Somatic Mutation			Bioinformatic Tool Scores					
Res #	Res L	Mutation Type	AA mutation	Tissue Histology	SIFT	FATHMM	1DMTR	3DMTR	PROVEAN	MutPRED2
		R=	Coding Silent	Large Intestine Carcinoma						
174	F						0.92	0.44		
176	K						0.90	0.48		

RGS10		Somatic Mutation			Bioinformatic Tool Scores					
Res #	Res L	Mutation Type	AA mutation	Tissue Histology	SIFT	FATHMM	1DMTR	3DMTR	PROVEAN	MutPRED2
64	S	Missense	T	Lung Carcinoma	0.01	0.96	0.85	0.91	-2.67	0.75
73	A	Coding Silent	A=	Lung Carcinoma	1.00	0.02	0.86	0.41		
89	K	Missense	M	Thyroid Carcinoma	0.00	0.84	0.69	0.48	-3.37	0.48
92	E						0.65	0.42		
93	I						0.70	0.31		
96	T						0.71	0.47		
97	F						0.68	0.32		
127	F						0.85	0.42		

RGS4		Somatic Mutation			Bioinformatic Tool Scores					
Res #	Res L	Mutation Type	AA mutation	Tissue Histology	SIFT	FATHMM	1DMTR	3DMTR	PROVEAN	MutPRED2
87	E	Missense	D	Large Intestine Carcinoma	0.00	0.83	0.89	0.70	-2.8	0.78
88	N						0.89	0.65		
89	I	Missense	N	Thyroid Carcinoma	0.00	0.95	0.87	0.68	-5.12	0.85
91	F						0.80	0.61		
92	W	Missense	C	Kidney Carcinoma	0.00	0.97	0.82	0.64	-11.65	0.95
113	K	Frameshift	Rfs*15	Large Intestine Carcinoma, Soft tissue haemagiolaoma			0.57	0.56		
		Missense	N	Endometrium Carcinoma	0.39	0.98				
114	I						0.58	0.67		
117	E						0.58	0.37		
118	F	Coding silent	F=	Skin Malignant Melanoma	1.00	0.94	0.58	0.41		
122	Q	Missense	H	Breast Carcinoma	0.07	0.94	0.83	0.71	-3.21	0.38
123	A	Missense	T	Stomach Carcinoma	0.01	0.95	0.88	0.56	-3.02	0.51

RGS4		Somatic Mutation			Bioinformatic Tool Scores					
Res #	Res L	Mutation Type	AA mutation	Tissue Histology	SIFT	FATHMM	1DMTR	3DMTR	PROVEAN	MutPRED2
		Missense	E	Breast Carcinoma	0.00	0.99				0.73
124	T						0.95	0.41		
125	K	Missense	Q	Lung Carcinoma	0.01	0.97	0.94	0.49	-2.68	0.47
		Coding silent	K=	Lung Carcinoma	1.00	0.99				
126	E	Missense	K	Skin malignant melanoma	0.00	1.00	0.99	0.42	-3.87	0.87
127	V	Coding silent	V=	NS Malignant melanoma, Salivary gland carcinoma	1.00	0.77	0.99	0.49		
135	E	Missense	K	Skun Carcinoma, Skin Malgnant Melanoma, Upper aerodigestive tract carcinoma	0.01	1.00	1.22	1.14	-3.46	0.62

CHAPTER 3: HUMAN RGS14 AND NHERF1 REGULATE PTH1R-G PROTEIN SIGNALING EVENTS LINKED TO PHOSPHATE UPTAKE IN KIDNEY

This chapter has been assembled in part from the published manuscript:
Friedman PA, Sneddon WB, Mamonova T, **Montanez-Miranda C**, Ramineni S, Harbin NH, Squires KE, Gefter JV, Magyar CE, Emler DR, Hepler JR (2022). **RGS14 regulates PTH- and FGF23-sensitive NPT2A-mediated renal phosphate uptake via binding to the NHERF1 scaffolding protein.** *J Biol Chem.* PMID: 35307350

3.1 ABSTRACT

Regulator of G Protein Signaling 14 is a multifunctional scaffolding protein that integrates G protein, MAPK, and Ca⁺⁺/CaM signaling pathways. Multiple GWAS studies have implicated RGS14 with Chronic Kidney Disease and disordered phosphate metabolism. How RGS14 impacts kidney function and phosphate homeostasis remains unexplored. Phosphate homeostasis is regulated by the kidney sodium/phosphate exchanger [NPT2A:NHERF1] complex, which mediates phosphate uptake in renal proximal tubule cells. Parathyroid hormone (PTH) activation of the parathyroid hormone receptor 1 (PTH1R) blocks phosphate uptake. Our recent studies (Friedman et al., 2022) show that RGS14 blocks PTH-sensitive phosphate uptake in renal cells. How RGS14 regulates PTHR1 signaling is unknown. Previous studies show that PTHR1 increases intracellular cAMP and calcium. Here we show in HEK and Opossum Kidney (OK) cells that PTHR1 stimulates intracellular cAMP and calcium, and directly couples to G_{αs} but, surprisingly, not G_{αq}. We find that RGS14 and NHERF1 block PTH-stimulated calcium, but not cAMP. We also show that human RGS14 binds to NHERF1, suggesting that RGS14 and NHERF1 regulate PTHR1-G signaling. Ongoing studies focus on understanding how RGS14 impacts PTH1R-G binding to NHERF1 to affect PTH1R downstream signaling and phosphate metabolism in the kidney.

3.2 INTRODUCTION

Numerous GWAS studies implicate RGS14 in kidney diseases (Kestenbaum et al., 2010; Long et al., 2018b; Mahajan et al., 2016; Robinson-Cohen et al., 2017; Urabe et al., 2012; Yasui et al., 2013), including disordered phosphate metabolism. The RGS14 gene on human chromosome 5 is adjacent to SLC34A1 that encodes the NPT2A sodium-phosphate cotransporter. RGS14 is an unusual multifunctional scaffolding protein that integrates G protein, MAPK, and Ca^{2+} /CaM signaling pathways (Evans et al., 2015; Evans et al., 2018a). RGS14 actions are best understood in rodent brain, but much less is known about human RGS14. Human and rodent RGS14 share a common domain structure that includes an amino-terminal RGS domain that binds Gai/o-GTP and acts as a GAP to limit G protein signaling (Cho et al., 2000c; Hollinger et al., 2001b); two tandem Ras/Rap-binding domains (RBD) that bind active H-Ras and Rap2 (Shu et al., 2010; Traver et al., 2000a; Willard et al., 2009); and a G protein regulator (GPR, also referred to as GoLoco) motif that binds inactive Gai1/3 to anchor RGS14 at membranes (Shu et al., 2007b). Human, primate, and ovine RGS14 differ from the rodent protein in that they contain a carboxy-terminal Class I PDZ-recognition sequence.

Recent Genome Wide Association Studies (GWAS) have linked human variants in RGS14 to Chronic Kidney Disease (Chen et al., 2019; Long et al., 2018a; Mahajan et al., 2016), specifically in disordered phosphate metabolism. Under basal conditions, phosphate uptake occurs through the NPT2A transporter bound to NHERF1 in proximal tubule kidney cells. Upon PTH (parathyroid hormone) stimulation of PTHR, downstream G protein signaling is activated leading to the activation of PKA or PKC, which phosphorylates NHERF1 and allows for dissociation from the transporter, which leads to

internalization of NPT2A blocking phosphate transport inside the cell. In a phosphate disordered metabolism model, either excess reabsorption of phosphate or excess excretion of phosphate occurs. However, how is RGS14 involved in this system?

Recent studies by our laboratory in collaboration with Peter Friedman (U Pittsburg School of Medicine) have described the interaction between RGS14 and NHERF1 and their role in kidney phosphate transport. RGS14 and NHERF1 colocalize and interact in human kidney cells and are recovered as a complex in coimmunoprecipitation assays (Friedman et al., 2022). RGS14 is endogenously expressed in proximal kidney cells and HPCT cell line, siRNA knockdown of RGS14 unmask hormone sensitivity and restores PTH and FGF23 capacity to block NPT2A Pi uptake (Friedman et al., 2022). These results describe RGS14 to have a tonic inhibition role of PTH and FGF23 actions in human kidney. This apparent tonic inhibition strongly suggests that RGS14 is a tightly regulated on/off switch for PTH and FGF23 control of NPT2A-mediated Pi uptake (Friedman et al., 2022). In addition, recent human variants have been identified in the DSAL PDZ recognition sequence of RGS14. Naturally occurring variants in D563 (D563G and D563N) and in A565 (A546S and A565V) effect on binding to NHERF1 and PTH sensitive uptake were explored (Friedman et al., 2022). Co-immunoprecipitation experiments of NHERF1 binding to RGS14 showed that mutations in D563N affected binding to NHERF1. Phosphate transport studies in OK cells (NHERF1-null) were transfected with WT RGS14 or RGS14 mutants and NHERF1. RGS14 variants D563N reversed the WT effects on blocking PTH inhibition of phosphate uptake.

This project focuses on understanding the actions of RGS14 downstream of hormone receptor signaling. PTH1R receptor is expressed in the apical and basolateral part of

renal proximal tubule cells (Weinman and Lederer, 2012). In the apical side of the cell, PTH1R exists as part of a complex that includes Npt2a, and NHERF1 (Gisler et al., 2001; Khundmiri et al., 2003). When PTH1R is bound to NHERF1 or NHERF2, the receptor signals through the PKC pathway, whereas in the absence of NHERF1 signaling is via cAMP/PKA pathway (Mahon et al., 2002). Studies by Friedman and colleagues have demonstrated NHERF1 regulates internalization and desensitization of the PTH1R and can also block desensitization by impairing binding between PTH1R and arrestin (Villardaga et al., 2011). PTHR couples to Gas to stimulate the production of cAMP and activate PKA which, in turn, phosphorylates NHERF1 to uncouple it from NPT2A (Deliot et al., 2005; Zhang et al., 2019; Zizak et al., 1999). PTHR also couples to Gαq/11 (Schwindinger et al., 1998b; Wang et al., 2010). RGS14 binds directly to active Gai/o and inactive Gai1/3 but does not directly engage either Gas or Gαq (Hollinger et al., 2001b; Vellano et al., 2011b). We sought to determine if RGS14 affects PTHR G protein coupling and second messenger signaling directly or by binding NHERF1.

3.3 MATERIALS AND METHODS

Kinetic BRET

HEK293 cells were cultured in 1× Dulbecco's modified Eagle's medium without phenol red supplemented with 10% fetal bovine serum (5% for transfection medium), 2 mM L-Gln, 100 units/mL penicillin, and 100 mg/mL streptomycin. HEK293 cells were maintained in a humidified incubator with 5% CO₂ at 37 °C. Polyethyleneimine (PEI) was used to carry out transfections for BRET assays in HEK293 cells. JetOptimus was used to carry out transfections for CALFUX BRET in Opossum Kidney (OK) cells. Cells were seeded 8×10⁵ in 2 mL of transfection medium per well in six-well plates. For PTHR Kinetic BRET, PTHR HEK293 cells were transfected with 200ng 3×HA-PTHR, 1000ng Gas-EE (short, (cDNA.org GNA0SSEIC0), 200ng Venus-Gβ1, 200ng Venus-Gγ2, 200ng, mas-GRK3ct-Luciferase, 200ng HA-NHERF1, and 200ng Human-FLAG RGS14. To monitor PTH1R G protein selectivity using a kinetic BRET assay, HEK293 cells were also transfected with 200ng 3×HA-PTHR, 200ng Venus-Gβ1, 200ng Venus-Gγ2, 200ng mas-GRK3ct-Luciferase and 1000ng of either Gα subunit of interest: Gas-EE (short), Gαq-EE, Gα11, Gα14, Gα16, Gai1 and Gai2. To monitor intracellular concentrations of cAMP in live cells, we used the CAMYEL sensor (cAMP sensor using YFP-Epac-RLuc) as previously described (Jiang et al., 2007). HEK293 cells were transfected with 350 ng CAMYEL sensor, 500 ng 3×HA-PTHR, 250 ng HA-NHERF1 and 250 ng of human-FLAG RGS14.

Kinetic BRET experiments were performed as previously described (Brown et al., 2016b). Forty-eight h following transfection, cells were resuspended in Tyrode's solution (140 mM NaCl, 5 mM KCl, 1 mM MgCl₂, 1 mM CaCl₂, 0.37 mM NaH₂PO₄, 24 mM

NaHCO₃, 10 mM HEPES, and 0.1% glucose, pH 7.4) and plated on white 96-well Optiplates (Perkin Elmer Life Sciences, Waltham, MA). To confirm acceptor (YFP or Ven) expression, fluorescence measurements were made using the TriStar LB 941 plate reader (Berthold Technologies, Bad Wildbad, Germany) with 485-nm excitation and 530-nm emission filters. After 5 min application of 5 μ M coelenterazine H (Nanolight Technologies, Pinetop, AZ), kinetic BRET was monitored in live cells using sequential measurements through 485- and 530-nm emission filters. BRET was recorded for 30 s with no stimulation to establish basal BRET. After basal BRET measurements, agonist PTH(1-34) (100 nM) was applied at 30 s. The change in BRET was calculated by dividing the mas-GRK3ct-Luc signal (530 nm) by the Ven-G β γ signal (485 nm) and subtracting the average BRET signal observed from the first 30 s of observation (basal BRET). For each experiment, a kinetic BRET control was performed. For PTHR kinetic BRET, cells were treated with vehicle (ddH₂O) and any signal recorded in these controls was considered as noise and subtracted from experimental kinetic BRET recording. For cAMP BRET experiments, cells were treated with vehicle and the signal recorded in these controls was considered as noise and plotted. Data were collected using MikroWin 2010 software (Mikrotek Laborsysteme GmbH, Overath, Germany) and analyzed using Microsoft Excel and GraphPad Prism 9.

To measure intracellular concentrations of calcium in live cells, we used the calcium BRET sensor Calflux-VTN (CALcium FLUX composed of Venus, Troponin and NanoLuc, Addgene plasmid #83926) as previously described (Yang et al., 2016). HEK293 cells were transfected with 100ng calflux-vtn BRET sensor, 250ng 3 \times HA-PTHR, 250ng HA-NHERF1 and 250ng of human-FLAG RGS14. To monitor calcium levels in a

physiologically relevant model, OK cells were transfected with 100ng calflux-vtn and plus or minus 250ng human-FLAG RGS14. Cells are transfected and kept in 5% FBS media for 48 hours. Next, cells are washed with 500uL of 5mM EDTA and incubated for 3 min to allow the cells to lift off the 6-well plate. Nano-luciferase substrate furimazine (Promega N2590) mix is made with BRET buffer and FBS (23.uL of BRET Buffer (Tryrode's solution), 10uL FBS and 1uL of furimazine). Cells are treated with 10uM of furimazine (30uL from furimazine mix into each well). After cells are incubated in the 96-well plate with furimazine for 1-2hrs at 37C, kinetic BRET is monitored in live cells using sequential measurements through 485- and 530-nm emission filters. BRET was recorded for 30 s with no stimulation to establish basal BRET. After basal BRET measurements, agonist PTH(1-34) (100 nM) was applied at 30 s. The change in BRET was calculated by dividing the nano-Luc signal (530 nm) by the Ven-G $\beta\gamma$ signal (485 nm) and subtracting the average BRET signal observed from the first 30 s of observation (basal BRET).

Analysis of immunoblots

Denatured HEK293 cell lysate samples in Laemmli Buffer were resolved on 13.5% SDS-PAGE, and samples were then transferred to nitrocellulose membranes. Membranes were blocked for 1 h at room temperature with 5% nonfat dried milk in Tris-buffered saline plus Tween 20 (TBST) (blocking buffer) and incubated with the primary antibodies (polyclonal anti-FLAG at 1:1000, polyclonal anti-HA at 1:1000) in blocking buffer overnight at 4 °C. The membranes were washed four times for 10 min in TBST and then incubated with goat anti-rabbit IgG conjugated to horseradish peroxidase at a 1:5000 dilution for 1 h at room temperature. Membranes were washed four times for 10 min in

TBST. Blots were developed using ECL and imaged using the ChemiDoc MP Imaging system (BioRad).

Statistical analysis

Results were analyzed using Prism 9 software (GraphPad, La Jolla, CA). Data represent the mean \pm SD or SEM as indicated of $n \geq 3$ independent experiments and were compared by analysis of variance with post hoc testing using the Bonferonni procedure or paired t-test as appropriate. p values < 0.05 were considered statistically significant.

3.4 RESULTS

PTH1R couples strongly to Gas but no other G proteins in transfected HEK293 cells

We sought to determine if RGS14 affects PTHR G protein coupling and second messenger signaling directly or by binding NHERF1. Here, we applied live-cell BRET bimolecular fluorescence complementation assays with Ven-G β 1 γ 2 and a mas-GRKct-Luc biosensor to detect G $\beta\gamma$ release (Hollins et al., 2009; Hynes, 2011). First, we focus on looking at PTH1R coupling with different G proteins. Studies have identified that PTH1R signals primarily through Gas but can also signal via G α q (Abou-Samra et al., 1992), and G α 12/13 (Singh et al., 2005). PTH1R has been shown to couple to Gas and G α q in C21 cells but not in C20 or HEK293 cells because coupling of G-proteins to PTHR/PTHrP is dependent on receptor density (Schwindinger et al., 1998a). To test PTH1R-G protein activation capabilities in HEK293 cells, we transfected HA-PTH1R, G $\beta\gamma$ -Ven and mas-GRKct-Luc, and different G α subunits (Gas, G α q, G α 11, G α 14, G α 16, G α i1 and G α i2). Upon PTH stimulation of PTH1R, results show that PTH1R couples strongly to Gas but no other G proteins (Fig 3.1).

RGS14 and NHERF1 do not affect PTHR-Gas coupling or cAMP formation

Next, we focus on PTH1R-Gas coupling and how does the presence of RGS14 alone or with NHERF1 affect signaling. HEK293 cells were transfected with PTH1R, Gas, GBY-Ven and GRK-Luc, and either NHERF1 alone or plus FLAG-RGS14 (Fig 3.2A). Upon PTH stimulation, presence of NHERF1 alone or in combination with RGS14 did not affect PTH1R-Gas activation (Fig 3.2B). Consistent with this finding, RGS14 also did not alter PTH-triggered cAMP production. PTH stimulation of cAMP in cells transfected with the

cAMP BRET sensor CAMYEL, PTHR, and either FLAG-RGS14 alone or NHERF1 plus RGS14 was not significantly altered in the presence of either RGS14 or NHERF1 alone, or when the two proteins were added in combination (Fig. 3.2C).

RGS14 and NHERF1 do not affect PTHR-Gαq coupling but do affect calcium levels

In osteosarcoma-derived osteoblast-like cells treated with PTH lead to the activation of Gαq/11 signaling (Abou-Samra et al., 1992). In HEK293 cells, we do not see PTH activation of Gαq/11 (Fig 3.1). Next, we test to see if the presence of NHERF1 or RGS14 can lead to activation of PTH-Gαq/11. HEK293 cells were transfected with PTH1R and Gq in presence of NHERF1 alone or in combination with RGS14. Upon PTH activation of PTHR-Gαq, no Gβγ release was detected in the presence of RGS14 alone, NHERF1 alone, or in combination RGS14 and NHERF1 (Fig 3.3A). The Gαq/11 signaling pathway has been implicated in PTH-induced inhibition of phosphate reabsorption via NPT2a cotransporter (Bastepe et al., 2017). Here we use a BRET assay in live cells to measure PTH stimulation of Gαq/PLCβ/DAG/IP3/Ca²⁺ by measuring intracellular calcium levels using the CALFLUX-VTN sensor. When transfected HEK293 cells with the calflux-vtn, PTH1R, and Gαq are stimulated with PTH, it leads to an increase of calcium levels measured by BRET (Ven 530/Luc485) (Fig 3.3B). Presence of NHERF1 leads to an increase in early intracellular response while RGS14 decreases overall response (Fig 3.3B). Presence of RGS14 leads to a decrease in calcium levels, and RGS14 plus NHERF1 rescues the calcium levels to an intermediate level when compared NHERF1 or RGS14 alone (Fig 3.3B). Expression of RGS14 and NHERF1 expression in HEK293 cells for calcium BRET studies is confirmed with immunoblots (Figure 3.3E). Next. we tested

the effect of increasing concentrations of RGS14 in HEK293 cells transfected with PTH1R and NHERF1. Results show the increasing concentrations of RGS14 lead to a decrease in PTH-stimulated calcium levels (Fig 3.3C). Opossum kidney (OK) cells endogenously express PTH1R and NHERF1. Using the calcium BRET sensor live cell assay, we can analyze how the presence of RGS14 in this renal physiology relevant model can affect the PTH calcium response. Upon PTH stimulation of OK cells expressed with RGS14, the presence of RGS14 blocks sustained calcium response (Fig 3.3D).

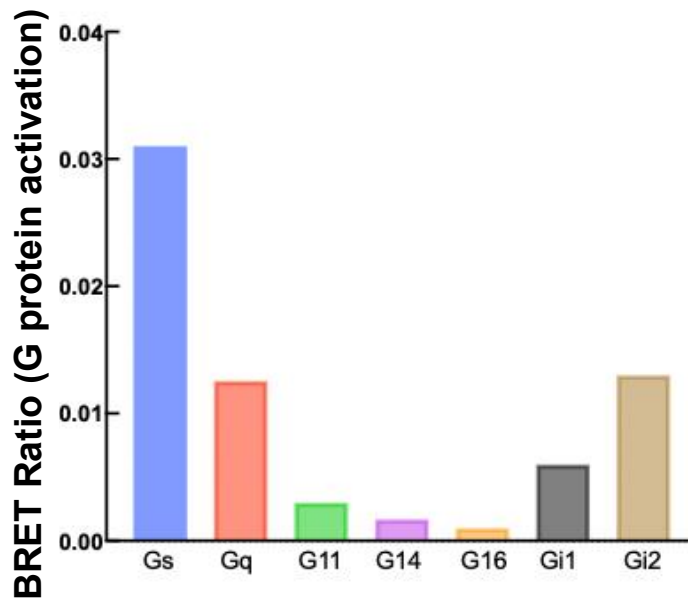


FIGURE 3.1: PTH1R signals strongly through G_s. HEK cells were transfected with 200ng 3×HA-PTH1R, 1000ng G_α, 200ng Venus-G_β1, 200ng Venus-G_γ2, and 200ng mas-GRK3ct-Luciferase. Agonist PTH(1-34) (100 nM) was applied at 30s and signal was recorded at 100s.

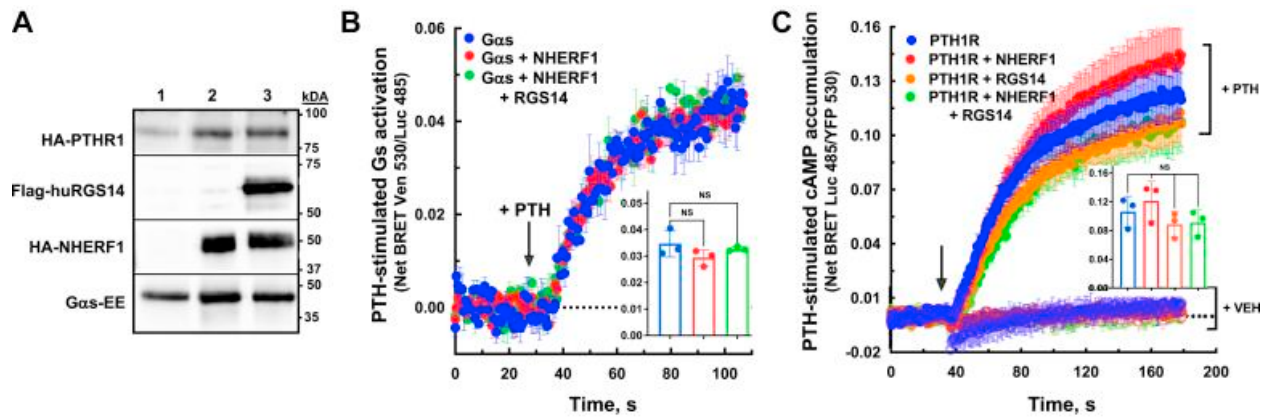


FIGURE 3.2: RGS14 and NHERF1 do not affect PTHR-G α_s coupling or cAMP formation.

A. Expression of proteins used in kinetic BRET studies. **B.** PTH–PTHR coupling to G α_s determined by BRET in live cells. Cells were treated with vehicle (ddH₂O) or 100 nM PTH(1–34) 30 s after measurements began. The hormone-stimulated BRET signal is measured as released Ven-G $\beta\gamma$ binding to membrane-associated mas-GRK3ct-Luc. **C.** PTH–PTHR-stimulated cAMP formation in live cells measured by BRET. HEK293 cells were transfected with cDNA encoding the cAMP BRET sensor CAMYEL and cotransfected with HA-PTHR alone or plus HA-NHERF1, FLAG-RGS14, or both HA-NHERF1 and FLAG-RGS14. About 48 h later, cells were treated with vehicle or 100 nM PTH(1–34) 40 s after initiating BRET measurement. The hormone-stimulated signal is measured as decreased BRET signal upon cAMP binding. Note that the BRET signal is inverted for simplicity. Data shown in A are representative of three separate experiments. Data presented in B and C are the pooled averages with SDs of $n = 3$. One-way ANOVA with Bartlett’s test for multiple comparisons shown as figure insets was made at 60 s (B, $F[2,6] = 0.2421$, $p = ns$) and 120 s (C, $F[3,8] = 1.519$, $p = ns$).

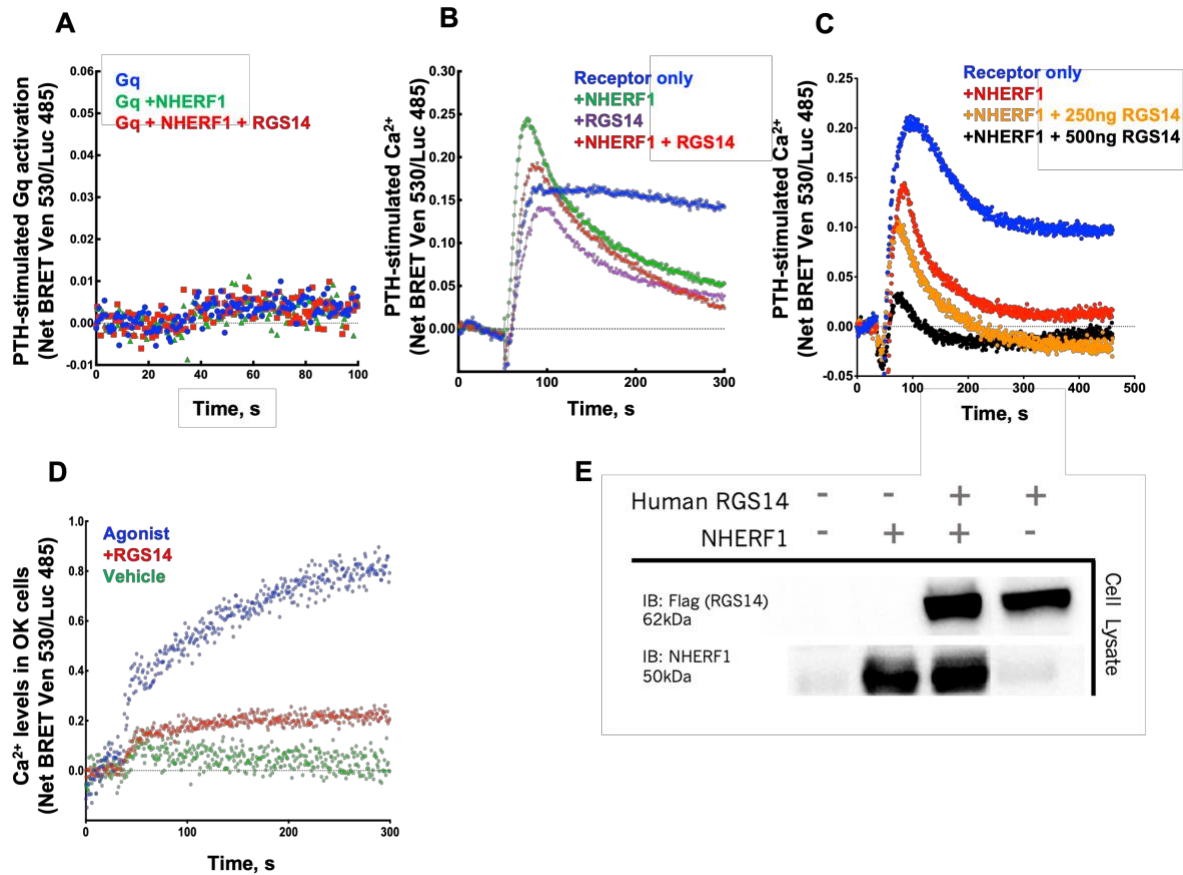


FIGURE 3.3: RGS14 and NHERF1 do not affect PTHR-Gαq coupling but do affect calcium levels. Cells were treated with vehicle (ddH₂O) or 100 nM PTH(1–34) 30 s after measurements began. The hormone-stimulated BRET signal is measured as released Ven-Gβγ binding to membrane-associated mas-GRK3ct-Luc. **A.** PTH–PTHR does not couple strongly to Gαq determined by BRET in live cells. **B.** PTH–PTHR-stimulated calcium formation in live cells measured by BRET. HEK293 cells were transfected calflux and with HA-PTHR alone or plus HA-NHERF1, FLAG-RGS14, or both HA-NHERF1 and FLAG-RGS14. About 48 h later, cells were treated with vehicle or 100 nM PTH(1–34) 30 s after initiating BRET measurement. Presence of NHERF1 increases early intracellular calcium response while RGS14 decreases overall response. **C.** Increasing concentrations of RGS14 in the presence of NHERF1 result in a decrease in calcium levels. **D.** OK cells were transfected with calflux BRET sensor in the presence or absence of Flag-RGS14. Presence of RGS14 causes a decrease in calflux measured signal.

E. Expression of proteins used in calflux BRET studies in HEK293 cells. Data presented in A, B and D is the mean of three separate experiments (n=3). Data presented in C represent an individual replicate (n=1).

3.5 Discussion

RGS14 does not modulate PTH1R-G α s signaling but might play a significant role in PTH1R-G α q-Ca $^{2+}$ signaling

RGS14 is a scaffolding protein that binds many signaling partners (e.g., active Gai/o and inactive Gai1/3 (Cho et al., 2000c; Hollinger et al., 2001b; Shu et al., 2007b), active H-Ras and Rap2A (Shu et al., 2010; Traver et al., 2000a; Vellano et al., 2013b), Ca $^{2+}$ /CaM (Evans et al., 2018c), 14-3-3 γ (Gerber et al., 2018b)). We initially speculated that upstream signaling events leading to the binding of one or more of these partners may serve as a regulatory on/off switch for RGS14 interactions with the NPT2A-NHERF1 and/or PTHR-NHERF1 complexes. Studies by Mahon *et. al.* (Mahon et al., 2002) have demonstrated that PTH1R binds NHERF1 and NHERF2, and that PTH stimulated PTHR in the presence of NHERF2 markedly activates phospholipase C beta and inhibits adenylyl cyclase through stimulation of Gai/o proteins. This unique mechanism, of NHERF2 mediating PTHR G protein signaling sparked our interest on the effect of NHERF1 in PTHR-G protein and how RGS14 may regulate the signaling events. However, our results show that presence of NHERF1 (and/or WT RGS14) does not mediate PTH1R-G α s or G α q protein signaling. It will be important to explore the effect of PTH1R signaling via Gai/o family members in the presence of NHERF1. NHERF1 and NHERF2 are similar proteins with 57% amino acid identity and they have the same domain structure (Boratkó and Csontos, 2013), the 43% difference between the two could explain why NHERF1 does not impact PTH1R-G protein signaling like NHERF2.

Other studies have focused on understanding the role of RGS14 in NPT2A-NHERF1 regulation of PTH-Pi transport in the kidney (See: (Friedman et al., 2022)). Here we

focused on what role RGS14 may exert at the level of the PTHR-G protein signaling. PTH activation of PTHR stimulates G α s-cAMP-PKA signaling and phosphorylation of NHERF1 which, in turn, uncouples NHERF1 from NPT2A thereby inhibiting phosphate uptake (Gattineni and Friedman, 2015). Like RGS14, the PTH receptor also contains a PDZ ligand that binds NHERF1 to stabilize its membrane localization and promote linked G protein signaling (Wang et al., 2010; Wang et al., 2007). We considered whether RGS14 may bind NHERF1 to uncouple it from the PTHR and block PTH signaling. RGS14, however, had no effect on PTHR signaling irrespective of NHERF1 presence. RGS14 notably failed to block PTHR G α s activation or cAMP formation. The effects of NHERF1 and RGS14 were also measured in PTH1R-G α q-Ca $^{2+}$ signaling. Interestingly, presence of NHERF1 increases early calcium response while RGS14 decreases overall response. Overall, our results show that presence of RGS14 causes a decrease in PTH-PTH1R stimulated calcium levels suggesting a blocking effect. This blocking effect is seen when RGS14 is alone or co-transfected with its binding partner NHERF1.

In summary, NHERF1 forms a complex with NPT2A to stabilize the transporter and allow phosphate uptake. RGS14 binds directly to NHERF1 to disrupt the NHERF1-NPT2A complex (Fig. 3.4). Agonist activation of PTH1R blocks phosphate uptake by phosphorylating NHERF1 and leading to a disassembly of the NHERF1-NPT2A complex. RGS14 causes a tonic inhibition of PTH actions on phosphate uptake by disrupting NHERF1 binding to NPT2A. The presence of RGS14 lowers calcium stimulated PTH increase independent of G α q activation. Future studies will explore how RGS14 regulates PTH-directed calcium, and how RGS14 binding to NHERF1 can impact PTH-stimulated

calcium. Possible interpretations and proposed future experiments are outlined in Chapter 4.

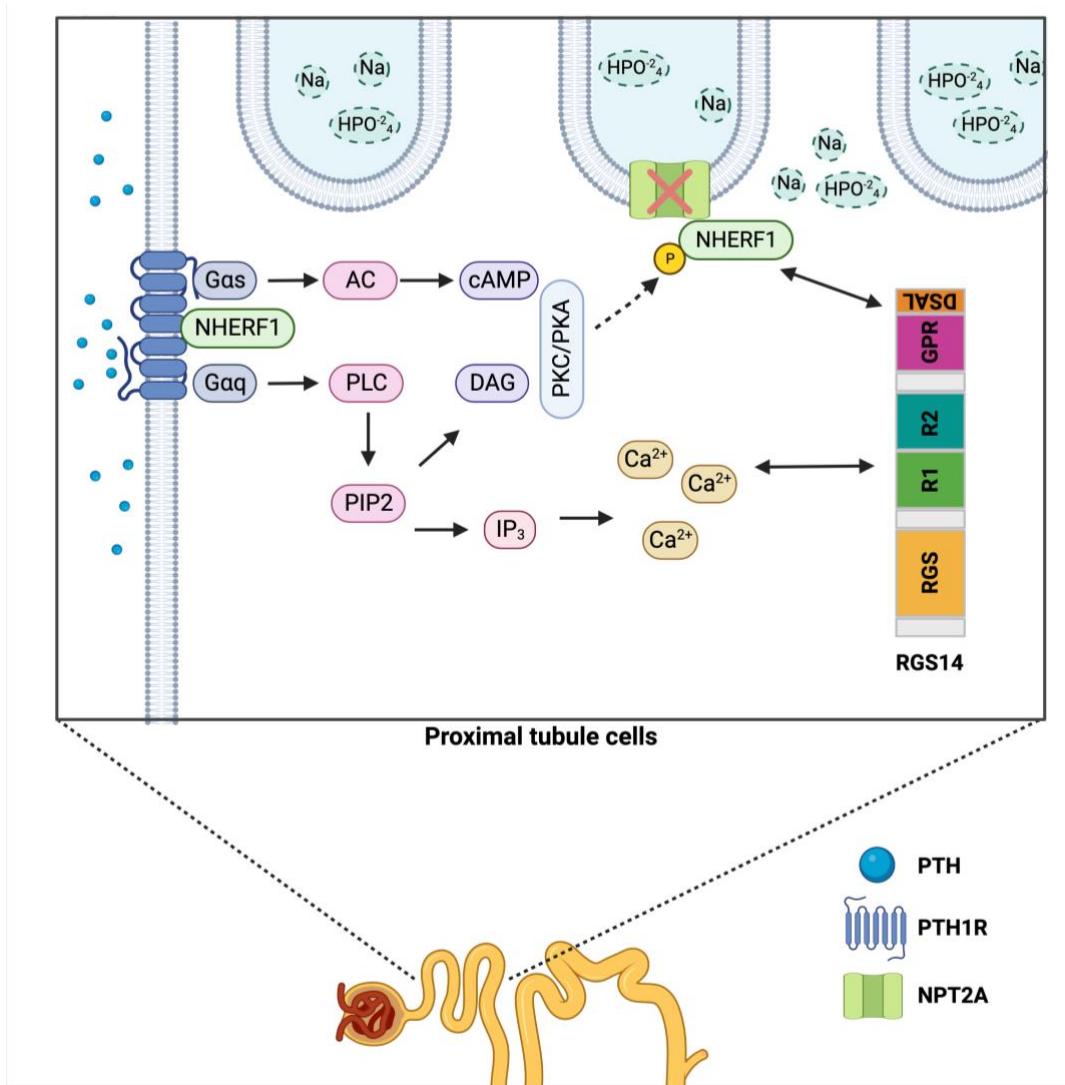


Figure 3.4 RGS14 role in PTH-PTHrP signaling. NHERF1 binds NPT2A at the plasma membrane to allow phosphate uptake into the cell. PTH acting through PTHrP-Gs-cAMP-PKA or PTHrP-Gq-PLC-PIP2-DAG-PKC phosphorylates NHERF1 causing it to dissociate from NPT2A and block phosphate uptake. Human RGS14 binds NHERF1 and stabilizes the NPT2A-NHERF1 complex, blocking PTH actions on phosphate inhibition. PTH-PTH1R-Gq-PLC-PIP2-IP3 leads to an increase in intracellular calcium levels, and presence of RGS14 decreases it.

CHAPTER 4: DISCUSSION AND CONCLUDING REMARKS

4.1 INTRODUCTION

RGS14 has been most extensively studied in the rodent brain (Evans et al., 2014; Evans et al., 2018d; Lee et al., 2010b) where it is highly expressed in regions essential for learning, memory, emotion, and stimulus-induced behaviors (Harbin et al., 2021). Most of our previous studies have centered on RGS14 roles in suppressing synaptic plasticity in hippocampal area CA2 (Evans et al., 2018d; Lee et al., 2010b). RGS14 controls synaptic signaling by binding proteins that are essential for plasticity, such as active Gai/o-GTP (Cho et al., 2000d; Hollinger et al., 2001a), Rap1 (Traver et al., 2000b), Rap2 (Traver et al., 2000b), H-Ras (Shu et al., 2010; Vellano et al., 2013a; Willard et al., 2009), 14-3-3 (Gerber et al., 2018a), calcium/calmodulin (Ca²⁺/CaM) and Ca²⁺/CaM-dependent kinase II (CaMKII) (Evans et al., 2018b), and inactive Gai1/3-GDP (Hollinger et al., 2001a; Kimple et al., 2001; Mittal and Linder, 2004). GWAS studies have identified variants in RGS proteins that are associated to diseases. These include RGS14 linked to glioblastoma (Yin et al., 2019), RGS10 associated to non-muscle invasive bladder cancer (Lee et al., 2013a), and RGS4 gene associated to psychiatric illness (Schwarz, 2018), among others. Due to the involvement of RGS proteins in complex diseases, genetic variants that cause a loss-of-function or a gain-of-function could potentially disrupt cellular equilibrium. However, determining the significance of these genetic variants in disease states (pathology) and different human traits (physiology) remains a challenge. In my studies, I applied for the first time a novel bioinformatic tool (3DMTR analysis) that compares the observed proportion of missense variation to the expected proportion given the protein-coding region of interest in 3D space. I used this tool to identify sensitive regions within the RGS domain of 15 members of the 20 highly evolutionary conserved

RGS protein family. Our analysis was limited to those RGS proteins with reported solved structure. I further expanded my studies to examine the functional effects of cancer-linked mutations in sensitive residues of RGS14, RGS10 and RGS4, and tested the capacity of 3D-MTR as a new bioinformatics tool to correctly predict key residues important for function. We found that 3D-MTR is a useful tool bioinformatics tool for this purpose.

In addition, RGS14 has been linked to kidney disease(Guan et al., 2021) where it is thought to play a crucial role in kidney phosphate transport. In the kidney, PTH acts on PTH1R and plays a role in calcium and phosphate homeostasis by increasing calcium reabsorption and inhibiting phosphate reabsorption (Khan et al., 2022). My studies expanded on RGS14 function on PTH1R-G protein signaling, Gas-AC-cAMP and Gq-PLCB-Ca²⁺. PTH controls serum phosphate by inhibiting NPT2A in the kidney and promoting regulated phosphate excretion. RGS14 blocks PTH action by acting as an regulated on/off switch for PTH and controlling NPT2A-mediated phosphate uptake. Since disorders of calcium and phosphate metabolism happen when calcium and phosphate levels deviate from basal condition leading to hypo/hyperphosphatemia or hypo/hypercalcemia (Sun et al., 2020), my studies focused on understanding how RGS14 regulates phosphate uptake and calcium downstream of PTH1R-G protein signaling. The studies explained above add to the field of RGS protein signaling by expanding on the role of RGS14/RGS10/RGS4 and the effect of naturally occurring mutants in signal transduction. Each of these findings will be discussed below.

4.2. DISCUSSION AND FUTURE DIRECTIONS

3DMTR and RGS mutations

Computational tools have been developed to predict variant effects with limited success (Schulz et al., 2015). Prioritizing which somatic mutations to test based on their predicted functional consequence is still an obstacle in biomedical research. Recently, a novel tool known as 3DMTR with a permutation analysis (Perszyk et al., 2021) has been developed but not yet widely tested. Research efforts focused on condensing large single-nucleotide variation within genes by giving scores to each residue based on a missense tolerance ratio (MTR). The MTR score equates the observed proportion of missense variation to the expected proportion given the protein-coding sequence of interest (Traynelis et al., 2017). However, the updated 3DMTR calculates the MTR for neighboring residues over a 3D distance from crystallography and cryo-EM data (Perszyk et al., 2021). Even so, this method can't be applied to the whole genome because structural data is not available for all proteins. This new approach makes this tool a more accurate diagnostic tool. The permutation analysis identifies the most significantly intolerant and tolerant residues by estimating the likelihood of a specific score in a given data set by providing a distribution of the possible scores that each residue can have (Perszyk et al., 2021).

For my main dissertation project, I applied for the first time the novel 3DMTR to the highly evolutionary conserved RGS protein family and identified sensitive regions within the RGS domain. RGS proteins are crucial for achieving physiological relevant timing and extent GPCR signaling (Hollinger and Hepler, 2002; Masuho et al., 2020) and loss of RGS mediated control leads to a range of pathologies observed in mouse models (Deng et al., 2012; Foster et al., 2021; Lee et al., 2010a; Rorabaugh et al., 2018; Vatner et al., 2018)

and associated with human disease (Squires et al., 2018b). GPCRs can only signal through the same limited amount of G proteins that they can activate, and RGS proteins selectively recognize and regulate specific G α proteins based on bar codes (specific binding residues) (Masuho et al., 2020). Naturally occurring variants and mutations affect RGS selectivity and may contribute to pathological dysregulation of GPCR signaling and variable response to drug treatments.

Using the 3DMTR permutation analysis, we were able to identify sensitive regions within the conserved RGS domain for 15/20 RGS proteins that had an available protein structure (Fig 4.1). The 3DMTR analysis predictive capabilities was compared with other bioinformatic tools. 3DMTR was the most accurate at predicting intolerant residues of a protein that if mutated would lead to deleterious effects and change-of-function phenotypes. RGS14, RGS10 and RGS4 were selected to study further.

Bioinformatic tools use algorithms to predict the pathogenic potential of reported somatic mutations. Using COSMIC, we were able to locate somatic mutations that overlap with residues in the RGS domain of RGS14, RGS10 and RGS4 identified by the 3DMTR to be either more sensitive or less sensitive to mutations. The effect of RGS mutations was tested downstream of GPCR activation. For RGS14, four mutations were tested, two were scored as tolerant (S127P and D137Y) (Fig. 2.3C-2.3F) and two as intolerant (R173C and R173H) (Fig. 2.3G-2.3J). Three of the four somatic mutations found in tolerant and intolerant residues of RGS14 as defined by 3DMTR behaved as predicted. Mutant D137Y inhibited agonist activation of α 2AR-Gao, and bound active Gao, whereas mutants S127P, R173H and R173C all failed to bind Gao. In the cAMP assay, intolerant mutant R173C in RGS14 lost capacity to reverse G protein inhibition of cAMP, whereas

tolerant mutant D137Y showed a robust capacity to enhance cAMP accumulation (Fig. 2.6D). When assessing the effect of WT RGS14 and mutants on forskolin-stimulated cAMP production directly, in the absence of agonist-activated GPCR-Gai/o inhibition, WT RGS14 (Fig. 2.7B) did not show an inhibition of FSK-stimulated cAMP levels. Interestingly, tolerant mutant D137Y in RGS14 showed a robust increase in cAMP levels in the absence of agonist-stimulated Gi/o-coupled receptor (Fig. 2.7B).

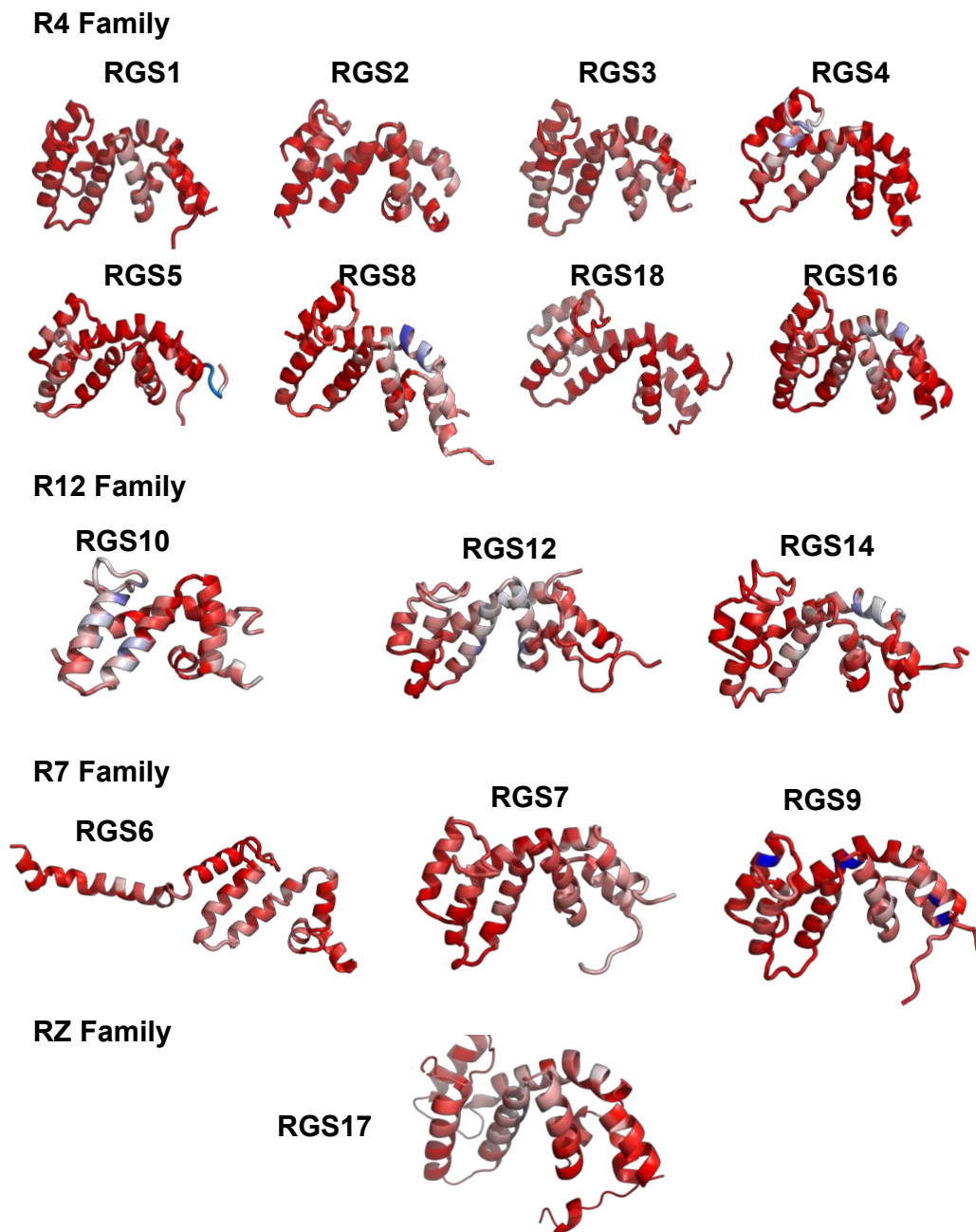


Figure 4.1. The 3DMTR permutation analysis identifies intolerant and tolerant residues within the RGS domain of RGS proteins. Structural view of the heatmap of the 21-residue 3DMTR score. Intolerant residues are identified in blue, neutral in white, and tolerant in red.

In the case of RGS10, two somatic mutations were tested which were scored by 3DMTR as either tolerant (S64T) (Fig. 2.4C-2.4D) or intolerant (K89M) (Fig. 2.4E-2.4F). Somatic mutations within the tolerant/intolerant residues of RGS10 exhibited phenotypes inconsistent with the 3DMTR prediction. In the cAMP assay, tolerant mutation S64T in RGS10 acted like WT RGS10, opposite to the effects in receptor-directed G protein activation and G protein binding (Fig. 2.4B-2.4D), while intolerant mutant K89M showed a robust capacity to enhance cAMP accumulation (Fig. 2.6E). Forskolin-stimulated cAMP results showed tolerant mutant S64T in RGS10 showed an increase in cAMP levels when compared to WT RGS10 that had no effect (Fig. 2.7C).

For RGS4, three somatic mutations were tested which were scored as either intolerant (K125Q and E126K) (Fig. 2.5C-2.5F) or tolerant (E135K) (Fig. 2.5G-2.5H). Intolerant mutants K125Q and E126K exhibit partial loss-of-function phenotypes (Fig. 2.5C-2.5F), largely failing to inhibit G α o activation, whereas tolerant mutation E135K (Fig. 2.5G-2.5H) behaved as wild type RGS4. Mutants K125Q and E135K each bound active G α o, whereas mutant E126K did not bind. In the cAMP assay, Intolerant mutant E126K in RGS4 lost the capacity to reverse G-protein inhibition of cAMP, while tolerant mutant E135K acted like RGS4 WT (Fig. 2.6F). Mutations in E126K and E135K of RGS4 showed similar results to the effects shown for WT RGS4 in forskolin-stimulated cAMP in the absence of agonist-activated GPCR-G α i/o inhibition (Fig. 2.7D).

The 3DMTR bioinformatic tool can be used to not only look at RGS proteins, but also proteins involved in other polygenic diseases. We can implement this tool to prioritize which mutations to test that can have a potential role in disease progression. The 3DMTR, when compared to its ancestor 1DMTR, has been greatly improved but was not perfect

in its predictive power. When compared to other bioinformatic tools, 3DMTR was the most accurate at predicting change-of-function. This novel tool can detect functionally relevant consequences of mutations in highly intolerant residues. In the future, the 3DMTR will develop into a more precise tool as the Genome Aggregation Database (gnomAD) expands with more human variant information, and the analysis will become more accurate leading to an improved predictive potential.

The role of GPCR-G protein mechanism in cancer have been identified in cancerous tissues where they mediate oncogenesis (Gutkind, 1998; Hurst and Hooks, 2009). Genome sequencing techniques have shown that the components of the GPCR-G protein axis are frequently mutated in cancer. However, less is known about the role RGS proteins play in GPCR-G protein signaling in cancer. In our study we use the information generated by the COSMIC database and the 3DMTR analysis to choose what somatic mutations to analyze using different functional assays. Here I show that some somatic mutations lead to a loss of GAP function and can speculate that these contribute to oncogenesis.

For future studies, I would like to expand on the effect of RGS change-of-function mutations (RGS14-S127P/R173C/R173H, RGS10-S64T/K89M, RGS4-K125Q/E126K) vs WT in cancer cell proliferation. The α 2AR has been characterized in breast tumor cells lines (Vazquez et al., 1999) and has been associated with increased cell proliferation in vitro (Vazquez et al., 2006) and increased tumor growth in vivo (Bruzzone et al., 2008). Studies have described the impact of α 2AR antagonist (rauwolscine) as an inhibitor of tumor growth and cell proliferation (Bruzzone et al., 2011). Using a proliferation assays, we would first examine the expression of WT RGS (RGS14, RGS10 and RGS4) proteins

in human breast cancer cell lines where $\alpha 2AR$ has been described to be expressed. Next, we would express the RGS mutants of interest and measure the effect of these mutants on cell proliferation in the presence or absence of the $\alpha 2AR$ antagonist. In addition, ERK signaling pathway is associated with cell proliferation and tumor growth as well. We would measure ERK phosphorylation in extracts from cancer cells and analyze the effect of the mutants on ERK activation. These experiments will help us further characterize the effect of RGS cancer-associated mutations in GPCR-G protein signaling.

While performing these studies, I made an unexpected discovery tangential to our main focus. I found preliminary evidence that RGS proteins can inhibit receptor-G α s stimulated adenylyl cyclase activity (Figure 4.2). These findings are very preliminary but warrant further study. Future studies will explore the role of RGS proteins (RGS14, RGS10, RGS4) on G $\alpha_{i/o}$ /G α_s -directed regulation of adenylyl cyclase (AC) activity. The results published on Chapter 2 focused on understanding the effect of RGS proteins and select mutants in $\alpha 2AR$ -G $\alpha_{i/o}$ inhibition of cAMP. Initially, I used a live cell $\alpha 2AR$ -G α_o model to test the effects of RGS protein mutants, although studies have shown that $\alpha 2AR$ can couple to G α_s as well (Wade et al., 1999). Under certain conditions $\alpha 2AR$ appears to both inhibit or stimulate intracellular cAMP (Eason et al., 1992; Fraser et al., 1989; Jones et al., 1991), or have a biphasic responses on AC activity displaying both inhibitory and stimulatory components (Eason et al., 1992). However, the molecular mechanisms for $\alpha 2AR$ signaling promiscuity at G $\alpha_{i/o}$ and G α_s are not well understood (Xu et al., 2022). My preliminary results in HEK293 cells (Fig 4.2A) show that upon $\alpha 2AR$ agonist stimulation, the presence of pertussis toxin (PTX) leads to an increase in G α_s -activation. Surprisingly, WT RGS10 and WT RGS14 inhibit $\alpha 2AR$ stimulated cAMP accumulation in

the presence of PTX treatment (100ng/mL) (Fig.4.2B). These unexpected results need to be expanded to determine if RGS proteins bind to Gas, inhibit Gas activation, and understand their role in AC-cAMP accumulation. We also examined RGS proteins on forskolin-stimulated cAMP production directly, in the absence of agonist-activated GPCR-Gai/o inhibition. RGS actions on AC have not been extensively studied. Our results on RGS mutants' effect on forskolin-stimulated AC raise the question of whether RGS proteins in general regulate AC differently with forskolin or GPCR-Gas activation. We can expand on these studies by looking at the interaction of AC and RGS proteins in the presence or absence of FSK. These studies can be done by using static BRET to determine direct association of RGS proteins with AC.

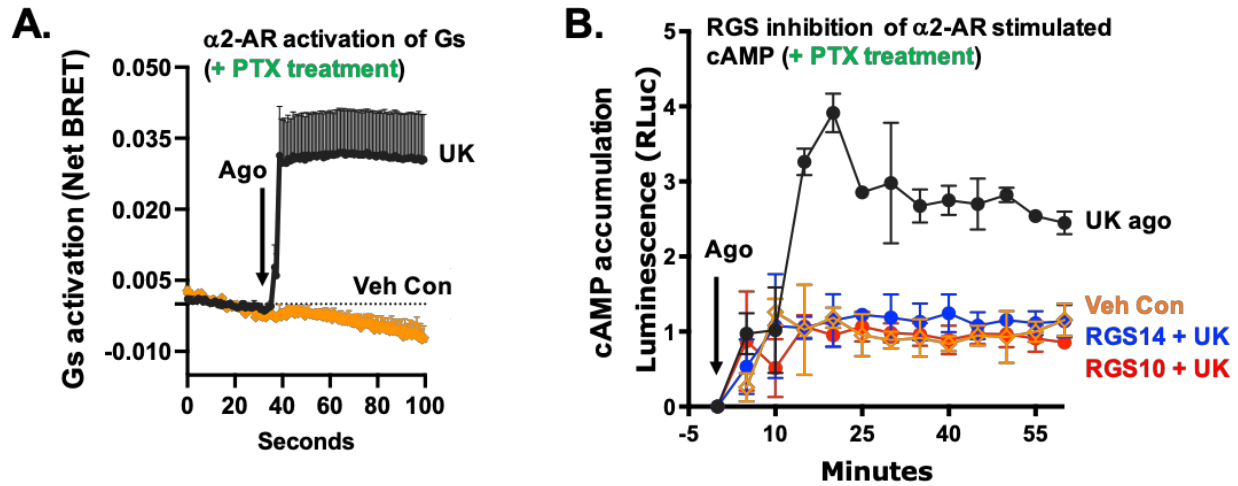


Figure 4.2. α 2AR signals via G α s in HEK cells and RGS14/RGS10 inhibit G α s-stimulated-cAMP accumulation. A) HEK cells were transfected with α 2AR + G α s, BRET biosensors, and treated with PTX (100ng/mL) overnight. Cells then were stimulated with 100 μ M α 2AR agonist UK or vehicle (DMSO) and BRET signal was measured. (B) HEK cells were transfected with cAMP Glo sensor, α 2AR, RGS and treated with PTX overnight. Cells then were stimulated with α 2AR agonist or vehicle, and cAMP luminescence was measured for 1 hr.

RGS14 regulation of PTHR-calcium signaling

PTHR signaling has been reported to be mediated by Gas, Gαq/11, Gai and Gα12/13 depending on the organ/cell type and experimental set-up (Gardella and Vilaradaga, 2015), but this coupling mechanism remains unclear. PTHR1 binds the adaptor protein NHERF1 which may serve as a switch to control PTHR1 signaling by Gas, Gαq/11 and Gai (Mahon et al., 2002; Wang et al., 2013). However, my findings show that RGS14 binds NHERF1 (Friedman et al., 2022), and that the presence of RGS14 does not affect PTH1R signaling through Gas or Gαq/11. For future studies, we want to expand on PTH1R coupling to other G proteins to include other Gαq family members (Gα11, Gα14, Gα16), Gai family members (Gai2, Gai3, Gao) and Gα12/13 and if the presence of RGS14 and NHERF1 controls PTH1R-G protein selectivity.

PTH activates Ca²⁺/PKC systems in addition to cAMP, and extracellular calcium influences renal phosphate absorption (Sneddon et al., 2000). In distal convoluted tubule cells, PTH reduces calcium excretion by stimulating calcium absorption (Costanzo and Windhager, 1980; Sneddon et al., 2000). In proximal tubule cells, PTH inhibits phosphate transport by involving calcium signaling but not stimulating calcium transport (Friedman et al., 1996). PTH activates phosphatidylinositol-specific phospholipase C (PI-PLC) linked to IP3 formation that causes an increase of intracellular calcium (Friedman et al., 1999). In distal tubule cells, PTH stimulates calcium transport without calcium signaling (Friedman et al., 1996).

In future studies, we will use OK cells to further explore the role of RGS14 in calcium signaling. My studies show PTHR1 stimulates calcium but does not couple to

Gαq. I want to examine if a G protein pathway is mediating PTH stimulated calcium levels involving other Gαq family members (G11, G14, G16) or Gi family members via Gβγ release. We will treat OK cells with pertussis toxin, and PTHR-Ca²⁺ will be stimulated with agonist. This will allow me to determine if PTH1R stimulated calcium is due to Gi/o activation or perhaps other Gαq family members. Once we determine whether G protein pathway leads to PTH stimulated calcium we can explore the role of RGS14 in this process.

RGS14 regulation of PTHR calcium signaling may be independent of G protein signaling. As such, I also want to explore if RGS14 impacts calcium flux at the extracellular or intracellular level. Initial studies will chelate extracellular calcium to determine if PTHR-stimulated calcium increases are exclusively from extracellular sources, intracellular stores, or both. Hormone activation of receptors coupled to PLC results in IP₃ production that stimulates a biphasic calcium signaling process (Bird et al., 2008). In this process calcium is released from intracellular organelles, followed by entry of calcium ions across the plasma membrane. Using genetically encoded calcium indicators (GECI) will allow for measurement of calcium dynamics in specific locations within living cells (McCombs and Palmer, 2008). GECIs can be targeted to a specific cellular localization by attaching a signal sequence to the calcium sensor. Using GECI targeted to nucleus, Golgi, mitochondria, plasma membrane and ER, we can detect where the calcium signaling is found in OK cells. Using the OK cell system, PTH stimulation will lead to an increase in signal, allowing quantification of calcium levels at a specific cellular localization. Next, I can determine the signaling change and specific localization in the presence or absence of overexpressed RGS14.

In neuronal cells, RGS14 inhibits calcium influx from CaV1 (L-type) voltage-gated calcium channels (VGCCs) (Martin-Montanez et al., 2010) and from ionotropic glutamate receptors (Evans et al., 2018d). Whether these actions of RGS14 are direct or indirect are unknown currently. Results in Chapter 3 show that the presence of RGS14 decreases overall PTH stimulated calcium response in HEK cells (Fig 3.3B) and in OK cells (Fig. 3.3D). In the proximal and distal convoluted tubules where RGS14 is localized (Friedman et al., 2022), Cav1.2 (L-type) calcium channels and transient receptor potential family member (TRP) calcium channels are found in the plasma membrane (Zhou and Greka, 2016). In renal cells, calcium uptake into the endoplasmic reticulum (ER) is mediated by Sarcoplasmic/ER Ca²⁺-ATPase (SERCA) pumps (Park et al., 2021) and Ca²⁺ emptying of the ER activates store-operated calcium (SOC) channels and calcium channel protein 1 (ORAI1) at the plasma membrane via the Ca²⁺ sensor Stromal Interaction Molecule 1 (STIM1) stimulating extracellular Ca²⁺ entry (Chaudhari et al., 2021). Cellular calcium homeostasis relies on the influx of calcium through the mentioned above channels in the plasma membrane, and internal calcium stores (ER, mitochondria (MIT), and golgi) (Park et al., 2021; Yang et al., 2018). We will explore calcium handling channels (e.g. ORAI1, SERCA, others that mediate the calcium flux in the presence or absence of RGS14 (Bagur and Hajnoczky, 2017). This assay will use calcium channel inhibitors and a calcium indicator (GCaMP6m-XC:(Yang et al., 2018)) to monitor cytosolic, or submembrane calcium levels (Fig 4.3A). Using OK cells, calcium influx can be measured in the presence and absence of RSG14 in complex with NHERF1 upon PTH stimulation.

In the kidney, CaSR (calcium sensing-receptor) senses extracellular levels of calcium ions and maintains calcium homeostasis by controlling PTH secretion and renal

calcium reabsorption and urinary calcium excretion (Abid et al., 2021). Ligand activation of CaSR inhibits PTH-dependent phosphate uptake (Ba et al., 2003). A recent publication from our lab in collaboration with the Friedman lab showed presence of RGS14 inhibits PTH-dependent phosphate uptake (Friedman et al., 2022). There is also coordinated modulation of the expression and brush border localization of CaSR and NPT2A in rats following chronic exposure to PTH (Riccardi et al., 2000). Since the CaSR plays a role in extracellular calcium homeostasis and phosphate homeostasis, maybe the presence of RGS14 linked to CaSR influences renal phosphate reabsorption (indirect of PTHR) (Fig. 4.3B). Using HEK cells, CaSR and RGS14 can be overexpressed in the presence or absence of NHERF1 and NPT2A to examine if RGS14-CaSR can be recovered as stable complex in immunoprecipitation studies. Immunoprecipitation studies can then be repeated in human kidney cells. Since our previous studies showed that RGS14 does not regulate phosphate uptake via PTH1R activation, these proposed experiments will explore if the effect of RGS14 in phosphate uptake are potentially via a complex with CaSR.

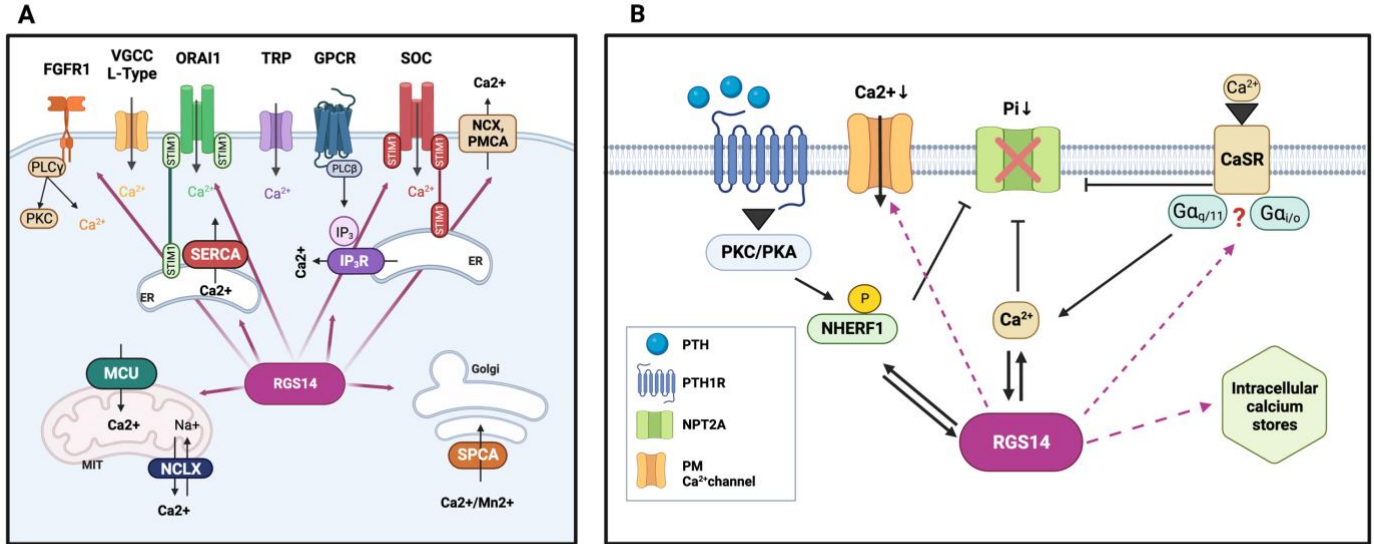


Figure 4.3. Model Figure: Possible mechanisms by which RGS14 inhibits phosphate uptake and regulates calcium flux in kidney cells. A. Cellular calcium is mediated by channels in the plasma membrane and intracellular stores. At the plasma membrane (PM) active transport of calcium occurs via PMCA pumps. Permeable voltage gated calcium channels (VGCC) and transient receptor potential family members (TRP) have constituent activity in some cells. Calcium levels can also be regulated by store release from the endoplasmic reticulum (ER) by IP₃ receptors (IP₃R). Depletion of intracellular Ca²⁺ stores is detected by the calcium sensor stromal interaction molecule (STIM1) that activates Ca²⁺ release activating the calcium channel protein 1 (ORAI1)-dependent calcium influx pathway and store-operated channels (SOC) to promote calcium store refilling through the Sarcoplasmic/ER Ca²⁺-ATPase (SERCA) pump. Calcium sequestration into the Golgi occurs via the secretory pathway Ca²⁺ ATPase (SPCA). Other calcium transporting proteins such as the mitochondrial calcium uniporter (MCU) and the Na/ Ca²⁺ exchanger (NCLX) can transport calcium into the cytoplasm. RGS14 could be regulating the calcium homeostasis inside the cell by mediating some of these pathways. **B.** PTH action through PTHR-PKA/PKC phosphorylates NHERF1 causing to dissociate from NPT2A and block

phosphate uptake. RGS14 binds NHERF1 and presence of RGS14 blocks PTH-phosphate uptake. RGS14 could potentially regulate PTH inhibition of NT2A phosphate uptake by regulating CaSR signaling. RGS14 is also expected to regulate calcium flux via plasma membrane channels or intracellular store channels. RGS14 is well positioned to modulate phosphate and calcium levels in the kidney suggesting that human variants associated with kidney disease are due to aberrant regulation of these pathways.

4.3 CONCLUDING REMARKS

The findings presented in this thesis have advanced our understanding of the role of RGS14 in signaling pathways outside of the brain, and the effect of human variants in RGS function. My studies expanded on the role of RGS proteins in GPCR-G protein pathways linked to disease, such as $\alpha 2AR$ in oncogenicity and PTH1R in renal phosphate uptake linked to chronic kidney disease. Genetic diversity makes us unique, however some variants can lead to negative biological functions. Advancements in the genomic field are rapidly identifying gene variants in human protein sequences, some are more likely to be pathogenic than others. The novel 3DMTR discussed in this document helps prioritize which variants to test. Human variants in sensitive regions of the protein impact cellular and organ physiology, and pharmacological responses.

Single point variants can have a great consequence in functional output, affecting the duration of the GPCR-G protein signaling cascade. Here I show the use of a combination of bioinformatic tools (COSMIC database and 3DMTR analysis) to detect important residues that overlap with disease linked genetic variants and prioritize which to functionally assess. We also explored the effect of cancer somatic mutations in RGS proteins in $\alpha 2AR$ signaling cascade. Future experiments will expand on the phenotype of these human variants in $\alpha 2AR$ cell proliferation and the relationship with tumor progression. In addition, the information gathered by the 3DMTR analysis and COSMIC database can be used to explore the effect of RGS somatic mutations in other GPCR signaling pathways related to disease. RGS14 linkage to kidney disease has motivated us to explore the role of this complex multi-signaling pathway protein in the context of kidney basal conditions. We expanded on the role of RGS14 in PTH1R signaling and

determined that upon PTH stimulation the presence of RGS14 decreases calcium levels. Future studies will uncover RGS14 mechanism in PTH stimulated calcium signaling and if mutations found in chronic kidney disease patients affect the native role of RGS14 in renal physiology.

BIBLIOGRAPHY

Abid HA, Inoue A and Gorvin CM (2021) Heterogeneity of G protein activation by the calcium-sensing receptor. *J Mol Endocrinol* **67**:41-53.

Abou-samra ab, juppner h, force t, freeman mw, kong xf, schipani e, urena p, richards j, bonventre jv, potts jt, jr. And et al. (1992) expression cloning of a common receptor for parathyroid hormone and parathyroid hormone-related peptide from rat osteoblast-like cells: a single receptor stimulates intracellular accumulation of both camp and inositol trisphosphates and increases intracellular free calcium. *Proc natl acad sci u s a* **89**:2732-2736.

Agudelo lz, ferreira dms, cervenka i, bryzgalova g, dadvar s, jannig pr, pettersson-klein at, lakshmikanth t, sustarsic eg, porsmyr-palmertz m, correia jc, izadi m, martinez-redondo v, ueland pm, midttun o, gerhart-hines z, brodin p, pereira t, berggren po and ruas jl (2018) kynurenic acid and gpr35 regulate adipose tissue energy homeostasis and inflammation. *Cell metab* **27**:378-392 e375.

Ahlers ke, chakravarti b and fisher ra (2016) rgs6 as a novel therapeutic target in cns diseases and cancer. *Aaps j* **18**:560-572.

Ahlers-dannen ke, spicer mm and fisher ra (2020) rgs proteins as critical regulators of motor function and their implications in parkinson's disease. *Mol pharmacol* **98**:730-738.

Ajit sk and young kh (2005) analysis of chimeric rgs proteins in yeast for the functional evaluation of protein domains and their potential use in drug target validation. *Cell signal* **17**:817-825.

Ali mw, cacan e, liu y, pierce jy, creasman wt, murph mm, govindarajan r, eblen st, greer sf and hooks sb (2013) transcriptional suppression, dna methylation, and histone deacetylation of the regulator of g-protein signaling 10 (rgs10) gene in ovarian cancer cells. *Plos one* **8**:e60185.

Alqinyah m, almutairi f, wendimu my and hooks sb (2018) rgs10 regulates the expression of cyclooxygenase-2 and tumor necrosis factor alpha through a g protein-independent mechanism. *Mol pharmacol* **94**:1103-1113.

Altman MK, Alshamrani AA, Jia W, Nguyen HT, Fambrough JM, Tran SK, Patel MB, Hoseinzadeh P, Beedle AM and Murph MM (2015) Suppression of the gtpase-activating protein RGS10 increases Rheb-GTP and mtor signaling in ovarian cancer cells. *Cancer Lett* **369**:175-183.

Anderson GR, Posokhova E and Martemyanov KA (2009) The R7 RGS protein family: multi-subunit regulators of neuronal G protein signaling. *Cell Biochem Biophys* **54**:33-46.

- Arang N and Gutkind JS (2020) G Protein-Coupled receptors and heterotrimeric G proteins as cancer drivers. *FEBS Lett* **594**:4201-4232.
- Ashrafi A, Garcia P, Kollmus H, Schughart K, Del Sol A, Buttini M and Glaab E (2017) Absence of regulator of G-protein signaling 4 does not protect against dopamine neuron dysfunction and injury in the mouse 6-hydroxydopamine lesion model of Parkinson's disease. *Neurobiol Aging* **58**:30-33.
- Ba J, Brown D and Friedman PA (2003) Calcium-sensing receptor regulation of PTH-inhibitable proximal tubule phosphate transport. *Am J Physiol Renal Physiol* **285**:F1233-1243.
- Bagur R and Hajnoczky G (2017) Intracellular Ca(2+) Sensing: Its Role in Calcium Homeostasis and Signaling. *Mol Cell* **66**:780-788.
- Bastepe M, Turan S and He Q (2017) Heterotrimeric G proteins in the control of parathyroid hormone actions. *J Mol Endocrinol* **58**:R203-R224.
- Bastin G, Singh K, Dissanayake K, Mighiu AS, Nurmohamed A and Heximer SP (2012) Amino-terminal cysteine residues differentially influence RGS4 protein plasma membrane targeting, intracellular trafficking, and function. *J Biol Chem* **287**:28966-28974.
- Beadling C, Druey KM, Richter G, Kehrl JH and Smith KA (1999) Regulators of G protein signaling exhibit distinct patterns of gene expression and target G protein specificity in human lymphocytes. *J Immunol* **162**:2677-2682.
- Bennett ML, Bennett FC, Liddel SA, Ajami B, Zamanian JL, Fernhoff NB, Mulinyawe SB, Bohlen CJ, Adil A, Tucker A, Weissman IL, Chang EF, Li G, Grant GA, Hayden Gephart MG and Barres BA (2016) New tools for studying microglia in the mouse and human CNS. *Proc Natl Acad Sci U S A* **113**:E1738-1746.
- Benovic JL, Shorr RG, Caron MG and Lefkowitz RJ (1984) The mammalian beta 2-adrenergic receptor: purification and characterization. *Biochemistry* **23**:4510-4518.
- Berman DM, Wilkie TM and Gilman AG (1996) GAIP and RGS4 are GTPase-activating proteins for the Gi subfamily of G protein alpha subunits. *Cell* **86**:445-452.
- Bernardinelli Y, Nikonenko I and Muller D (2014) Structural plasticity: mechanisms and contribution to developmental psychiatric disorders. *Front Neuroanat* **8**:123.
- Bernstein LS, Grillo AA, Loranger SS and Linder ME (2000) RGS4 binds to membranes through an amphipathic alpha-helix. *J Biol Chem* **275**:18520-18526.
- Bernstein LS, Ramineni S, Hague C, Cladman W, Chidiac P, Levey AI and Hepler JR (2004) RGS2 binds directly and selectively to the M1 muscarinic acetylcholine receptor third intracellular loop to modulate Gq/11alpha signaling. *J Biol Chem* **279**:21248-21256.

- Bird CM and Burgess N (2008) The hippocampus and memory: insights from spatial processing. *Nat Rev Neurosci* **9**:182-194.
- Bird GS, DeHaven WI, Smyth JT and Putney JW, Jr. (2008) Methods for studying store-operated calcium entry. *Methods* **46**:204-212.
- Bliss-Moreau E, Bauman MD and Amaral DG (2011) Neonatal amygdala lesions result in globally blunted affect in adult rhesus macaques. *Behav Neurosci* **125**:848-858.
- Bodenstein J, Sunahara RK and Neubig RR (2007) N-terminal residues control proteasomal degradation of RGS2, RGS4, and RGS5 in human embryonic kidney 293 cells. *Mol Pharmacol* **71**:1040-1050.
- Boratkó A and Csontos C (2013) NHERF2 is crucial in ERM phosphorylation in pulmonary endothelial cells. *Cell Communication and Signaling* **11**:99.
- Bourne HR, Sanders DA and McCormick F (1990) The GTPase superfamily: a conserved switch for diverse cell functions. *Nature* **348**:125-132.
- Branch MR and Hepler JR (2017) Endogenous RGS14 is a cytoplasmic-nuclear shuttling protein that localizes to juxtannuclear membranes and chromatin-rich regions of the nucleus. *PLoS One* **12**:e0184497.
- Broadbent NJ, Gaskin S, Squire LR and Clark RE (2010) Object recognition memory and the rodent hippocampus. *Learn Mem* **17**:5-11.
- Broadbent NJ, Squire LR and Clark RE (2004) Spatial memory, recognition memory, and the hippocampus. *Proc Natl Acad Sci U S A* **101**:14515-14520.
- Brown NE, Goswami D, Branch MR, Ramineni S, Ortlund EA, Griffin PR and Hepler JR (2015) Integration of G protein alpha (Galpha) signaling by the regulator of G protein signaling 14 (RGS14). *J Biol Chem* **290**:9037-9049.
- Brown NE, Lambert NA and Hepler JR (2016a) RGS14 regulates the lifetime of Galpha-GTP signaling but does not prolong Gbetagamma signaling following receptor activation in live cells. *Pharmacol Res Perspect* **4**:e00249.
- Brown NE, Lambert NA and Hepler JR (2016b) RGS14 regulates the lifetime of Galpha-GTP signaling but does not prolong G $\beta\gamma$ signaling following receptor activation in live cells. *Pharmacol Res Perspect* **4**:e00249.
- Brown RB and Razzaque MS (2015) Dysregulation of phosphate metabolism and conditions associated with phosphate toxicity. *Bonekey Rep* **4**:705.
- Bruzzozone A, Pinero CP, Castillo LF, Sarappa MG, Rojas P, Lanari C and Luthy IA (2008) Alpha2-adrenoceptor action on cell proliferation and mammary tumour growth in mice. *Br J Pharmacol* **155**:494-504.

Bruzzozone A, Pinero CP, Rojas P, Romanato M, Gass H, Lanari C and Luthy IA (2011) alpha(2)-Adrenoceptors enhance cell proliferation and mammary tumor growth acting through both the stroma and the tumor cells. *Curr Cancer Drug Targets* **11**:763-774.

Burgon PG, Lee WL, Nixon AB, Peralta EG and Casey PJ (2001) Phosphorylation and nuclear translocation of a regulator of G protein signaling (RGS10). *J Biol Chem* **276**:32828-32834.

Cacan E, Ali MW, Boyd NH, Hooks SB and Greer SF (2014) Inhibition of HDAC1 and DNMT1 modulate RGS10 expression and decrease ovarian cancer chemoresistance. *PLoS One* **9**:e87455.

Campbell DB, Ebert PJ, Skelly T, Stroup TS, Lieberman J, Levitt P and Sullivan PF (2008) Ethnic stratification of the association of RGS4 variants with antipsychotic treatment response in schizophrenia. *Biol Psychiatry* **63**:32-41.

Carman CV, Parent J-L, Day PW, Pronin AN, Sternweis PM, Wedegaertner PB, Gilman AG, Benovic JL and Kozasa T (1999) Selective regulation of Gαq/11 by an RGS domain in the G protein-coupled receptor kinase, GRK2. *Journal of Biological Chemistry* **274**:34483-34492.

Chan RK and Otte CA (1982) Isolation and genetic analysis of *Saccharomyces cerevisiae* mutants supersensitive to G1 arrest by a factor and alpha factor pheromones. *Mol Cell Biol* **2**:11-20.

Chatterjee TK and Fisher RA (2000) Novel alternative splicing and nuclear localization of human RGS12 gene products. *J Biol Chem* **275**:29660-29671.

Chatterjee TK and Fisher RA (2002) RGS12TS-S localizes at nuclear matrix-associated subnuclear structures and represses transcription: structural requirements for subnuclear targeting and transcriptional repression. *Mol Cell Biol* **22**:4334-4345.

Chaudhari S, Mallet RT, Shotorbani PY, Tao Y and Ma R (2021) Store-operated calcium entry: Pivotal roles in renal physiology and pathophysiology. *Exp Biol Med (Maywood)* **246**:305-316.

Chaudhary PK and Kim S (2021) An Insight into GPCR and G-Proteins as Cancer Drivers. *Cells* **10**.

Chen TC, Hinton DR, Zidovetzki R and Hofman FM (1998) Up-regulation of the cAMP/PKA pathway inhibits proliferation, induces differentiation, and leads to apoptosis in malignant gliomas. *Lab Invest* **78**:165-174.

Chen TC, Wadsten P, Su S, Rawlinson N, Hofman FM, Hill CK and Schonthal AH (2002) The type IV phosphodiesterase inhibitor rolipram induces expression of the cell cycle inhibitors p21(Cip1) and p27(Kip1), resulting in growth inhibition, increased differentiation, and subsequent apoptosis of malignant A-172 glioma cells. *Cancer Biol Ther* **1**:268-276.

Chen WC, Chou WH, Chu HW, Huang CC, Liu X, Chang WP, Chou YH and Chang WC (2019) The rs1256328 (ALPL) and rs12654812 (RGS14) Polymorphisms are Associated with Susceptibility to Calcium Nephrolithiasis in a Taiwanese population. *Sci Rep* **9**:17296.

Chen X, Dunham C, Kendler S, Wang X, O'Neill FA, Walsh D and Kendler KS (2004) Regulator of G-protein signaling 4 (RGS4) gene is associated with schizophrenia in Irish high density families. *Am J Med Genet B Neuropsychiatr Genet* **129B**:23-26.

Cho H, Kim DU and Kehrl JH (2005) RGS14 is a centrosomal and nuclear cytoplasmic shuttling protein that traffics to promyelocytic leukemia nuclear bodies following heat shock. *J Biol Chem* **280**:805-814.

Cho H, Kozasa T, Takekoshi K, De Gunzburg J and Kehrl JH (2000a) RGS14, a GTPase-Activating Protein for $G_{i\alpha}$, Attenuates $G_{i\alpha}$ - and $G_{13\alpha}$ -mediated signaling pathways. *Mol Pharmacology* **58**:569-576.

Cho H, Kozasa T, Takekoshi K, De Gunzburg J and Kehrl JH (2000b) RGS14, a GTPase-activating protein for $G_{i\alpha}$, attenuates $G_{i\alpha}$ - and $G_{13\alpha}$ -mediated signaling pathways. *Mol Pharmacol* **58**:569-576.

Cho H, Kozasa T, Takekoshi K, De Gunzburg J and Kehrl JH (2000c) RGS14, a GTPase-activating protein for $G_{i\alpha}$, attenuates $G_{i\alpha}$ - and $G_{13\alpha}$ -mediated signaling pathways. *Mol Pharmacol* **58**:569-576.

Cho H, Kozasa T, Takekoshi K, De Gunzburg J and Kehrl JH (2000d) RGS14, a GTPase-activating protein for $G_{i\alpha}$, attenuates $G_{i\alpha}$ - and $G_{13\alpha}$ -mediated signaling pathways. *Molecular pharmacology* **58**:569-576.

Chowdari KV, Bamne M, Wood J, Talkowski ME, Mirnics K, Levitt P, Lewis DA and Nimgaonkar VL (2008) Linkage disequilibrium patterns and functional analysis of RGS4 polymorphisms in relation to schizophrenia. *Schizophr Bull* **34**:118-126.

Chowdari KV, Mirnics K, Semwal P, Wood J, Lawrence E, Bhatia T, Deshpande SN, B KT, Ferrell RE, Middleton FA, Devlin B, Levitt P, Lewis DA and Nimgaonkar VL (2002) Association and linkage analyses of RGS4 polymorphisms in schizophrenia. *Hum Mol Genet* **11**:1373-1380.

Coleman DE, Berghuis AM, Lee E, Linder ME, Gilman AG and Sprang SR (1994) Structures of active conformations of G_i α 1 and the mechanism of GTP hydrolysis. *Science* **265**:1405-1412.

Collingridge GL, Isaac JT and Wang YT (2004) Receptor trafficking and synaptic plasticity. *Nat Rev Neurosci* **5**:952-962.

Costanzo LS and Windhager EE (1980) Effects of PTH, ADH, and cyclic AMP on distal tubular Ca and Na reabsorption. *Am J Physiol* **239**:F478-485.

- Dai J, Gu J, Lu C, Lin J, Stewart D, Chang D, Roth JA and Wu X (2011) Genetic variations in the regulator of G-protein signaling genes are associated with survival in late-stage non-small cell lung cancer. *PLoS One* **6**:e21120.
- Davydov IV and Varshavsky A (2000) RGS4 is arginylated and degraded by the N-end rule pathway in vitro. *J Biol Chem* **275**:22931-22941.
- Day PW, Wedegaertner PB and Benovic JL (2004) Analysis of G-protein-coupled receptor kinase RGS homology domains. *Methods Enzymol* **390**:295-310.
- De Vries L, Elenko E, Hubler L, Jones TL and Farquhar MG (1996) GAIP is membrane-anchored by palmitoylation and interacts with the activated (GTP-bound) form of G alpha i subunits. *Proc Natl Acad Sci U S A* **93**:15203-15208.
- Deliot N, Hernando N, Horst-Liu Z, Gisler SM, Capuano P, Wagner CA, Bacic D, O'Brien S, Biber J and Murer H (2005) Parathyroid hormone treatment induces dissociation of type IIa Na⁺-P_i cotransporter-Na⁺/H⁺ exchanger regulatory factor-1 complexes. *Am J Physiol Cell Physiol* **289**:C159-C167.
- Deng W, Wang X, Xiao J, Chen K, Zhou H, Shen D, Li H and Tang Q (2012) Loss of regulator of G protein signaling 5 exacerbates obesity, hepatic steatosis, inflammation and insulin resistance. *PLoS One* **7**:e30256.
- Dhami GK, Anborgh PH, Dale LB, Sterne-Marr R and Ferguson SS (2002) Phosphorylation-independent regulation of metabotropic glutamate receptor signaling by G protein-coupled receptor kinase 2. *Journal of Biological Chemistry* **277**:25266-25272.
- Dietzel C and Kurjan J (1987) Pheromonal regulation and sequence of the *Saccharomyces cerevisiae* SST2 gene: a model for desensitization to pheromone. *Mol Cell Biol* **7**:4169-4177.
- DiGiacomo V, Maziarz M, Luebbbers A, Norris JM, Laksono P and Garcia-Marcos M (2020) Probing the mutational landscape of regulators of G protein signaling proteins in cancer. *Sci Signal* **13**.
- Ding J, Guzman JN, Tkatch T, Chen S, Goldberg JA, Ebert PJ, Levitt P, Wilson CJ, Hamm HE and Surmeier DJ (2006) RGS4-dependent attenuation of M4 autoreceptor function in striatal cholinergic interneurons following dopamine depletion. *Nat Neurosci* **9**:832-842.
- Dixon RA, Kobilka BK, Strader DJ, Benovic JL, Dohlman HG, Frielle T, Bolanowski MA, Bennett CD, Rands E, Diehl RE, Mumford RA, Slater EE, Sigal IS, Caron MG, Lefkowitz RJ and Strader CD (1986) Cloning of the gene and cDNA for mammalian beta-adrenergic receptor and homology with rhodopsin. *Nature* **321**:75-79.

- Dohlman HG, Apaniesk D, Chen Y, Song J and Nusskern D (1995) Inhibition of G-protein signaling by dominant gain-of-function mutations in Sst2p, a pheromone desensitization factor in *Saccharomyces cerevisiae*. *Mol Cell Biol* **15**:3635-3643.
- Dohlman HG and Thorner J (1997) RGS proteins and signaling by heterotrimeric G proteins. *J Biol Chem* **272**:3871-3874.
- Dou Y, Gold HD, Luquette LJ and Park PJ (2018) Detecting Somatic Mutations in Normal Cells. *Trends Genet* **34**:545-557.
- Dunn HA and Ferguson SS (2015) PDZ Protein Regulation of G Protein-Coupled Receptor Trafficking and Signaling Pathways. *Mol Pharmacol* **88**:624-639.
- Eason MG, Kurose H, Holt BD, Raymond JR and Liggett SB (1992) Simultaneous coupling of alpha 2-adrenergic receptors to two G-proteins with opposing effects. Subtype-selective coupling of alpha 2C10, alpha 2C4, and alpha 2C2 adrenergic receptors to Gi and Gs. *J Biol Chem* **267**:15795-15801.
- Emilsson L, Saetre P and Jazin E (2006) Low mRNA levels of RGS4 splice variants in Alzheimer's disease: association between a rare haplotype and decreased mRNA expression. *Synapse* **59**:173-176.
- Ennaceur A and Delacour J (1988) A new one-trial test for neurobiological studies of memory in rats. 1: Behavioral data. *Behav Brain Res* **31**:47-59.
- Epi PMC (2015) A roadmap for precision medicine in the epilepsies. *Lancet Neurol* **14**:1219-1228.
- Evans PR, Dudek SM and Hepler JR (2015) Regulator of G Protein Signaling 14: A Molecular Brake on Synaptic Plasticity Linked to Learning and Memory. *Prog Mol Biol Transl Sci* **133**:169-206.
- Evans PR, Gerber KJ, Dammer EB, Duong DM, Goswami D, Lustberg DJ, Zou J, Yang JJ, Dudek SM, Griffin PR, Seyfried NT and Hepler JR (2018a) Interactome analysis reveals regulator of G Protein signaling 14 (RGS14) is a novel calcium/calmodulin (Ca²⁺/CaM) and CaM Kinase II (CaMKII) binding partner. *J Proteome Res* **17**:1700-1711.
- Evans PR, Gerber KJ, Dammer EB, Duong DM, Goswami D, Lustberg DJ, Zou J, Yang JJ, Dudek SM, Griffin PR, Seyfried NT and Hepler JR (2018b) Interactome Analysis Reveals Regulator of G Protein Signaling 14 (RGS14) is a Novel Calcium/Calmodulin (Ca(2+)/CaM) and CaM Kinase II (CaMKII) Binding Partner. *J Proteome Res* **17**:1700-1711.
- Evans PR, Lee SE, Smith Y and Hepler JR (2014) Postnatal developmental expression of regulator of G protein signaling 14 (RGS14) in the mouse brain. *J Comp Neurol* **522**:186-203.

Evans PR, Parra-Bueno P, Smirnov MS, Lustberg DJ, Dudek SM, Hepler JR and Yasuda R (2018c) RGS14 restricts plasticity in hippocampal CA2 by limiting postsynaptic calcium signaling. *eNeuro* **5**:pii: ENEURO.0353-0317.2018. doi: 0310.1523/ENEURO.0353-0317.2018.

Evans PR, Parra-Bueno P, Smirnov MS, Lustberg DJ, Dudek SM, Hepler JR and Yasuda R (2018d) RGS14 Restricts Plasticity in Hippocampal CA2 by Limiting Postsynaptic Calcium Signaling. *eNeuro* **5**.

Felkin LE, Lara-Pezzi EA, Hall JL, Birks EJ and Barton PJ (2011) Reverse remodelling and recovery from heart failure are associated with complex patterns of gene expression. *J Cardiovasc Transl Res* **4**:321-331.

Ferguson JN, Young LJ and Insel TR (2002) The neuroendocrine basis of social recognition. *Front Neuroendocrinol* **23**:200-224.

Foster SL, Lustberg DJ, Harbin NH, Bramlett SN, Hepler JR and Weinshenker D (2021) RGS14 modulates locomotor behavior and ERK signaling induced by environmental novelty and cocaine within discrete limbic structures. *Psychopharmacology (Berl)* **238**:2755-2773.

Fraser CM, Arakawa S, McCombie WR and Venter JC (1989) Cloning, sequence analysis, and permanent expression of a human alpha 2-adrenergic receptor in Chinese hamster ovary cells. Evidence for independent pathways of receptor coupling to adenylate cyclase attenuation and activation. *J Biol Chem* **264**:11754-11761.

Friedman PA, Coutermarsh BA, Kennedy SM and Gesek FA (1996) Parathyroid hormone stimulation of calcium transport is mediated by dual signaling mechanisms involving protein kinase A and protein kinase C. *Endocrinology* **137**:13-20.

Friedman PA, Gesek FA, Morley P, Whitfield JF and Willick GE (1999) Cell-specific signaling and structure-activity relations of parathyroid hormone analogs in mouse kidney cells. *Endocrinology* **140**:301-309.

Friedman PA, Sneddon WB, Mamonova T, Montanez-Miranda C, Ramineni S, Harbin NH, Squires KE, Gefter JV, Magyar CE, Emler DR and Hepler JR (2022) RGS14 regulates PTH- and FGF23-sensitive NPT2A-mediated renal phosphate uptake via binding to the NHERF1 scaffolding protein. *J Biol Chem* **298**:101836.

Gao B, Mumby S and Gilman AG (1987) The G protein beta 2 complementary DNA encodes the beta 35 subunit. *J Biol Chem* **262**:17254-17257.

Garcia-Marcos M, Ghosh P and Farquhar MG (2011) Molecular basis of a novel oncogenic mutation in GNAO1. *Oncogene* **30**:2691-2696.

Gardella TJ and Vilardaga JP (2015) International Union of Basic and Clinical Pharmacology. XCIII. The parathyroid hormone receptors--family B G protein-coupled receptors. *Pharmacol Rev* **67**:310-337.

- Gattineni J and Friedman PA (2015) Regulation of hormone-sensitive renal phosphate transport. *Vitam Horm* **98**:249-306.
- Gerber KJ, Squires KE and Hepler JR (2016) Roles for Regulator of G Protein Signaling Proteins in Synaptic Signaling and Plasticity. *Mol Pharmacol* **89**:273-286.
- Gerber KJ, Squires KE and Hepler JR (2018a) 14-3-3 γ binds regulator of G protein signaling 14 (RGS14) at distinct sites to inhibit the RGS14:G α _i-AIF4(-) signaling complex and RGS14 nuclear localization. *J Biol Chem* **293**:14616-14631.
- Gerber KJ, Squires KE and Hepler JR (2018b) 14-3-3 γ binds regulator of G protein signaling 14 (RGS14) at distinct sites to inhibit the RGS14:G α _i-AIF4⁻ signaling complex and RGS14 nuclear localization. *J Biol Chem* **293**:14616-14631.
- Ghavami A, Hunt RA, Olsen MA, Zhang J, Smith DL, Kalgaonkar S, Rahman Z and Young KH (2004) Differential effects of regulator of G protein signaling (RGS) proteins on serotonin 5-HT_{1A}, 5-HT_{2A}, and dopamine D₂ receptor-mediated signaling and adenylyl cyclase activity. *Cell Signal* **16**:711-721.
- Gilman AG (1987) G proteins: transducers of receptor-generated signals. *Annu Rev Biochem* **56**:615-649.
- Gisler SM, Stagljar I, Traebert M, Bacic D, Biber J and Murer H (2001) Interaction of the type IIa Na/Pi cotransporter with PDZ proteins. *J Biol Chem* **276**:9206-9213.
- Glick JL, Meigs TE, Miron A and Casey PJ (1998) RGSZ1, a G α _z-selective regulator of G protein signaling whose action is sensitive to the phosphorylation state of G α . *J Biol Chem* **273**:26008-26013.
- Gold SJ, Ni YG, Dohlman HG and Nestler EJ (1997) Regulators of G-protein signaling (RGS) proteins: region-specific expression of nine subtypes in rat brain. *J Neurosci* **17**:8024-8037.
- Goldenstein BL, Nelson BW, Xu K, Luger EJ, Pribula JA, Wald JM, O'Shea LA, Weinshenker D, Charbeneau RA, Huang X, Neubig RR and Doze VA (2009) Regulator of G protein signaling protein suppression of G α _h protein-mediated α _{2A} adrenergic receptor inhibition of mouse hippocampal CA3 epileptiform activity. *Mol Pharmacol* **75**:1222-1230.
- Graziano MP, Casey PJ and Gilman AG (1987) Expression of cDNAs for G proteins in *Escherichia coli*. Two forms of G α stimulate adenylyl cyclase. *J Biol Chem* **262**:11375-11381.
- Gu S, He J, Ho WT, Ramineni S, Thal DM, Natesh R, Tesmer JJ, Hepler JR and Heximer SP (2007) Unique hydrophobic extension of the RGS2 amphipathic helix domain imparts increased plasma membrane binding and function relative to other RGS R4/B subfamily members. *J Biol Chem* **282**:33064-33075.

Guan F, Han W, Ni T, Zhao L, Li X, Zhang B and Zhang T (2020) Genetic Polymorphisms of RGS14 and Renal Stone Disease: A Case-control Study Based on the Chinese Han Population. *Arch Med Res*.

Guan F, Han W, Ni T, Zhao L, Li X, Zhang B and Zhang T (2021) Genetic Polymorphisms of RGS14 and Renal Stone Disease. *Arch Med Res* **52**:332-338.

Guo S, Tang W, Shi Y, Huang K, Xi Z, Xu Y, Feng G and He L (2006) RGS4 polymorphisms and risk of schizophrenia: an association study in Han Chinese plus meta-analysis. *Neurosci Lett* **406**:122-127.

Gurevich VV and Gurevich EV (2019) GPCR Signaling Regulation: The Role of GRKs and Arrestins. *Front Pharmacol* **10**:125.

Gutkind JS (1998) Cell growth control by G protein-coupled receptors: from signal transduction to signal integration. *Oncogene* **17**:1331-1342.

Haller C, Fillatreau S, Hoffmann R and Agenes F (2002) Structure, chromosomal localization and expression of the mouse regulator of G-protein signaling10 gene (mRGS10). *Gene* **297**:39-49.

Hamm HE (1998) The many faces of G protein signaling. *J Biol Chem* **273**:669-672.

Harbin NH, Bramlett SN, Montanez-Miranda C, Terzioglu G and Hepler JR (2021) RGS14 Regulation of Post-Synaptic Signaling and Spine Plasticity in Brain. *Int J Mol Sci* **22**.

Harris BA, Robishaw JD, Mumby SM and Gilman AG (1985) Molecular cloning of complementary DNA for the alpha subunit of the G protein that stimulates adenylate cyclase. *Science* **229**:1274-1277.

Hauser AS, Attwood MM, Rask-Andersen M, Schioth HB and Gloriam DE (2017) Trends in GPCR drug discovery: new agents, targets and indications. *Nat Rev Drug Discov* **16**:829-842.

Hazeki O and Ui M (1981) Modification by islet-activating protein of receptor-mediated regulation of cyclic AMP accumulation in isolated rat heart cells. *Journal of Biological Chemistry* **256**:2856-2862.

He W, Lu L, Zhang X, El-Hodiri HM, Chen CK, Slep KC, Simon MI, Jamrich M and Wensel TG (2000) Modules in the photoreceptor RGS9-1.Gbeta 5L GTPase-accelerating protein complex control effector coupling, GTPase acceleration, protein folding, and stability. *J Biol Chem* **275**:37093-37100.

He Z, Yu L, Luo S, Li Q, Huang S and An Y (2019) RGS4 Regulates Proliferation And Apoptosis Of NSCLC Cells Via microRNA-16 And Brain-Derived Neurotrophic Factor. *Onco Targets Ther* **12**:8701-8714.

Hensch NR, Karim ZA, Druey KM, Tansey MG and Khasawneh FT (2016) RGS10 Negatively Regulates Platelet Activation and Thrombogenesis. *PLoS One* **11**:e0165984.

Hepler JR (1999) Emerging roles for RGS proteins in cell signalling. *Trends Pharmacol Sci* **20**:376-382.

Hepler JR, Berman DM, Gilman AG and Kozasa T (1997) RGS4 and GAIP are GTPase-activating proteins for Gq alpha and block activation of phospholipase C beta by gamma-thio-GTP-Gq alpha. *Proc Natl Acad Sci U S A* **94**:428-432.

Hepler JR and Gilman AG (1992) G proteins. *Trends Biochem Sci* **17**:383-387.

Heximer SP (2004) RGS2-mediated regulation of Gqalpha. *Methods Enzymol* **390**:65-82.

Heximer SP, Lim H, Bernard JL and Blumer KJ (2001) Mechanisms governing subcellular localization and function of human RGS2. *J Biol Chem* **276**:14195-14203.

Heximer SP, Srinivasa SP, Bernstein LS, Bernard JL, Linder ME, Hepler JR and Blumer KJ (1999) G protein selectivity is a determinant of RGS2 function. *J Biol Chem* **274**:34253-34259.

Heximer SP, Watson N, Linder ME, Blumer KJ and Hepler JR (1997) RGS2/G0S8 is a selective inhibitor of Gqalpha function. *Proc Natl Acad Sci U S A* **94**:14389-14393.

Hishimoto A, Shirakawa O, Nishiguchi N, Aoyama S, Ono H, Hashimoto T and Maeda K (2004) Novel missense polymorphism in the regulator of G-protein signaling 10 gene: analysis of association with schizophrenia. *Psychiatry Clin Neurosci* **58**:579-581.

Ho AM, MacKay RK, Dodd PR and Lewohl JM (2010) Association of polymorphisms in RGS4 and expression of RGS transcripts in the brains of human alcoholics. *Brain Res* **1340**:1-9.

Hollinger S and Hepler JR (2002) Cellular regulation of RGS proteins: modulators and integrators of G protein signaling. *Pharmacol Rev* **54**:527-559.

Hollinger S, Taylor JB, Goldman EH and Hepler JR (2001a) RGS14 is a bifunctional regulator of Galphai/o activity that exists in multiple populations in brain. *J Neurochem* **79**:941-949.

Hollinger S, Taylor JB, Goldman EH and Hepler JR (2001b) RGS14 is a bifunctional regulator of G $\alpha_{i/o}$ activity that exists in multiple populations in brain. *J Neurochem* **79**:941-949.

Hollins B, Kuravi S, Digby GJ and Lambert NA (2009) The c-terminus of GRK3 indicates rapid dissociation of G protein heterotrimer. *Cell Signal* **21**:1015-1021.

Homologene Regulator of G-protein signaling 14, National Library of Medicine (US), National Center for Biotechnology Information, Bethesda (MD).

Hooks SB, Callihan P, Altman MK, Hurst JH, Ali MW and Murph MM (2010) Regulators of G-Protein signaling RGS10 and RGS17 regulate chemoresistance in ovarian cancer cells. *Mol Cancer* **9**:289.

Hooks SB and Murph MM (2015) Cellular deficiency in the RGS10 protein facilitates chemoresistant ovarian cancer. *Future Med Chem* **7**:1483-1489.

Hooks SB, Waldo GL, Corbitt J, Bodor ET, Krumins AM and Harden TK (2003) RGS6, RGS7, RGS9, and RGS11 stimulate GTPase activity of Gi family G-proteins with differential selectivity and maximal activity. *J Biol Chem* **278**:10087-10093.

Huang C, Hepler JR, Gilman AG and Mumby SM (1997) Attenuation of Gi- and Gq-mediated signaling by expression of RGS4 or GAIP in mammalian cells. *Proc Natl Acad Sci U S A* **94**:6159-6163.

Hunt TW, Fields TA, Casey PJ and Peralta EG (1996) RGS10 is a selective activator of G alpha i GTPase activity. *Nature* **383**:175-177.

Hurst JH and Hooks SB (2009) Regulator of G-protein signaling (RGS) proteins in cancer biology. *Biochem Pharmacol* **78**:1289-1297.

Hurst JH, Mendpara N and Hooks SB (2009) Regulator of G-protein signalling expression and function in ovarian cancer cell lines. *Cell Mol Biol Lett* **14**:153-174.

Hynes RO (2011) Metastatic cells will take any help they can get. *Cancer Cell* **20**:689-690.

Ideno N, Yamaguchi H, Ghosh B, Gupta S, Okumura T, Steffen DJ, Fisher CG, Wood LD, Singhi AD, Nakamura M, Gutkind JS and Maitra A (2018) GNAS(R201C) Induces Pancreatic Cystic Neoplasms in Mice That Express Activated KRAS by Inhibiting YAP1 Signaling. *Gastroenterology* **155**:1593-1607 e1512.

Ingi T and Aoki Y (2002) Expression of RGS2, RGS4 and RGS7 in the developing postnatal brain. *Eur J Neurosci* **15**:929-936.

Jaba IM, Zhuang ZW, Li N, Jiang Y, Martin KA, Sinusas AJ, Papademetris X, Simons M, Sessa WC, Young LH and Tirziu D (2013) NO triggers RGS4 degradation to coordinate angiogenesis and cardiomyocyte growth. *J Clin Invest* **123**:1718-1731.

Jiang LI, Collins J, Davis R, Lin KM, DeCamp D, Roach T, Hsueh R, Rebres RA, Ross EM, Taussig R, Fraser I and Sternweis PC (2007) Use of a cAMP BRET sensor to characterize a novel regulation of cAMP by the sphingosine 1-phosphate/G13 pathway. *J Biol Chem* **282**:10576-10584.

Jones SB, Halenda SP and Bylund DB (1991) Alpha 2-adrenergic receptor stimulation of phospholipase A2 and of adenylate cyclase in transfected Chinese hamster ovary cells is mediated by different mechanisms. *Molecular Pharmacology* **39**:239-245.

Kan Z, Jaiswal BS, Stinson J, Janakiraman V, Bhatt D, Stern HM, Yue P, Haverty PM, Bourgon R, Zheng J, Moorhead M, Chaudhuri S, Tomsho LP, Peters BA, Pujara K, Cordes S, Davis DP, Carlton VE, Yuan W, Li L, Wang W, Eigenbrot C, Kaminker JS, Eberhard DA, Waring P, Schuster SC, Modrusan Z, Zhang Z, Stokoe D, de Sauvage FJ, Faham M and Seshagiri S (2010) Diverse somatic mutation patterns and pathway alterations in human cancers. *Nature* **466**:869-873.

Kannarkat GT, Lee JK, Ramsey CP, Chung J, Chang J, Porter I, Oliver D, Shepherd K and Tansey MG (2015) Age-related changes in regulator of G-protein signaling (RGS)-10 expression in peripheral and central immune cells may influence the risk for age-related degeneration. *Neurobiol Aging* **36**:1982-1993.

Kardestuncer T, Wu H, Lim AL and Neer EJ (1998) Cardiac myocytes express mRNA for ten RGS proteins: changes in RGS mRNA expression in ventricular myocytes and cultured atria. *FEBS Lett* **438**:285-288.

Katada T, Bokoch GM, Smigel MD, Ui M and Gilman AG (1984) The inhibitory guanine nucleotide-binding regulatory component of adenylate cyclase. Subunit dissociation and the inhibition of adenylate cyclase in S49 lymphoma cyc- and wild type membranes. *J Biol Chem* **259**:3586-3595.

Kaur K, Kehrl JM, Charbeneau RA and Neubig RR (2011) RGS-insensitive Galpha subunits: probes of Galpha subtype-selective signaling and physiological functions of RGS proteins. *Methods Mol Biol* **756**:75-98.

Kestenbaum B, Glazer NL, Kottgen A, Felix JF, Hwang SJ, Liu Y, Lohman K, Kritchevsky SB, Hausman DB, Petersen AK, Gieger C, Ried JS, Meitinger T, Strom TM, Wichmann HE, Campbell H, Hayward C, Rudan I, de Boer IH, Psaty BM, Rice KM, Chen YD, Li M, Arking DE, Boerwinkle E, Coresh J, Yang Q, Levy D, van Rooij FJ, Dehghan A, Rivadeneira F, Uitterlinden AG, Hofman A, van Duijn CM, Shlipak MG, Kao WH, Witteman JC, Siscovick DS and Fox CS (2010) Common genetic variants associate with serum phosphorus concentration. *J Am Soc Nephrol* **21**:1223-1232.

Khan M, Jose A and Sharma S (2022) Physiology, Parathyroid Hormone, in *StatPearls*, Treasure Island (FL).

Khundmiri SJ, Rane MJ and Lederer ED (2003) Parathyroid hormone regulation of type II sodium-phosphate cotransporters is dependent on an A kinase anchoring protein. *J Biol Chem* **278**:10134-10141.

Kimple RJ, De Vries L, Tronchere H, Behe CI, Morris RA, Gist Farquhar M and Siderovski DP (2001) RGS12 and RGS14 GoLoco motifs are G alpha(i) interaction sites with guanine nucleotide dissociation inhibitor Activity. *J Biol Chem* **276**:29275-29281.

- Kimple RJ, Kimple ME, Betts L, Sondek J and Siderovski DP (2002) Structural determinants for GoLoco-induced inhibition of nucleotide release by Galpha subunits. *Nature* **416**:878-881.
- Kimple RJ, Willard FS and Siderovski DP (2004) Purification and in vitro functional analyses of RGS12 and RGS14 GoLoco motif peptides. *Methods Enzymol* **390**:416-436.
- Koelle MR and Horvitz HR (1996) EGL-10 regulates G protein signaling in the *C. elegans* nervous system and shares a conserved domain with many mammalian proteins. *Cell* **84**:115-125.
- Kozasa T, Jiang X, Hart MJ, Sternweis PM, Singer WD, Gilman AG, Bollag G and Sternweis PC (1998) p115 RhoGEF, a GTPase activating protein for Galpha12 and Galpha13. *Science* **280**:2109-2111.
- Krupinski J, Coussen F, Bakalyar HA, Tang WJ, Feinstein PG, Orth K, Slaughter C, Reed RR and Gilman AG (1989) Adenylyl cyclase amino acid sequence: possible channel- or transporter-like structure. *Science* **244**:1558-1564.
- Lambert NA, Johnston CA, Cappell SD, Kuravi S, Kimple AJ, Willard FS and Siderovski DP (2010) Regulators of G-protein signaling accelerate GPCR signaling kinetics and govern sensitivity solely by accelerating GTPase activity. *Proc Natl Acad Sci U S A* **107**:7066-7071.
- Lee EK, Ye Y, Kamat AM and Wu X (2013a) Genetic variations in regulator of G-protein signaling (RGS) confer risk of bladder cancer. *Cancer* **119**:1643-1651.
- Lee JK, Chung J, Kannarkat GT and Tansey MG (2013b) Critical role of regulator G-protein signaling 10 (RGS10) in modulating macrophage M1/M2 activation. *PLoS One* **8**:e81785.
- Lee JK, Chung J, McAlpine FE and Tansey MG (2011) Regulator of G-protein signaling-10 negatively regulates NF-kappaB in microglia and neuroprotects dopaminergic neurons in hemiparkinsonian rats. *J Neurosci* **31**:11879-11888.
- Lee JK, Kannarkat GT, Chung J, Joon Lee H, Graham KL and Tansey MG (2016) RGS10 deficiency ameliorates the severity of disease in experimental autoimmune encephalomyelitis. *J Neuroinflammation* **13**:24.
- Lee JK, McCoy MK, Harms AS, Ruhn KA, Gold SJ and Tansey MG (2008) Regulator of G-protein signaling 10 promotes dopaminergic neuron survival via regulation of the microglial inflammatory response. *J Neurosci* **28**:8517-8528.
- Lee JK and Tansey MG (2015) Physiology of RGS10 in Neurons and Immune Cells. *Prog Mol Biol Transl Sci* **133**:153-167.

Lee MJ, Kim DE, Zakrzewska A, Yoo YD, Kim SH, Kim ST, Seo JW, Lee YS, Dorn GW, 2nd, Oh U, Kim BY and Kwon YT (2012) Characterization of arginylation branch of N-end rule pathway in G-protein-mediated proliferation and signaling of cardiomyocytes. *J Biol Chem* **287**:24043-24052.

Lee SE, Simons SB, Heldt SA, Zhao M, Schroeder JP, Vellano CP, Cowan DP, Ramineni S, Yates CK, Feng Y, Smith Y, Sweatt JD, Weinshenker D, Ressler KJ, Dudek SM and Hepler JR (2010a) RGS14 is a natural suppressor of both synaptic plasticity in CA2 neurons and hippocampal-based learning and memory. *Proc Natl Acad Sci U S A* **107**:16994-16998.

Lee SE, Simons SB, Heldt SA, Zhao M, Schroeder JP, Vellano CP, Cowan DP, Ramineni S, Yates CK, Feng Y, Smith Y, Sweatt JD, Weinshenker D, Ressler KJ, Dudek SM and Hepler JR (2010b) RGS14 is a natural suppressor of both synaptic plasticity in CA2 neurons and hippocampal-based learning and memory. *Proceedings of the National Academy of Sciences of the United States of America* **107**:16994–16998.

Lerner TN and Kreitzer AC (2012) RGS4 is required for dopaminergic control of striatal LTD and susceptibility to parkinsonian motor deficits. *Neuron* **73**:347-359.

Li Y, Tang XH, Li XH, Dai HJ, Miao RJ, Cai JJ, Huang ZJ, Chen AF, Xing XW, Lu Y and Yuan H (2016) Regulator of G protein signalling 14 attenuates cardiac remodelling through the MEK-ERK1/2 signalling pathway. *Basic Res Cardiol* **111**:47.

Lim J, Thompson J, May RC, Hotchin NA and Caron E (2013) Regulator of G-Protein Signalling-14 (RGS14) Regulates the Activation of alphaMbeta2 Integrin during Phagocytosis. *PLoS One* **8**:e69163.

Linder ME, Ewald DA, Miller RJ and Gilman AG (1990) Purification and characterization of Go alpha and three types of Gi alpha after expression in Escherichia coli. *J Biol Chem* **265**:8243-8251.

Lomasney JW, Leeb-Lundberg LM, Cotecchia S, Regan JW, DeBernardis JF, Caron MG and Lefkowitz RJ (1986) Mammalian alpha 1-adrenergic receptor. Purification and characterization of the native receptor ligand binding subunit. *J Biol Chem* **261**:7710-7716.

Long J, Chen Y, Lin H, Liao M, Li T, Tong L, Wei S, Xian X, Zhu J, Chen J, Tian J, Wang Q and Mo Z (2018a) Significant association between RGS14 rs12654812 and nephrolithiasis risk among Guangxi population in China. *J Clin Lab Anal* **32**:e22435.

Long J, Chen Y, Lin H, Liao M, Li T, Tong L, Wei S, Xian X, Zhu J, Chen J, Tian J, Wang Q and Mo Z (2018b) Significant association between RGS14 rs12654812 and nephrolithiasis risk among Guangxi population in China. *J Clin Lab Anal*:e22435.

Lynch G, Kessler M, Arai A and Larson J (1990) The nature and causes of hippocampal long-term potentiation. *Prog Brain Res* **83**:233-250.

Mahajan A, Rodan AR, Le TH, Gaulton KJ, Haessler J, Stilp AM, Kamatani Y, Zhu G, Sofer T, Puri S, Schellinger JN, Chu PL, Cechova S, van Zuydam N, Consortium S, BioBank Japan P, Arnlov J, Flessner MF, Giedraitis V, Heath AC, Kubo M, Larsson A, Lindgren CM, Madden PAF, Montgomery GW, Papanicolaou GJ, Reiner AP, Sundstrom J, Thornton TA, Lind L, Ingelsson E, Cai J, Martin NG, Kooperberg C, Matsuda K, Whitfield JB, Okada Y, Laurie CC, Morris AP and Franceschini N (2016) Trans-ethnic Fine Mapping Highlights Kidney-Function Genes Linked to Salt Sensitivity. *Am J Hum Genet* **99**:636-646.

Mahon MJ, Donowitz M, Yun CC and Segre GV (2002) Na(+)/H(+) exchanger regulatory factor 2 directs parathyroid hormone 1 receptor signalling. *Nature* **417**:858-861.

Mao H, Zhao Q, Daigle M, Ghahremani MH, Chidiac P and Albert PR (2004) RGS17/RGSZ2, a novel regulator of Gi/o, Gz, and Gq signaling. *J Biol Chem* **279**:26314-26322.

Martemyanov KA and Arshavsky VY (2004) Kinetic approaches to study the function of RGS9 isoforms. *Methods Enzymol* **390**:196-209.

Martin-Montanez E, Acevedo MJ, Lopez-Tellez JF, Duncan RS, Mateos AG, Pavia J, Koulen P and Khan ZU (2010) Regulator of G-protein signaling 14 protein modulates Ca(2)+ influx through Cav1 channels. *Neuroreport* **21**:1034-1039.

Masuh I, Balaji S, Muntean BS, Skamangas NK, Chavali S, Tesmer JJG, Babu MM and Martemyanov KA (2020) A Global Map of G Protein Signaling Regulation by RGS Proteins. *Cell* **183**:503-521 e519.

Masuh I, Xie K and Martemyanov KA (2013) Macromolecular composition dictates receptor and G protein selectivity of regulator of G protein signaling (RGS) 7 and 9-2 protein complexes in living cells. *J Biol Chem* **288**:25129-25142.

May DC, Ross EM, Gilman AG and Smigel MD (1985) Reconstitution of catecholamine-stimulated adenylate cyclase activity using three purified proteins. *J Biol Chem* **260**:15829-15833.

McCombs JE and Palmer AE (2008) Measuring calcium dynamics in living cells with genetically encodable calcium indicators. *Methods* **46**:152-159.

McCoy KL and Hepler JR (2009) Regulators of G protein signaling proteins as central components of G protein-coupled receptor signaling complexes. *Prog Mol Biol Transl Sci* **86**:49-74.

Min C, Cheong SY, Cheong SJ, Kim M, Cho DI and Kim KM (2012) RGS4 exerts inhibitory activities on the signaling of dopamine D2 receptor and D3 receptor through the N-terminal region. *Pharmacol Res* **65**:213-220.

Mirnic K, Middleton FA, Stanwood GD, Lewis DA and Levitt P (2001) Disease-specific changes in regulator of G-protein signaling 4 (RGS4) expression in schizophrenia. *Mol Psychiatry* **6**:293-301.

Mittal V and Linder ME (2004) The RGS14 GoLoco domain discriminates among Galphai isoforms. *J Biol Chem* **279**:46772-46778.

Mittmann C, Chung CH, Hoppner G, Michalek C, Nose M, Schuler C, Schuh A, Eschenhagen T, Weil J, Pieske B, Hirt S and Wieland T (2002) Expression of ten RGS proteins in human myocardium: functional characterization of an upregulation of RGS4 in heart failure. *Cardiovasc Res* **55**:778-786.

Moon EY, Lee GH, Lee MS, Kim HM and Lee JW (2012) Phosphodiesterase inhibitors control A172 human glioblastoma cell death through cAMP-mediated activation of protein kinase A and Epac1/Rap1 pathways. *Life Sci* **90**:373-380.

Moore AR, Ceraudo E, Sher JJ, Guan Y, Shoushtari AN, Chang MT, Zhang JQ, Walczak EG, Kazmi MA, Taylor BS, Huber T, Chi P, Sakmar TP and Chen Y (2016) Recurrent activating mutations of G-protein-coupled receptor CYSLTR2 in uveal melanoma. *Nat Genet* **48**:675-680.

Nairismagi ML, Tan J, Lim JQ, Nagarajan S, Ng CC, Rajasegaran V, Huang D, Lim WK, Laurensia Y, Wijaya GC, Li ZM, Cutcutache I, Pang WL, Thangaraju S, Ha J, Khoo LP, Chin ST, Dey S, Poore G, Tan LH, Koh HK, Sabai K, Rao HL, Chuah KL, Ho YH, Ng SB, Chuang SS, Zhang F, Liu YH, Pongpruttipan T, Ko YH, Cheah PL, Karim N, Chng WJ, Tang T, Tao M, Tay K, Farid M, Quek R, Rozen SG, Tan P, Teh BT, Lim ST, Tan SY and Ong CK (2016) JAK-STAT and G-protein-coupled receptor signaling pathways are frequently altered in epitheliotropic intestinal T-cell lymphoma. *Leukemia* **30**:1311-1319.

Nance MR, Kreutz B, Tesmer VM, Sterne-Marr R, Kozasa T and Tesmer JJ (2013) Structural and functional analysis of the regulator of G protein signaling 2-galphaq complex. *Structure* **21**:438-448.

Neitzel KL and Hepler JR (2006) Cellular mechanisms that determine selective RGS protein regulation of G protein-coupled receptor signaling. *Semin Cell Dev Biol* **17**:383-389.

Nikolova DN, Zembutsu H, Sechanov T, Vidinov K, Kee LS, Ivanova R, Becheva E, Kocova M, Toncheva D and Nakamura Y (2008) Genome-wide gene expression profiles of thyroid carcinoma: Identification of molecular targets for treatment of thyroid carcinoma. *Oncol Rep* **20**:105-121.

Nishihara H, Hwang M, Kizaka-Kondoh S, Eckmann L and Insel PA (2004) Cyclic AMP promotes cAMP-responsive element-binding protein-dependent induction of cellular inhibitor of apoptosis protein-2 and suppresses apoptosis of colon cancer cells through ERK1/2 and p38 MAPK. *J Biol Chem* **279**:26176-26183.

- Nobles M, Benians A and Tinker A (2005) Heterotrimeric G proteins precouple with G protein-coupled receptors in living cells. *Proc Natl Acad Sci U S A* **102**:18706-18711.
- Nobrega MA and Pennacchio LA (2004) Comparative genomic analysis as a tool for biological discovery. *J Physiol* **554**:31-39.
- Northup JK, Sternweis PC, Smigel MD, Schleifer LS, Ross EM and Gilman AG (1980) Purification of the regulatory component of adenylate cyclase. *Proc Natl Acad Sci U S A* **77**:6516-6520.
- Nunn C, Mao H, Chidiac P and Albert PR (2006) RGS17/RGSZ2 and the RZ/A family of regulators of G-protein signaling. *Semin Cell Dev Biol* **17**:390-399.
- O'Hayre M, Degese MS and Gutkind JS (2014) Novel insights into G protein and G protein-coupled receptor signaling in cancer. *Curr Opin Cell Biol* **27**:126-135.
- O'Hayre M, Vazquez-Prado J, Kufareva I, Stawiski EW, Handel TM, Seshagiri S and Gutkind JS (2013) The emerging mutational landscape of G proteins and G-protein-coupled receptors in cancer. *Nat Rev Cancer* **13**:412-424.
- Olafsson S and Anderson CA (2021) Somatic mutations provide important and unique insights into the biology of complex diseases. *Trends Genet* **37**:872-881.
- Opel A, Nobles M, Montaigne D, Finlay M, Anderson N, Breckenridge R and Tinker A (2015) Absence of the Regulator of G-protein Signaling, RGS4, Predisposes to Atrial Fibrillation and Is Associated with Abnormal Calcium Handling. *J Biol Chem* **290**:19233-19244.
- Owen VJ, Burton PB, Mullen AJ, Birks EJ, Barton P and Yacoub MH (2001) Expression of RGS3, RGS4 and Gi alpha 2 in acutely failing donor hearts and end-stage heart failure. *Eur Heart J* **22**:1015-1020.
- Park HJ, Kim SH and Moon DO (2017) Growth inhibition of human breast carcinoma cells by overexpression of regulator of G-protein signaling 4. *Oncol Lett* **13**:4357-4363.
- Park SJ, Li C and Chen YM (2021) Endoplasmic Reticulum Calcium Homeostasis in Kidney Disease: Pathogenesis and Therapeutic Targets. *Am J Pathol* **191**:256-265.
- Perszyk RE, Kristensen AS, Lyuboslavsky P and Traynelis SF (2021) Three-dimensional missense tolerance ratio analysis. *Genome Res* **31**:1447-1461.
- Popov S, Yu K, Kozasa T and Wilkie TM (1997) The regulators of G protein signaling (RGS) domains of RGS4, RGS10, and GAIP retain GTPase activating protein activity in vitro. *Proc Natl Acad Sci U S A* **94**:7216-7220.
- Posner BA, Gilman AG and Harris BA (1999) Regulators of G protein signaling 6 and 7. Purification of complexes with gbeta5 and assessment of their effects on g protein-mediated signaling pathways. *J Biol Chem* **274**:31087-31093.

Prasad KM, Chowdari KV, Nimgaonkar VL, Talkowski ME, Lewis DA and Keshavan MS (2005) Genetic polymorphisms of the RGS4 and dorsolateral prefrontal cortex morphometry among first episode schizophrenia patients. *Mol Psychiatry* **10**:213-219.

Puiffe ML, Le Page C, Filali-Mouhim A, Zietarska M, Ouellet V, Tonin PN, Chevrette M, Provencher DM and Mes-Masson AM (2007) Characterization of ovarian cancer ascites on cell invasion, proliferation, spheroid formation, and gene expression in an in vitro model of epithelial ovarian cancer. *Neoplasia* **9**:820-829.

Qutob N, Masuho I, Alon M, Emmanuel R, Cohen I, Di Pizio A, Madore J, Elkahloun A, Ziv T, Levy R, Gartner JJ, Hill VK, Lin JC, Hevroni Y, Greenberg P, Brodezki A, Rosenberg SA, Kosloff M, Hayward NK, Admon A, Niv MY, Scolyer RA, Martemyanov KA and Samuels Y (2018) RGS7 is recurrently mutated in melanoma and promotes migration and invasion of human cancer cells. *Sci Rep* **8**:653.

Regan JW, Nakata H, DeMarinis RM, Caron MG and Lefkowitz RJ (1986) Purification and characterization of the human platelet alpha 2-adrenergic receptor. *J Biol Chem* **261**:3894-3900.

Reif K and Cyster JG (2000) RGS molecule expression in murine B lymphocytes and ability to down-regulate chemotaxis to lymphoid chemokines. *J Immunol* **164**:4720-4729.

Ribeiro FM, Ferreira LT, Paquet M, Cregan T, Ding Q, Gros R and Ferguson SS (2009) Phosphorylation-independent regulation of metabotropic glutamate receptor 5 desensitization and internalization by G protein-coupled receptor kinase 2 in neurons. *Journal of Biological Chemistry* **284**:23444-23453.

Riccardi D, Traebert M, Ward DT, Kaissling B, Biber J, Hebert SC and Murer H (2000) Dietary phosphate and parathyroid hormone alter the expression of the calcium-sensing receptor (CaR) and the Na⁺-dependent Pi transporter (NaPi-2) in the rat proximal tubule. *Pflugers Arch* **441**:379-387.

Robinson-Cohen C, Bartz TM, Lai D, Ikizler TA, Peacock M, Imel EA, Michos ED, Foroud TM, Akesson K, Taylor KD, Malmgren L, Matsushita K, Nethander M, Eriksson J, Ohlsson C, Mellstrom D, Wolf M, Ljunggren O, McGuigan F, Rotter JI, Karlsson M, Econs MJ, Ix JH, Lutsey PL, Psaty BM, de Boer IH and Kestenbaum BR (2018) Genetic Variants Associated with Circulating Fibroblast Growth Factor 23. *J Am Soc Nephrol* **29**:2583-2592.

Robinson-Cohen C, Lutsey PL, Kleber ME, Nielson CM, Mitchell BD, Bis JC, Eny KM, Portas L, Eriksson J, Lorentzon M, Koller DL, Milaneschi Y, Teumer A, Pilz S, Nethander M, Selvin E, Tang W, Weng LC, Wong HS, Lai D, Peacock M, Hannemann A, Volker U, Homuth G, Nauk M, Murgia F, Pattee JW, Orwoll E, Zmuda JM, Riancho JA, Wolf M, Williams F, Penninx B, Econs MJ, Ryan KA, Ohlsson C, Paterson AD, Psaty BM, Siscovick DS, Rotter JI, Pirastu M, Streeten E, Marz W, Fox C, Coresh J, Wallaschofski H, Pankow JS, de Boer IH and Kestenbaum B (2017) Genetic Variants Associated with Circulating Parathyroid Hormone. *J Am Soc Nephrol* **28**:1553-1565.

Robison GA and Sutherland EW (1971) Cyclic AMP and the function of eukaryotic cells: an introduction. *Ann N Y Acad Sci* **185**:5-9.

Rodbell M, Birnbaumer L, Pohl SL and Krans HM (1971) The glucagon-sensitive adenyl cyclase system in plasma membranes of rat liver. V. An obligatory role of guanylnucleotides in glucagon action. *J Biol Chem* **246**:1877-1882.

Rorabaugh BR, Rose MJ, Stoops TS, Stevens AA, Seeley SL and D'Souza MS (2018) Regulators of G-protein signaling 2 and 4 differentially regulate cocaine-induced rewarding effects. *Physiol Behav* **195**:9-19.

Ross EM and Gilman AG (1977) Resolution of some components of adenylate cyclase necessary for catalytic activity. *J Biol Chem* **252**:6966-6969.

Ross EM and Wilkie TM (2000) GTPase-Activating Proteins for Heterotrimeric G Proteins: Regulators of G Protein Signaling (RGS) and RGS-Like Proteins. *Annual Review of Biochemistry* **69**:795-827.

Roy AA, Baragli A, Bernstein LS, Hepler JR, Hebert TE and Chidiac P (2006) RGS2 interacts with Gs and adenylyl cyclase in living cells. *Cell Signal* **18**:336-348.

Sakloth F, Polizu C, Bertherat F and Zachariou V (2020) Regulators of G Protein Signaling in Analgesia and Addiction. *Mol Pharmacol* **98**:739-750.

Salaga M, Storr M, Martemyanov KA and Fichna J (2016) RGS proteins as targets in the treatment of intestinal inflammation and visceral pain: New insights and future perspectives. *Bioessays* **38**:344-354.

Salim S, Sinnarajah S, Kehrl JH and Dessauer CW (2003) Identification of RGS2 and type V adenylyl cyclase interaction sites. *J Biol Chem* **278**:15842-15849.

Sambi BS, Hains MD, Waters CM, Connell MC, Willard FS, Kimple AJ, Pyne S, Siderovski DP and Pyne NJ (2006) The effect of RGS12 on PDGFbeta receptor signalling to p42/p44 mitogen activated protein kinase in mammalian cells. *Cell Signal* **18**:971-981.

Schoneberg T and Liebscher I (2021) Mutations in G Protein-Coupled Receptors: Mechanisms, Pathophysiology and Potential Therapeutic Approaches. *Pharmacol Rev* **73**:89-119.

Schulz WL, Tormey CA and Torres R (2015) Computational Approach to Annotating Variants of Unknown Significance in Clinical Next Generation Sequencing. *Lab Med* **46**:285-289.

Schwarz E (2018) A gene-based review of RGS4 as a putative risk gene for psychiatric illness. *Am J Med Genet B Neuropsychiatr Genet* **177**:267-273.

Schwindinger WF, Fredericks J, Watkins L, Robinson H, Bathon JM, Pines M, Suva LJ and Levine MA (1998a) Coupling of the PTH/PTHrP receptor to multiple G-proteins. Direct demonstration of receptor activation of G_s, G_{q/11}, and G_{i(1)} by [α -³²P]GTP- γ -azidoanilide photoaffinity labeling. *Endocrine* **8**:201-209.

Schwindinger WF, Fredericks J, Watkins L, Robinson H, Bathon JM, Pines M, Suva LJ and Levine MA (1998b) Coupling of the PTH/PTHrP receptor to multiple G-proteins. Direct demonstration of receptor activation of G_s, G_{q/11}, and G_{i(1)} by [α -³²P]GTP- γ -azidoanilide photoaffinity labeling. *Endocrine* **8**:201-209.

Shihab HA, Rogers MF, Gough J, Mort M, Cooper DN, Day INM, Gaunt TR and Campbell C (2015) An integrative approach to predicting the functional effects of non-coding and coding sequence variation. *Bioinformatics* **31**:1536-1543.

Shorr RG, Lefkowitz RJ and Caron MG (1981) Purification of the beta-adrenergic receptor. Identification of the hormone binding subunit. *J Biol Chem* **256**:5820-5826.

Shu FJ, Ramineni S, Amyot W and Hepler JR (2007a) Selective interactions between Gi α 1 and Gi α 3 and the GoLoco/GPR domain of RGS14 influence its dynamic subcellular localization. *Cell Signal* **19**:163-176.

Shu FJ, Ramineni S, Amyot W and Hepler JR (2007b) Selective interactions between Gi α 1 and Gi α 3 and the GoLoco/GPR domain of RGS14 influence its dynamic subcellular localization. *Cell Signal* **19**:163-176.

Shu FJ, Ramineni S and Hepler JR (2010) RGS14 is a multifunctional scaffold that integrates G protein and Ras/Raf MAPkinase signalling pathways. *Cell Signal* **22**:366-376.

Silver J, Rodriguez M and Slatopolsky E (2012) FGF23 and PTH--double agents at the heart of CKD. *Nephrol Dial Transplant* **27**:1715-1720.

Singh AT, Gilchrist A, Voyno-Yasenetskaya T, Radeff-Huang JM and Stern PH (2005) G α 12/G α 13 subunits of heterotrimeric G proteins mediate parathyroid hormone activation of phospholipase D in UMR-106 osteoblastic cells. *Endocrinology* **146**:2171-2175.

Sjogren B (2011) Regulator of G protein signaling proteins as drug targets: current state and future possibilities. *Adv Pharmacol* **62**:315-347.

Sjogren B and Neubig RR (2010) Thinking outside of the "RGS box": new approaches to therapeutic targeting of regulators of G protein signaling. *Mol Pharmacol* **78**:550-557.

Sneddon WB, Liu F, Gesek FA and Friedman PA (2000) Obligate mitogen-activated protein kinase activation in parathyroid hormone stimulation of calcium transport but not calcium signaling. *Endocrinology* **141**:4185-4193.

Snow BE, Antonio L, Suggs S, Gutstein HB and Siderovski DP (1997) Molecular cloning and expression analysis of rat Rgs12 and Rgs14. *Biochem Biophys Res Commun* **233**:770-777.

Snow BE, Hall RA, Krumins AM, Brothers GM, Bouchard D, Brothers CA, Chung S, Mangion J, Gilman AG, Lefkowitz RJ and Siderovski DP (1998a) GTPase activating specificity of RGS12 and binding specificity of an alternatively spliced PDZ (PSD-95/Dlg/ZO-1) domain. *J Biol Chem* **273**:17749-17755.

Snow BE, Krumins AM, Brothers GM, Lee SF, Wall MA, Chung S, Mangion J, Arya S, Gilman AG and Siderovski DP (1998b) A G protein gamma subunit-like domain shared between RGS11 and other RGS proteins specifies binding to Gbeta5 subunits. *Proc Natl Acad Sci U S A* **95**:13307-13312.

So HC, Chen RY, Chen EY, Cheung EF, Li T and Sham PC (2008) An association study of RGS4 polymorphisms with clinical phenotypes of schizophrenia in a Chinese population. *Am J Med Genet B Neuropsychiatr Genet* **147B**:77-85.

Soundararajan M, Willard FS, Kimple AJ, Turnbull AP, Ball LJ, Schoch GA, Gileadi C, Fedorov OY, Dowler EF, Higman VA, Hutsell SQ, Sundstrom M, Doyle DA and Siderovski DP (2008) Structural diversity in the RGS domain and its interaction with heterotrimeric G protein alpha-subunits. *Proc Natl Acad Sci U S A* **105**:6457-6462.

Squires KE, Gerber KJ, Pare JF, Branch MR, Smith Y and Hepler JR (2018a) Regulator of G protein signaling 14 (RGS14) is expressed pre- and postsynaptically in neurons of hippocampus, basal ganglia, and amygdala of monkey and human brain. *Brain Struct Funct* **223**:233-253.

Squires KE, Gerber KJ, Tillman MC, Lustberg DJ, Montanez-Miranda C, Zhao M, Ramineni S, Scharer CD, Saha RN, Shu FJ, Schroeder JP, Ortlund EA, Weinshenker D, Dudek SM and Hepler JR (2021) Human genetic variants disrupt RGS14 nuclear shuttling and regulation of LTP in hippocampal neurons. *J Biol Chem* **296**:100024.

Squires KE, Montanez-Miranda C, Pandya RR, Torres MP and Hepler JR (2018b) Genetic Analysis of Rare Human Variants of Regulators of G Protein Signaling Proteins and Their Role in Human Physiology and Disease. *Pharmacol Rev* **70**:446-474.

Stewart A and Fisher RA (2015) Introduction: G Protein-coupled Receptors and RGS Proteins. *Prog Mol Biol Transl Sci* **133**:1-11.

Stewart A, Huang J and Fisher RA (2012) RGS Proteins in Heart: Brakes on the Vagus. *Front Physiol* **3**:95.

Stewart A, Maity B, Anderegg SP, Allamargot C, Yang J and Fisher RA (2015) Regulator of G protein signaling 6 is a critical mediator of both reward-related behavioral and pathological responses to alcohol. *Proc Natl Acad Sci U S A* **112**:E786-795.

Sun M, Wu X, Yu Y, Wang L, Xie D, Zhang Z, Chen L, Lu A, Zhang G and Li F (2020) Disorders of Calcium and Phosphorus Metabolism and the Proteomics/Metabolomics-Based Research. *Front Cell Dev Biol* **8**:576110.

Sunahara RK, Tesmer JJ, Gilman AG and Sprang SR (1997) Crystal structure of the adenylyl cyclase activator G α . *Science* **278**:1943-1947.

Tansey MG and Goldberg MS (2010) Neuroinflammation in Parkinson's disease: its role in neuronal death and implications for therapeutic intervention. *Neurobiol Dis* **37**:510-518.

Tate JG, Bamford S, Jubb HC, Sondka Z, Beare DM, Bindal N, Boutselakis H, Cole CG, Creatore C, Dawson E, Fish P, Harsha B, Hathaway C, Jupe SC, Kok CY, Noble K, Ponting L, Ramshaw CC, Rye CE, Speedy HE, Stefancsik R, Thompson SL, Wang S, Ward S, Campbell PJ and Forbes SA (2018) COSMIC: the Catalogue Of Somatic Mutations In Cancer. *Nucleic Acids Research* **47**:D941-D947.

Tatenhorst L, Senner V, Puttmann S and Paulus W (2004) Regulators of G-protein signaling 3 and 4 (RGS3, RGS4) are associated with glioma cell motility. *J Neuropathol Exp Neurol* **63**:210-222.

Terzi D, Stergiou E, King SL and Zachariou V (2009) Regulators of G protein signaling in neuropsychiatric disorders. *Prog Mol Biol Transl Sci* **86**:299-333.

Tesmer JJ, Berman DM, Gilman AG and Sprang SR (1997a) Structure of RGS4 bound to AIF4--activated G(i alpha1): stabilization of the transition state for GTP hydrolysis. *Cell* **89**:251-261.

Tesmer JJ, Sunahara RK, Gilman AG and Sprang SR (1997b) Crystal structure of the catalytic domains of adenylyl cyclase in a complex with G α .GTPgammaS. *Science* **278**:1907-1916.

Thusberg J and Vihinen M (2009) Pathogenic or not? And if so, then how? Studying the effects of missense mutations using bioinformatics methods. *Hum Mutat* **30**:703-714.

Traver S, Bidot C, Spassky N, Baltauss T, De Tand MF, Thomas JL, Zalc B, Janoueix-Lerosey I and Gunzburg JD (2000a) RGS14 is a novel Rap effector that preferentially regulates the GTPase activity of galphao. *Biochem J* **350 Pt 1**:19-29.

Traver S, Bidot C, Spassky N, Baltauss T, De Tand MF, Thomas JL, Zalc B, Janoueix-Lerosey I and Gunzburg JD (2000b) RGS14 is a novel Rap effector that preferentially regulates the GTPase activity of galphao. *Biochem J* **350 Pt 1**:19-29.

Traynelis J, Silk M, Wang Q, Berkovic SF, Liu L, Ascher DB, Balding DJ and Petrovski S (2017) Optimizing genomic medicine in epilepsy through a gene-customized approach to missense variant interpretation. *Genome Res* **27**:1715-1729.

- Tu Y, Popov S, Slaughter C and Ross EM (1999) Palmitoylation of a conserved cysteine in the regulator of G protein signaling (RGS) domain modulates the GTPase-activating activity of RGS4 and RGS10. *J Biol Chem* **274**:38260-38267.
- Tu Y, Wang J and Ross EM (1997) Inhibition of brain Gz GAP and other RGS proteins by palmitoylation of G protein alpha subunits. *Science* **278**:1132-1135.
- Tu Y, Woodson J and Ross EM (2001) Binding of regulator of G protein signaling (RGS) proteins to phospholipid bilayers. Contribution of location and/or orientation to Gtpase-activating protein activity. *J Biol Chem* **276**:20160-20166.
- Tzakis N and Holahan MR (2019) Social Memory and the Role of the Hippocampal CA2 Region. *Front Behav Neurosci* **13**:233.
- Ueda N, Iniguez-Lluhi JA, Lee E, Smrcka AV, Robishaw JD and Gilman AG (1994) G protein beta gamma subunits. Simplified purification and properties of novel isoforms. *J Biol Chem* **269**:4388-4395.
- Uhlen M, Zhang C, Lee S, Sjostedt E, Fagerberg L, Bidkhorji G, Benfeitas R, Arif M, Liu Z, Edfors F, Sanli K, von Feilitzen K, Oksvold P, Lundberg E, Hober S, Nilsson P, Mattsson J, Schwenk JM, Brunnstrom H, Glimelius B, Sjoblom T, Edqvist PH, Djureinovic D, Micke P, Lindskog C, Mardinoglu A and Ponten F (2017) A pathology atlas of the human cancer transcriptome. *Science* **357**.
- Urabe Y, Tanikawa C, Takahashi A, Okada Y, Morizono T, Tsunoda T, Kamatani N, Kohri K, Chayama K, Kubo M, Nakamura Y and Matsuda K (2012) A genome-wide association study of nephrolithiasis in the Japanese population identifies novel susceptible Loci at 5q35.3, 7p14.3, and 13q14.1. *PLoS Genet* **8**:e1002541.
- Van Raamsdonk CD, Bezrookove V, Green G, Bauer J, Gaugler L, O'Brien JM, Simpson EM, Barsh GS and Bastian BC (2009) Frequent somatic mutations of GNAQ in uveal melanoma and blue naevi. *Nature* **457**:599-602.
- Van Raamsdonk CD, Griewank KG, Crosby MB, Garrido MC, Vemula S, Wiesner T, Obenaus AC, Wackernagel W, Green G, Bouvier N, Sozen MM, Baimukanova G, Roy R, Heguy A, Dolgalev I, Khanin R, Busam K, Speicher MR, O'Brien J and Bastian BC (2010) Mutations in GNA11 in uveal melanoma. *N Engl J Med* **363**:2191-2199.
- Vatner DE, Zhang J, Oydanich M, Guers J, Katsyuba E, Yan L, Sinclair D, Auwerx J and Vatner SF (2018) Enhanced longevity and metabolism by brown adipose tissue with disruption of the regulator of G protein signaling 14. *Aging Cell* **17**:e12751.
- Vazquez SM, Mladovan AG, Perez C, Bruzzone A, Baldi A and Luthy IA (2006) Human breast cell lines exhibit functional alpha2-adrenoceptors. *Cancer Chemother Pharmacol* **58**:50-61.
- Vazquez SM, Pignataro O and Luthy IA (1999) Alpha2-adrenergic effect on human breast cancer MCF-7 cells. *Breast Cancer Res Treat* **55**:41-49.

Vellano CP, Brown NE, Blumer JB and Hepler JR (2013a) Assembly and function of the regulator of G protein signaling 14 (RGS14).H-Ras signaling complex in live cells are regulated by Galphai1 and Galphai-linked G protein-coupled receptors. *J Biol Chem* **288**:3620-3631.

Vellano CP, Brown NE, Blumer JB and Hepler JR (2013b) Assembly and function of the regulator of G protein signaling 14 (RGS14).H-Ras signaling complex in live cells are regulated by Galphai1 and Galphai-linked G protein-coupled receptors. *J Biol Chem* **288**:3620-3631.

Vellano CP, Lee SE, Dudek SM and Hepler JR (2011a) RGS14 at the interface of hippocampal signaling and synaptic plasticity. *Trends Pharmacol Sci* **32**:666-674.

Vellano CP, Maher EM, Hepler JR and Blumer JB (2011b) G protein-coupled receptors and resistance to inhibitors of cholinesterase-8A (Ric-8A) both regulate the regulator of g protein signaling 14 RGS14.Galphai1 complex in live cells. *J Biol Chem* **286**:38659-38669.

Villardaga JP, Romero G, Friedman PA and Gardella TJ (2011) Molecular basis of parathyroid hormone receptor signaling and trafficking: a family B GPCR paradigm. *Cell Mol Life Sci* **68**:1-13.

Vitale G, Dicitore A, Mari D and Cavagnini F (2009) A new therapeutic strategy against cancer: cAMP elevating drugs and leptin. *Cancer Biol Ther* **8**:1191-1193.

Vorhees CV and Williams MT (2006) Morris water maze: procedures for assessing spatial and related forms of learning and memory. *Nat Protoc* **1**:848-858.

Wade SM, Lim WK, Lan KL, Chung DA, Nanamori M and Neubig RR (1999) G(i) activator region of alpha(2A)-adrenergic receptors: distinct basic residues mediate G(i) versus G(s) activation. *Mol Pharmacol* **56**:1005-1013.

Wall MA, Coleman DE, Lee E, Iniguez-Lluhi JA, Posner BA, Gilman AG and Sprang SR (1995) The structure of the G protein heterotrimer Gi alpha 1 beta 1 gamma 2. *Cell* **83**:1047-1058.

Walsh DA, Perkins JP and Krebs EG (1968) An adenosine 3',5'-monophosphate-dependant protein kinase from rabbit skeletal muscle. *J Biol Chem* **243**:3763-3765.

Wang B, Ardura JA, Romero G, Yang Y, Hall RA and Friedman PA (2010) Na/H exchanger regulatory factors control PTH receptor signaling by differential activation of G α protein subunits. *J Biol Chem* **285**:26976-26986.

Wang B, Bisello A, Yang Y, Romero GG and Friedman PA (2007) NHERF1 regulates parathyroid hormone receptor membrane retention without affecting recycling. *J Biol Chem* **282**:36214-36222.

Wang B, Yang Y, Liu L, Blair HC and Friedman PA (2013) NHERF1 regulation of PTH-dependent bimodal Pi transport in osteoblasts. *Bone* **52**:268-277.

Watson N, Linder ME, Druey KM, Kehrl JH and Blumer KJ (1996) RGS family members: GTPase-activating proteins for heterotrimeric G-protein α -subunits. *Nature* **383**:172-175.

Waugh JL, Lou AC, Eisch AJ, Monteggia LM, Muly EC and Gold SJ (2005) Regional, cellular, and subcellular localization of RGS10 in rodent brain. *J Comp Neurol* **481**:299-313.

Weiler M, Pfenning PN, Thiebold AL, Blaes J, Jestaedt L, Gronych J, Dittmann LM, Berger B, Jugold M, Kosch M, Combs SE, von Deimling A, Weller M, Bendszus M, Platten M and Wick W (2013) Suppression of proinvasive RGS4 by mTOR inhibition optimizes glioma treatment. *Oncogene* **32**:1099-1109.

Weinman EJ and Lederer ED (2012) PTH-mediated inhibition of the renal transport of phosphate. *Exp Cell Res* **318**:1027-1032.

Willard FS, Willard MD, Kimple AJ, Soundararajan M, Oestreich EA, Li X, Sowa NA, Kimple RJ, Doyle DA, Der CJ, Zylka MJ, Snider WD and Siderovski DP (2009) Regulator of G-protein signaling 14 (RGS14) is a selective H-Ras effector. *PLoS One* **4**:e4884.

Willars GB (2006) Mammalian RGS proteins: multifunctional regulators of cellular signalling. *Semin Cell Dev Biol* **17**:363-376.

Williams NM, Preece A, Spurlock G, Norton N, Williams HJ, McCreadie RG, Buckland P, Sharkey V, Chowdari KV, Zammit S, Nimgaonkar VL, Kirov G, Owen MJ and O'Donovan MC (2004) Support for RGS4 as a Susceptibility Gene for Schizophrenia. *BIOL PSYCHIATRY*:192-195.

Wright SC, Kozielwicz P, Kowalski-Jahn M, Petersen J, Bowin CF, Slodkowicz G, Marti-Solano M, Rodriguez D, Hot B, Okashah N, Strakova K, Valnohova J, Babu MM, Lambert NA, Carlsson J and Schulte G (2019) A conserved molecular switch in Class F receptors regulates receptor activation and pathway selection. *Nat Commun* **10**:667.

Wu J, Matthaei H, Maitra A, Dal Molin M, Wood LD, Eshleman JR, Goggins M, Canto MI, Schulick RD, Edil BH, Wolfgang CL, Klein AP, Diaz LA, Jr., Allen PJ, Schmidt CM, Kinzler KW, Papadopoulos N, Hruban RH and Vogelstein B (2011) Recurrent GNAS mutations define an unexpected pathway for pancreatic cyst development. *Sci Transl Med* **3**:92ra66.

Wu V, Yeerna H, Nohata N, Chiou J, Harismendy O, Raimondi F, Inoue A, Russell RB, Tamayo P and Gutkind JS (2019) Illuminating the Onco-GPCRome: Novel G protein-coupled receptor-driven oncocrine networks and targets for cancer immunotherapy. *J Biol Chem* **294**:11062-11086.

- Xie GX and Palmer PP (2007) How regulators of G protein signaling achieve selective regulation. *J Mol Biol* **366**:349-365.
- Xie Y, Wolff DW, Wei T, Wang B, Deng C, Kirui JK, Jiang H, Qin J, Abel PW and Tu Y (2009) Breast cancer migration and invasion depend on proteasome degradation of regulator of G-protein signaling 4. *Cancer Res* **69**:5743-5751.
- Xie Z, Chan EC and Druey KM (2016) R4 Regulator of G Protein Signaling (RGS) Proteins in Inflammation and Immunity. *AAPS J* **18**:294-304.
- Xu J, Cao S, Hubner H, Weikert D, Chen G, Lu Q, Yuan D, Gmeiner P, Liu Z and Du Y (2022) Structural insights into ligand recognition, activation, and signaling of the alpha2A adrenergic receptor. *Sci Adv* **8**:eabj5347.
- Xue X, Wang L, Meng X, Jiao J and Dang N (2017) Regulator of G protein signaling 4 inhibits human melanoma cells proliferation and invasion through the PI3K/AKT signaling pathway. *Oncotarget* **8**:78530-78544.
- Yang J, Cumberbatch D, Centanni S, Shi SQ, Winder D, Webb D and Johnson CH (2016) Coupling optogenetic stimulation with NanoLuc-based luminescence (BRET) Ca(++) sensing. *Nat Commun* **7**:13268.
- Yang Y, Liu N, He Y, Liu Y, Ge L, Zou L, Song S, Xiong W and Liu X (2018) Improved calcium sensor GCaMP-X overcomes the calcium channel perturbations induced by the calmodulin in GCaMP. *Nat Commun* **9**:1504.
- Yasui T, Okada A, Urabe Y, Usami M, Mizuno K, Kubota Y, Tozawa K, Sasaki S, Higashi Y, Sato Y, Kubo M, Nakamura Y, Matsuda K and Kohri K (2013) A replication study for three nephrolithiasis loci at 5q35.3, 7p14.3 and 13q14.1 in the Japanese population. *J Hum Genet* **58**:588-593.
- Yin W, Tang G, Zhou Q, Cao Y, Li H, Fu X, Wu Z and Jiang X (2019) Expression Profile Analysis Identifies a Novel Five-Gene Signature to Improve Prognosis Prediction of Glioblastoma. *Front Genet* **10**:419.
- Zhang H, Kong Q, Wang J, Jiang Y and Hua H (2020) Complex roles of cAMP-PKA-CREB signaling in cancer. *Exp Hematol Oncol* **9**:32.
- Zhang P and Mende U (2011) Regulators of G-protein signaling in the heart and their potential as therapeutic targets. *Circ Res* **109**:320-333.
- Zhang Q, Xiao K, Paredes JM, Mamonova T, Sneddon WB, Liu H, Wang D, Li S, McGarvey JC, Uehling D, Al-awar R, Joseph B, Jean-Alphonse F, Orte A and Friedman PA (2019) Parathyroid hormone initiates dynamic NHERF1 phosphorylation cycling and conformational changes that regulate NPT2A-dependent phosphate transport. *J Biol Chem* **294**:4546-4571.

Zhang S, Watson N, Zahner J, Rottman JN, Blumer KJ and Muslin AJ (1998) RGS3 and RGS4 are GTPase activating proteins in the heart. *J Mol Cell Cardiol* **30**:269-276.

Zhang Y, Chen K, Sloan SA, Bennett ML, Scholze AR, O'Keefe S, Phatnani HP, Guarnieri P, Caneda C, Ruderisch N, Deng S, Liddelow SA, Zhang C, Daneman R, Maniatis T, Barres BA and Wu JQ (2014) An RNA-sequencing transcriptome and splicing database of glia, neurons, and vascular cells of the cerebral cortex. *J Neurosci* **34**:11929-11947.

Zhao P, Nunn C, Ramineni S, Hepler JR and Chidiac P (2013) The Ras-binding domain region of RGS14 regulates its functional interactions with heterotrimeric G proteins. *J Cell Biochem* **114**:1414-1423.

Zhou Y and Greka A (2016) Calcium-permeable ion channels in the kidney. *Am J Physiol Renal Physiol* **310**:F1157-1167.

Zizak M, Lamprecht G, Steplock D, Tariq N, Shenolikar S, Donowitz M, Yun CH and Weinman EJ (1999) cAMP-induced phosphorylation and inhibition of Na⁺/H⁺ exchanger 3 (NHE3) are dependent on the presence but not the phosphorylation of NHE regulatory factor. *J Biol Chem* **274**:24753-24758.